CHARACTERIZATION OF AN INDUCIBLE ENHANCER ELEMENT AND THE SIGNALING PATHWAYS INVOLVED IN MANGANESE SUPEROXIDE DISMUTASE GENE REGULATION

By

RICHARD JAMES ROGERS

A DISSERTATION PRESENTED TO THE GRADUATE SCHOOL
OF THE UNIVERSITY OF FLORIDA IN PARTIAL FULFILLMENT
OF THE REQUIREMENTS FOR THE DEGREE OF
DOCTOR OF PHILOSOPHY

UNIVERSITY OF FLORIDA

2000

To my parents who understood the significance of education.

Live as if you were to die tomorrow. Learn as if you were to live forever.

– Ghandi

ACKNOWLEDGMENTS

I would like to thank Dr. Harry S. Nick, chairman of my graduate advisory committee, for his support, trust, friendship, guidance, and encouragement throughout my graduate studies. I am also grateful to the other committee members--Drs. Brian Cain, Sarah Chesrown, Robert Ferl, and Michael Kilberg--for their assistance. I would like to thank all members, professors and staff, from the Department of Biochemistry and Molecular Biology from the University of Florida College of Medicine. I am deeply indebted to the members of my laboratory, both past (Maureen, Jan-Ling, Michael, Yemi, and Jane) and present (Yang, Chris, Nikki, and Ann), for their help along this journey. I also wish to extend a special, heartfelt thanks to Joan Monnier, my second mom, for her support, technical help and spiritual guidance, during the most emotionally trying time in my personal life. I can never fully repay my debt to her. Finally, I would like to express my gratitude, respect and love to Ming Ming Chow for helping me in countless ways to become a better person, but especially for showing me how to feel joy again.

TABLE OF CONTENTS

page

ACKNOWLEDGMENTS iii

ABSTRACT vii

CHAPTERS

1 INTRODUCTION 1

Oxygen and Free Radicals 1
Superoxide Dismutases 3
Inflammation 5
Lipopolysaccharide 6
Tumor Necrosis Factor 7
Interleukin-1 9
Molecular Biology of *MnSOD* 11
Enhancers 14

2 MATERIALS AND METHODS 18

Materials 18
Methods 20
Tissue Culture 20
Polymerase Chain Reaction (PCR) 21
TA Cloning of PCR Products 22
Reporter Vector Cloning 23
Plasmid Purification 24
Transient Transfection of Mammalian Cells 26
RNA Isolation 27
Northern Analysis 28
Genomic DNA Isolation 29
Electrophoretic Mobility Shift Assay (EMSA) 30
In Vivo DMS Treatment 31
Ligation-Mediated PCR (LMPCR) 33
Site-Directed Mutagenesis and Substitutions by PCR 37
Radiolabeled Probe Synthesis 40
Hybridization of Northern and Southern Blots 41

3 CYTOKINE-INDUCIBLE ENHANCER WITH PROMOTER ACTIVITY IN BOTH THE RAT AND HUMAN SUPEROXIDE DISMUTASE GENES 42

Introduction 42
Results 44
An Inducible *Cis*-Acting Element Exists within *MnSOD* 44
The *MnSOD* Inducible Enhancer Element is Located within Intron 2 48
The Enhancer Is Likely Composed of A Complex Set of Interacting Elements 54
The Inducible Enhancer Elements within Rat and Human *MnSOD* Can Act with A Heterologous Promoter 60
Evaluation of Promoter-Enhancer Interactions 63
The Rat and Human Enhancer Elements Contain Inducible Promoter Activity 69
Discussion 70

4 *IN VIVO* FOOTPRINTING AND MUTAGENESIS OF THE RAT MANGANESE SUPEROXIDE DISMUTASE ENHANCER 75

Introduction 75
Results 77
Multiple Potential Protein Binding Sites Exist within the *MnSOD* Enhancer 77
Mutagenesis of Putative DNA Binding Sites Alters Inducible *MnSOD* Expression 83

Discussion 89

5 REACTIVE OXYGEN SPECIES AND MITOCHONDRIA-TO-NUCLEUS SIGNALING 91

Introduction 91
Results 93
Mitochondrial Electron Transport Inhibitors Modulate TNF-α-Induced Expression of *MnSOD* in Pulmonary Epithelial Cells 93
Antimycin A Strongly Decreases TNF-α-Inducible *MnSOD* Expression in Pulmonary Endothelial Cells 96
The Signaling Pathway of TNF-α Is Different from the Pathways of LPS- or IL-1-Stimulated Expression of *MnSOD* 100
Inhibition of Mitochondrial ATPase with Oligomycin also Represses TNF-α-Stimulated Expression of *MnSOD* 103
Reactive Oxygen Species Are Important for TNF-α-Stimulated Expression of *MnSOD* 108

TNF-α-Stimulated Expression of *MnSOD* in Endothelial Cells Is Dependent on Cytoplasmic Phospholipase A_2 (cPLA_2) 108
TNF-α-Inducible Expression of *MnSOD* Is Not Dependent on Nuclear Factor- κB (NF-κB) 115

Discussion 116

6 CONCLUSIONS AND FUTURE DIRECTIONS 121

Conclusions 121
Future Directions 127

REFERENCES 130

BIOGRAPHICAL SKETCH 153

Abstract of Dissertation Presented to the Graduate School
of the University of Florida in Partial Fulfillment of the
Requirements for the Degree of Doctor of Philosophy

CHARACTERIZATION OF AN INDUCIBLE ENHANCER ELEMENT AND THE SIGNALING PATHWAYS INVOLVED IN MANGANESE SUPEROXIDE DISMUTASE GENE REGULATION

By

Richard James Rogers

December 2000

Chairman: Dr. Harry S. Nick
Major Department: Biochemistry and Molecular Biology

Manganese superoxide dismutase (MnSOD), an enzyme localized to the mitochondria, converts superoxide ($O_2^{\bullet}$) into oxygen (O_2) and hydrogen peroxide (H_2O_2). The superoxide dismutases (SODs) are the first line of cellular defense against the damaging effects of superoxide anion radicals. Manganese superoxide dismutase is the most highly regulated of the three SODs. Multiple studies have shown that increased cellular levels of MnSOD are cytoprotective during cellular oxidative stress or inflammatory challenges. The major goals of this dissertation were to identify within the MnSOD gene the regions of DNA that are responsible for inducible expression and to understand some of the intracellular signaling pathways that control this induction. To do so, I utilized the polymerase chain reaction method to create deletions of a large region

within the MnSOD gene as a means of creating reporter vectors, which could be evaluated by transient transfection studies in a rat lung epithelial cell line. The results of these experiments defined a small region (260 bp) within intron 2 as an enhancer, which regulates the inducible expression seen in the endogenous MnSOD gene. In addition, by utilizing a variety of specific pharmacologic inhibitors, I was able to show the differences between signaling pathways (lipopolysaccharide, tumor necrosis factor, interleukin-1) responsible for the inducible expression of MnSOD. Interestingly, reactive oxygen species, which are byproducts of the mitochondrial electron transport chain, appear to be important regulators of the tumor necrosis factor pathway, but not that of lipopolysaccharide or interleukin-1. Finally, by using the method of *in vivo* footprinting, I was able to identify putative protein-DNA binding sites within the enhancer region. Using this data, I created a number of reporter vectors with mutations within the enhancer region. By transiently transfecting these reporter vectors into rat lung epithelial cells, I may have identified at least one important putative protein-DNA binding site in the enhancer region. It is likely that the MnSOD enhancer contains multiple protein-DNA binding sites which work to create a protein complex necessary for the inducible expression seen in the endogenous MnSOD gene. This work will add to the understanding of how the inducible MnSOD gene is regulated.

CHAPTER 1
INTRODUCTION

Oxygen and Free Radicals

The element oxygen (chemical symbol O) exists in air as a diatomic molecule, O_2, which strictly should be called dioxygen. Over 99% of the O_2 in the atmosphere is the isotope oxygen-16 but there are traces of oxygen-17 (about 0.04%) and oxygen-18 (about 0.2%). Except for certain anaerobic and aero-tolerant unicellular organisms, all animals, plants, and bacteria require O_2 for efficient production of energy by the use of O_2-dependent electron-transport chains, such as those in the mitochondria of eukaryotic cells. This need for O_2 obscures the fact that O_2 is a toxic mutagenic gas; aerobes survive because they have antioxidant defenses to protect against it.

Perhaps the earliest suggestion made to explain O_2 toxicity was that O_2 inhibits cellular enzymes (Balentine, 1982; Haugaard, 1968). Indeed, direct inhibition by O_2 is thought to account for the loss of nitrogenase activity in O_2-exposed *C. pasterianum* (Gallon, 1981). Another good example of the direct effect of O_2 comes from green plants. During photosynthesis, illuminated green plants fix CO_2 into sugars by a complex metabolic pathway know as the Calvin cycle. The first enzyme in this pathway, ribulose bisphosphate carboxylase, catalyses the reaction of CO_2 with a five-carbon sugar (ribulose 1,5-bisphosphate) to produce two molecules of phoshoglyceric acid. Oxygen is an alternative substrate for this enzyme, competitive with CO_2, and so at elevated O_2 concentrations there is less CO_2 fixation and hence less plant growth (Halliwell, 1984).

In general, however, the rates of direct inactivation of enzymes by O_2 in aerobic cells are too slow and too limited in extent to account for the rate at which toxic effects develop; most enzymes are totally unaffected by O_2. In 1954, Rebecca Gershman and Daniel L. Gilbert drew a parallel between the effects of O_2 and those of ionizing radiation and proposed that most of the damaging effects of O_2 could be attributed to the formation of free oxygen radicals (Gilbert, 1981).

The growth inhibition observed after exposing *E. coli* to high-pressure O_2 can be relieved by adding valine to the culture medium. Valine synthesis is impaired because of a rapid inhibition of the enzyme dihydoxyacid dehydratase, which catalyzes a reaction in the metabolic pathway leading to valine. This is probably not a direct inhibition by O_2, but rather by oxygen radicals such as superoxide (Flint et al., 1993). Other enzymes inactivated by superoxide radical ($O_2^{\bullet-}$) in *E. coli* exposed to high pressure O_2 include the Krebs cycle enzymes aconitase and fumarase. *E. coli* contains three fumarases: fumarase A and B are inactivated by $O_2^{\bullet-}$ whereas fumarase C is not. Levels of fumarase C increase when *E. coli* is exposed to oxidizing conditions, perhaps as a replacement for the superoxide-sensitive fumarases A and B. Aconitase may also be an important target of damage by $O_2^{\bullet-}$ in mammalian tissues exposed to excess O_2 (Hausladen and Fridovich, 1994; Morton et al., 1998). The onset of O_2-induced convulsions in animals is correlated with a decrease in the cerebral content of the neurotransmitter GABA (γ-aminobutyric acid), perhaps because of an inhibition of the enzyme glutamate decarboxylase (glutamine → GABA + CO_2) by O_2 (Hori, 1982); it has not, however, been shown that

the enzyme inhibition *in vivo* is due to O_2 itself rather than to the effects of an increased production of oxygen radicals (Haugaard, 1968).

The term "free radical" has several definitions, however, the simplest one describes a free radical as any species capable of independent existence and contains one or more unpaired electrons (Halliwell and Gutteridge, 1999). The presence of one or more unpaired electrons usually causes free radicals to be attracted slightly to a magnetic field (i.e., to be paramagnetic), and sometimes makes them highly reactive, although the chemical reactivity of radicals varies over a wide spectrum. Radicals can be formed when a covalent bond is broken if one electron from each of the pair shared remains with each atom, a process known as hemolytic fission (von Sonntag, 1987).

$$A{:}B \rightarrow A^{\bullet} + B^{\bullet}$$

For example, hemolytic fission of one of the O-H covalent bonds in the H_2O molecule will yield a hydrogen radical ($H^{\bullet}$) and a hydroxyl radical ($^{\bullet}OH$). The opposite of hemolytic fission is heterolytic fission, in which one atom receives both electrons when a covalent bond breaks, i.e.

$$A{:}B \rightarrow A^{-} + B^{+}$$

Where A receives both electrons. A is now negatively charged and this gives A a negative charge and B is left with a positive charge. Heterolytic fission of water gives the hydrogen ion H+ and the hydoxide ion OH-.

Superoxide Dismutases

The superoxide dismutases (SODs) catalyze the dismutation of superoxide anion radical ($O_2^{\bullet -}$) into hydrogen peroxide and oxygen as follows:

$$2H^{+} + 2\,O_2^{\bullet -} \rightarrow H_2O_2 + O_2$$

SODs, isolated from a wide range of organisms, fall into three types depending on the metals found in their active centers: copper/zinc, manganese, and iron. Cu/ZnSOD is found mainly in the cytosol of eukaryotes (Slot et al., 1986) and in chloroplasts; MnSOD, in prokaryotes and in the mitochondria of eukaryotes; and FeSOD, in prokaryotes and in a few families of plants. In addition, an extracellular SOD similar to the Cu/ZnSOD had also been found in the extracellular fluid of eukaryotic cells (Marklund, 1984; Hjalmarsson et al., 1987). Amino acid sequence data had shown that these three types of SODs fall into two distinct families (Bannister et al., 1987). The FeSOD and MnSOD show a high degree of amino acid sequence and structural homology, while the second family, which includes the Cu/ZnSOD, is completely unrelated.

Two major forms of SOD have been purified from rat liver (Assayama and Burr, 1985). The Cu/ZnSOD consists of two identical subunits with a total molecular weight of 32 kilodaltons (kD). Each subunit contains a single Cu and Zn atom, noncovalently linked. The copper ion appears to function in the enzymatic reaction, whereas the zinc ion is noncatalytic and serves to stabilize the enzyme. The complete amino acid sequence of Cu/ZnSOD has been determined from various species with a high level of conservation (Bannister et al., 1987).

The rat MnSOD is a tetrameric enzyme containing four identical 21 kD subunits with a total molecular weight of approximately 80 kD whereas most bacterial MnSODs are dimeric enzymes of approximately 40 kD. The amino acid sequences of the MnSOD enzyme from various species, including rat, mouse, and human, as well as from bacteria, have been compared and are very similar (Bannister et al., 1987). These enzymes contain Mn at the active site and the mammalian forms have been localized primarily in the

mitochondria, particularly in the matrix between the cristae (Slot et al., 1986). Mitochondrial DNA and membranes are particularly prone to oxidation because mitochondria themselves are a major source of free radicals. When mitochondria are severely damaged, aerobically growing cells are starved for energy. The localization of the MnSOD exclusively within the mitochondria suggests an important role for this antioxidant enzyme in this organelle.

Both rat Cu/ZnSOD and MnSOD cDNAs have been isolated and characterized by our laboratory and others (Ho and Crapo, 1987). The rat MnSOD cDNA encodes a protein of 222 amino acids, which includes a putative mitochondrial targeting sequence of 24 amino acids. The Cu/ZnSOD is sensitive to cyanide, whereas MnSOD is resistant to this reagent (Weisinger and Fridovich, 1973; Fridovich, 1974). This difference in the cyanide sensitivity makes it possible to distinguish the enzymatic activities of these two SODs.

In general, the synthesis of Cu/ZnSOD is constitutive whereas MnSOD is inducible. Induction of MnSOD in eukaryotes has been observed following treatment with paraquat (Krall et al., 1988), X-irradiation (Oberley et al., 1987), and hyperoxia (Freeman et al., 1986), suggesting that MnSOD induction is important for protection against oxidative stress. Since inflammatory responses often result in generation of a variety of free radicals, which can directly or indirectly lead to tissue injury, it is of interest to further characterize the role of SOD in such inflammatory responses.

Inflammation

Microbial invasion, immunological reactions, and inflammatory processes induce a complex set of responses in the host, collectively referred to as the acute phase response

(Kushner et al., 1989). This response is characterized by fever, metabolic changes, increased peripheral white blood cell count, and an increased synthesis of acute phase proteins including C-reactive protein, ceruloplasmin, serum amyloid A protein, and various complement proteins.

In addition, the immune system produces a variety of inflammatory mediators including cytokines, arachidonic acid metabolites, and oxygen free radicals to protect the host when threatened by inflammatory agents, microbial invasion, or injury. In some cases this complex defense network successfully restores normal homeostasis, but at other times the overproduction of inflammatory mediators may actually prove deleterious to the host (Welbourn and Young, 1992). For example, septic shock associated with infection is generally caused by wide-spread and uncontrolled activation of the mononuclear phagocyte cell population and the release of massive quantities of inflammatory mediators (Molloy et al., 1993). The clinical characteristics of this condition include fever, hypotension, hypoglycemia, disseminated intravascular coagulation and increased vascular permeability. The acute phase response, characterized by the release of pro-inflammatory mediators and the activation of immune cells, can be produced upon exposure to bacterial cell wall materials, most notably, lipopolysaccharide.

Lipopolysaccharide

One of the major toxic components contributing to the inflammatory response during microbial invasions is lipopolysaccharide (LPS). LPS, a constituent of the cell wall of gram-negative bacteria, consists of a polysaccharide portion and a covalently linked lipid moiety termed lipid A (Rietschel and Brade, 1992). Wide derangements

including acute inflammatory responses, altered energy metabolism, and multiple tissue injury are observed after LPS administration (Ghosh et al, 1993). The toxic properties of LPS account for its other name, bacterial endotoxin.

Several lipopolysaccharide binding proteins (LBP), which specifically interact with LPS, have been reported (Tobias et al., 1988). For example, Schumann et al. (1990) have characterized a LBP which is a 60 kD plasma glycoprotein synthesized in hepatocytes. After the LBP interacts with LPS, this LPS-LBP complex then binds to the cell surface protein CD14 and presumably elicits the cellular and tissue responses to LPS (Wright et al., 1990). In addition, a membrane-localized 80 kD LPS-specific binding protein has been identified in B lymphocytes, T lymphocytes, and macrophages (Lei and Morrison, 1988). However, the roles of these different LBPs and the interaction between them are still not clear.

Tumor Necrosis Factor

Tumor necrosis factor (TNF), also called cachectin, is synthesized principally by monocytes and macrophages in response to macrophage activators such as endotoxin. Human TNF has a molecular weight of 17 kD, which is synthesized as a propeptide of 233 amino acids with a precursor sequence of 76 amino acids (Pennica et al., 1984; Aggarwal et al., 1985). The amino acid sequences of both the pro- and mature peptides are highly conserved between mouse and human, with about 80% homology (Beutler et al., 1985; Cseh and Beutler, 1989). A wide spectrum of possible physiological actions for TNF, including its use in the management of certain tumors, its role in an inflammatory reaction, and its involvement in the immune response, have been documented (Beutler and Cerami, 1989).

TNF and lymphotoxin (a tumoricidal protein produced by lymphocytes), sometimes referred to as TNF-α and TNF-β respectively, are structurally and functionally related (Goeddel et al., 1986). They share about 28% homology and have been shown to interact with the same receptors and exhibit a number of shared biological activities. The genes for TNF and lymphotoxin are closely linked and separated by about 1 kb in humans (Nedwin et al., 1985). Lymphotoxin lies 5' to TNF, and both genes reside within the major histocompatibility complex locus on chomosome 6, indicating that these two genes may have evolved from a gene duplication event.

Most cell types including liver, kidney, muscle, and adipose tissue have been shown to possess specific high affinity receptors for TNF. Two distinct TNF receptors of 55-69 kD (p55) and 70-80 kD (p75) have been identified in the mouse (Goodwin et al., 1991) and human systems which demonstrate ligand specificity for both TNF-α and TNF-β (Hohmann et al., 1990). The p75 receptor possesses greater affinity for TNF than the p55 receptor (Tartaglia and Goeddel, 1992). The genes for the p55 and p75 receptors map to chromosomes 12 and 1 in humans, and to chomosome 6 and 4 in the mouse, respectively (Goodwin et al., 1991).

Based on their amino acid sequence, the two receptors are only 29% identical to each other, and both share four cysteine-rich repeats in their extracellular domains that are characteristic of the nerve growth factor (NGF) receptor family. For both proteins, aggregation of receptors mediated by binding of dimeric or trimeric TNF is believed to initiate the signaling process. However, several lines of evidence suggest that subsequent steps of the signal transduction process may diverge. Studies have been conducted using antibodies specific for either the p55 or p75 receptor. Heller et al. (1992) reported that

the cytotoxicity of TNF was mediated through the p75 receptor. Tartaglia et al. (1993) provided evidence indicating that the cytotoxicity of TNF is signaled by the p55 receptor. The controversy between these two hypotheses needs further investigation, but also demonstrates the complexity of the TNF function.

Soluble forms of the TNF receptors are released from the cell surface by proteolytic cleavage (Lantz et al., 1990; Gullberg et al., 1992). These soluble receptors act as TNF binding proteins, which subsequently inhibit TNF interactions with surface receptors. In addition, the release of soluble receptors results in the down-regulation of cell surface receptors. Therefore, shedding of surface receptors enables target cells to decrease their responsiveness to TNF. Binding of TNF to its receptor is followed by rapid internalization and degradation via a lysosomal pathway (Tsujimoto et al., 1985; Niitsu et al., 1985)

Interleukin-1

Interleukin-1 (IL-1), initially recognized as a factor producing high fever and a shock-like state (Okusawa et al., 1988; Fischer et al., 1991), is primarily synthesized by macrophages and monocytes, but may also be produced by epithelial cells, endothelial cells, keratinocytes, and glial cells. IL-1 is an inflammatory cytokine, more closely related to tumor necrosis factor (TNF) than any other cytokine, although the structure and receptors for IL-1 and TNF are clearly distinct. IL-1 is biologically active in the low picomolar or even femtomolar range. There is little evidence that cytokines, such as IL-1, play any role in normal homeostasis such as hormonal regulation, metabolism or in physiological regulation. In the absence of injury or damage, however, it is unclear whether IL-1 is needed.

During inflammation, injury, immunological challenge or infection, IL-1 is produced and because of its multiple biological properties, this cytokine appears to affect the pathogenesis of disease. Specific physiological activities of IL-1 include lymphocyte stimulation, induction of acute phase proteins, helper activity for immunoglobulin production by B lymphocytes, induction of interferon β-2, and radioprotection (Neta et al., 1986; Fibbe et al., 1989). Most studies on IL-1 are derived from experiments in which bacterial products such as lipopolysaccharide (LPS), endotoxins from Gram-negative bacteria or exotoxins from Gram-positive organisms are used to stimulate macrophages (Ikejima et al., 1988).

Two distinct genes, located on chromosome 2, code for the IL-1α and IL-1β precursor polypeptides both having molecular masses of 31 kD (Auron et al., 1984; Lomedico et al., 1984; Clark et al., 1986; Dinarello, 1992). However, unlike most proteins, both IL-1α and β lack a leader sequence of amino acids, which would enable the precursor protein to be inserted into the Golgi and cleaved to a smaller, mature size to be transported out of the cell. The mature protein of both IL-1α and β is approximately 17 kD after enzymatic cleavage. IL-1α and IL-1β have very different amino acid sequences, sharing only 26% similarity; however, structurally the two isoforms of IL-1 are related at the three dimensional level, having been crystallized (Preistle et al., 1988, 1989). These two proteins have been found in human, mouse, rat, pig, and rabbit and exhibit significant interspecies homology at the amino acid level (62% homology between human and mouse IL-1α, Auron et al., 1985). The third member of the IL-1 gene family is IL-1 receptor antagonist (IL-1Ra). The three members of the IL-1 family

recognize and bind to the same cell surface receptors. IL-1α and IL-1β binding to the IL-1 receptors transmits a signal whereas IL-1Ra does not.

IL-1 is rapidly synthesized by mononuclear cells, which are stimulated by microbial products or inflammatory agents. Because of the lack of a leader peptide, most IL-1α remains in the cytosol of cells. There is some evidence that the precursor IL-1α is transported to the cell surface where it has been identified as membrane IL-1 (Brody and Durum, 1989). In human monocytes, between 40-60% of IL-1β is transported out of the cell but in contrast to IL-1α, IL-1β enters the circulation. Various mechanisms for transport include exocytosis from vesicles, active transport via multiple-drug-resistance carrier proteins, or following cell death. Unlike the IL-1α precursor, the IL-1β precursor requires cleavage for optimal biological activity. Several common enzymes will cut the IL-1β precursor into smaller and more active forms. However, one particular protease appears highly specific for cleaving the IL-1β precursor from 31 to 17.5 kD, its most active form (Cerretti et al., 1992; Thornberry et al., 1992). This enzyme is known as the IL-1β converting enzyme (ICE) and is a member of the cysteine protease family. ICE does not cleave the IL-1α precursor. Other enzymes have been found which cleave the IL-1α precursor, but these other enzymes seem less specific than ICE.

Molecular Biology of *MnSOD*

Our laboratory has previously characterized the rat *MnSOD* cDNA (Dougall, 1990). The rat *MnSOD* genomic locus was first sequenced by Ho et al. (1991). The promoter region of *MnSOD* contains neither a "CAAT box" nor a "TATA box." Our laboratory has also identified and characterized the rat *MnSOD* gene, which contains five exons. Exon one encodes the 5' untranslated leader sequence, the mitochondrial signal

sequence, and the N-terminus of the rat MnSOD protein. Exon 2, 3, 4, and 5 encode the mature MnSOD protein. Exon 5 contains the stop codon, TGA, and the 3' untranslated region (Dougall, 1990). Primer extension analysis was used to locate the transcription initiation site at between 70 and 74 nucleotides 5' to the start of translation (Hurt et al, 1992). There are five species of *MnSOD* mRNA identified by Northern analysis. Our laboratory has demonstrated that these five species of *MnSOD* mRNA are the result of differential polyadenylation (Hurt et al., 1992).

The regulation of *MnSOD* biosynthesis in *E. coli* is under rigorous control. The induction of this enzyme is in response to the cellular environmental redox state. *E. coli* grown in iron-poor medium or in the presence of iron-chelating agents results in an induction of the bacterial *MnSOD* gene. On the other hand, cells grown in iron-enriched medium produces an inhibition of *MnSOD* expression. All of these observations led Fridovich to suggest that *E. coli MnSOD* is controlled by an iron-containing repressor (Fridovich, 1986). More recently, the transcriptional regulators, Fnr, Fur, and Arc, were identified (Hassan and Sun, 1992; Privalle and Fridovich, 1993) and found to negatively regulate the expression of *MnSOD* in *E. coli*. Unlike bacteria, MnSOD synthesis in eukaryotic cells is upregulated dramatically by proinflammatory mediators including lipopolysaccharide (LPS), tumor necrosis factor alpha (TNF-α), interleukins-1 and -6 (IL-1, IL-6), and interferon gamma (IFN-γ) (Wong and Goeddel, 1988; Shaffer et al., 1990; Del-Vecchio and Shaffer, 1991; Dougall and Nick, 1991; Borg et al., 1992; Eddy et al., 1992, Gibbs et al., 1992; Valentine and Nick, 1992; Visner et al., 1992; Whitsett et al., 1992; Eastgate et al., 1993; Melendez and Baglioni, 1993; Bigdeli et al., 1994;

Jacoby et al., 1994; Akashi et al., 1995; Gwinner et al., 1995; Jones et al., 1995; Lontz et al., 1995; Stephanz et al., 1996). In L2 cells, a rat pulmonary epithelial-like cell line, *MnSOD* mRNA levels show an 18-23 fold induction after stimulation with LPS (Visner et al., 1990). Cells treated with TNF-α or IL-1 showed similar results.

To evaluate the importance of on-going protein synthesis and *de novo* transcription, studies with cycloheximide, an inhibitor of protein synthesis, showed no effect on LPS-, TNF-α-, or IL-1-dependent induction of *MnSOD* mRNA level. On the other hand, L2 cells co-treated with stimulant (LPS, TNF-α, or IL-1) and actinomycin, an inhibitor of mRNA transcription, inhibited the stimulus-dependent induction of *MnSOD* mRNA expression (Visner et al., 1990). Furthermore, nuclear-run on data showed a 9 fold induction in *MnSOD* mRNA level (Hsu, 1993). The above evidence suggests that the regulation of *MnSOD* gene expression is, at least partly, transcriptionally dependent. The difference between nuclear run-on analysis and *in vivo* data on mRNA level following LPS treatment may be caused by the stability of the mRNA or the loss of some transcription factors during the preparation of nuclei for nuclear run-on experiments. Examinations of other cell types treated with LPS, TNF-α, or IL-1 also showed similar results at the mRNA level, including rat pulmonary artery endothelial cells (Visner et al., 1992), porcine pulmonary artery endothelial cells (Visner et al., 1991), and intestinal epithelial cells (Valentine and Nick, 1992). Interestingly, though Cu/ZnSOD contributes the major part of the total cellular SOD activity, its mRNA level is not regulated by any known stimulant to any large degree.

Enhancers

The control of transcription in prokaryotes is largely governed by sequences in the vicinity of the transcriptional start site. Most prokaryotic promoters consist of short sequence motifs approximately 10 to 35 base pairs upstream of the transcriptional start site; these motifs make direct contact with RNA polymerase and thus serve to position the start site (Rosenberg and Court, 1979). The initial characterization of eukaryotic promoters revealed a similar arrangement of sequence elements. Many eukaryotic promoters possess the conserved sequence motif TATAAA (the TATA box) in the –20 to –30 region, and some promoters contain an additional upstream conserved element GG(T or C)CAATCT (the CAAT box). However, unlike the corresponding prokaryotic element, deletion of the TATA box does not necessarily abolish expression, as shown by early studies on the histones H2A gene (Grosschedl and Birnstiel, 1980a). In addition, these studies revealed that DNA sequences lying several hundred base pairs (bp) upstream of the transcriptional start site can positively influence transcription, even when positioned in an inverted orientation (Grosschedl and Birnstiel, 1980b).

Similar work with the simian virus 40 (SV40) early region indicated that the TATA box was not required for early gene expression (Benoist and Chambon, 1980) and that its deletion resulted in heterogeneous transcriptional start sites (Benoist and Chambon, 1981). In addition, deletion of sequences about 150 bp upstream of the transcriptional start site had an adverse effect on early gene expression. Deletion of one of the two 72 bp repeat elements upstream of the early gene did not greatly reduce early gene expression or virus viability, but the additional removal of a portion of the second repeat reduced expression dramatically (Gruss et al., 1981; Benoist and Chambon, 1981).

Thus, it was found that DNA sequences lying a considerable distance upstream of transcriptional start sites play a significant role in transcriptional regulation.

Further characterization of these sequences revealed a surprising result. When a 366 bp DNA segment of the SV40 promoter region was linked to a β-globin gene, transcription of the gene was enhanced up to 200-fold (Banerji et al., 1981). This enhancement of transcription occurred only when the SV40 sequences were present in *cis*, did not depend upon DNA replication, and could occur when the sequences were placed in both orientations either 1400 bp 5' or 3300 bp 3' of the gene. Enhancement was observed as long as one copy of the 72 bp repeats was present. Similar results were obtained when the SV40 promoter region was placed adjacent to the chicken conablumin or adenovirus major late promoters, or within the T antigen gene intron sequences (Moreau et al., 1981; Fromm and Berg, 1983). Thus, sequences within and flanking the SV40 72 bp repeats are important for enhancing the expression of *cis*-linked promoters in an orientation and distance independent fashion, although in some cases distance effects were observed (Moreau et al., 1981). Studies with polyoma virus also revealed the existence of a DNA segment essential for viral viability and capable of enhancing expression of *cis*-linked genes (Tyndall et al., 1981; de Villiers and Schaffner, 1981). Shortly thereafter, retroviruses were found to possess similar DNA elements in their long terminal repeat (LTR) regions (Levinson et al., 1982; Gorman et al., 1982).

The properties of these viral transcriptional control elements now constitute the definition of an enhancer element. These properties include the ability to (*a*) increase transcription of *cis*-linked promoters, (*b*) operate in an orientation independent manner,

(*c*) exert an effect over large distances independent of position, and (*d*) enhance the expression of heterologous promoters.

Since the first identified enhancer was observed in viral genomes it was conceivable that these transcriptional control elements might be unique to viruses and represent a means that enables them to compete for the host cell transcriptional machinery. However, the discovery and characterization of mammalian cellular enhancer elements within the immunoglobulin (Ig) genes eliminated this possibility (Banerji et al., 1983; Gillies et al., 1983; Neuberger 1983; Mercola et al., 1983). Banerji et al. (1983) showed that a several hundred bp DNA segment derived from the Ig heavy chain locus could enhance expression of a linked β-globin promoter in an orientation and position-independent manner. This effect occurred only when the Ig sequences were present in *cis* and did not depend upon DNA replication. Furthermore, enhancement occurred in three different lymphoid cell lines, but not in mouse 3T6, mink lung, or human HeLa cells. Gillies et al. (1983) concurrently demonstrated that the same DNA segment increased expression of the Igγ2b gene in an orientation and position independent manner, and functioned in lymphoid cells but not in L cells. Thus, the enhancing sequences operated in a tissue-specific manner. Similar results were obtained with the Ig κ gene, which indicated that a tissue-specific transcriptional enhancer element is located within the intron separating the joining (Jκ) and constant (Cκ) regions (Queen and Baltimore, 1983; Stafford and Queen, 1983; Queen and Stafford, 1984; Picard and Shaffner, 1984). The identification of enhancers in cellular genes indicated that enhancers are not transcriptional control elements peculiar to viral genomes.

Previous work from our laboratory demonstrated that the regulatory element responsible for the dramatic inductions in *MnSOD* mRNA was not contained within the 5' flanking region of the gene (Chesrown, 1994). Further work suggested that another region of DNA within the gene might be responsible for the transcriptional regulation by inflammatory mediators (Chesrown, 1994). The main objective of the research presented in this dissertation was to investigate the molecular mechanisms responsible for the dramatic inductions of *MnSOD* expression in response to inflammatory stimuli. The ultimate goal of this study was to characterize the *cis*-element(s) within the gene responsible for the inducibility of *MnSOD*. These results will provide information for future identification of the *trans*-acting factors, and other steps and components involved in the inflammatory pathway of *MnSOD*.

CHAPTER 2
MATERIALS AND METHODS

Materials

Ham's F12K Medium (Cat# N-3520), bovine serum albumin (Cat# A-7511), and dithiothreitol (Cat# D-0632), bacterial lipopolysaccharide (LPS) *E.coli* serotype 055:B5 (Cat#L 2880), amobarbital (Amytal) (Cat#A 4430), 2-heptyl-4-hydroxyquinoline N-oxide (HQNO) (Cat#H 3875), oligomycin (Cat#O 4876), and myxothiazol (Cat#M 5779) were purchased from Sigma Chemical Company, St. Louis, MO. Oligonucleotides, deprotected, desalted, and dephosphorylated, Medium 199 with Earle's salts (Cat#31100-035), fetal bovine serum (Cat# 16000-044), antibiotic-antimycotic solution (ABAM) (Cat#15240-062), restriction enzymes, *Taq* DNA Polymerase (Cat# 18038-018), T4 DNA Ligase (Cat# 15224), DH5α *E. coli* competent cells (Cat# 18265017), and Random Primers DNA Labeling System (Cat# 18187-013) were purchased from Gibco BRL, Gaitherburg, MD. Recombinant human TNF-α was a gift from Genentech. IL-1β was a gift from the National Cancer Institute. Antimycin A (Cat#1782), N-acetyl cysteine (Cat#106425), SB 203580 (559389), and PD 98059 (Cat#513000) were purchased from Calbiochem, San Diego, CA. The I kappa kinase inhibitor, Bay 11-7082, was purchased from BioMol, Plymouth Meeting, PA. (Sigma Corp, St. Louis, MO.). $Vent_R$ DNA Polymerase (Cat# 254S), restriction enzymes, T4 Polynucleotide Kinase (Cat#201S), and calf intestinal alkaline phosphatase (CIP) (Cat#290S) were purchased from New England

Biolabs, Inc., Beverly, MA. Long Ranger Gel Solution (Cat# 50611), and Seakem HGT agarose (Cat# 50040) were purchased from FMC BioProducts, Rockland, ME. Proteinase K (Cat# 161519) and *E. coli* tRNA (Cat# 109541) were purchased from Boehringer-Mannheim, Indianapolis, IN. TA Cloning kit (Cat# K2000) was purchased from Invitrogen Corporation, Carlsbad, CA. pCRScript Cloning kit (Cat# 211188-5) was purchased from Stratagene, La Jolla, CA. Zetabind positively charged nylon transfer membrane (Cat# NM511-01-045SP) was purchased from Cuno, Meriden, CT. Dimethyl sulfate (Cat#18,630-9) amd sodium cacodylate (Cat#23,385-4) were purchased from Aldrich, Milwaukee, WI. Piperidine (Cat# P125-100) was purchased from Fisher Scientific, Pittsburg, PA. QIAquick Nucleotide Removal kit (Cat#28304), QIAquick Gel Extraction kit (Cat#12162), QIAprep Spin Miniprep kit (Cat#27106), Qiagen Plasmid Midi kit (Cat#12144), Qiagen Plasmid Maxi kit (Cat# 12162) were obtained from Qiagen, Valencia, CA. Hyperfilm MP (Cat# RNP 1677K, Cat#RNP30H), Ultrapure dNTP Set (Cat# 27-2035-01), and adenosine 5'-triphosphate (Cat#27-1006-01) were purchased from Amersham-Pharmacia, Piscataway, NJ. [α-^{32}P]dATP (3,000 Ci (111TBq)/mmol) (Cat# BLU013H) and [γ-^{32}P]ATP (3,000 Ci (111TBq)/mmol) (Cat#BLU002A) were purchased from New England Nuclear (NEN) Life Sciences Products, Boston, MA. Cell lines rat pulmonary epithelial-like L2 (Cat# ATCC CCL 149) was purchased from American Type Culture Collection, Manassas, VA. pϕGH and pTKGH were obtained as a kit (Cat# 40-2205) from Nichols Institute Diagnostics, San Juan Capistrano, CA. All other chemicals not mentioned were obtained through either Sigma Chemical Co. or Fisher Scientific.

Methods

Tissue Culture

The cell lines used in the studies described in this thesis were: L2 rat pulmonary epithelial-like cells (ATCC CCL 149), rat pulmonary artery endothelial cells, VA cells, isolated from segments of pulmonary artery by mechanical methods (Visner et al., 1992), and, mouse fibroblast antimycin-resistant mutant cells, LA9 cells (generously provided by Dr. Neil Howell, Howell et al., 1983). All cells were cultured as adherent monolayers. The L2 rat pulmonary epithelial-like cell line (ATCC CCL 149) was grown as a monolayer in 150 mm tissue culture plates containing Ham's modified F12K medium (GIBCO) supplemented with 10% fetal bovine serum, 10 μg/ml penicillin G, 0.1 mg/ml streptomycin, and 0.25 μg/ml amphotericin B at 37°C in humidified air with 5% CO_2. If cells were used for *in vivo* footprinting experiments, then at approximately 90% confluence, cells were treated with 0.5 μg/ml Escherischia coli (*E. coli*) LPS (*E.coli* serotype 055:B5, Sigma), 10 ng/ml TNF-α (kindly provided by the Genentech Corp.), or 2 ng/ml IL-1β (kindly provided by the National Cancer Institute) for 2 or 4 hours to induce MnSOD gene expression. Untreated cells were used as controls. VA cells, a rat pulmonary artery endothelial cell line, were grown in Medium 199 with Earle's salts (Sigma Corp., St. Louis, MO.) with sodium bicarbonate to pH 7.4, 10% fetal bovine serum, 10 mM L-glutamine and antibiotic-antimycotic solution at 37° C in room air, 5% CO_2. LA9 cells, a mouse fibroblast antimycin-resistant mutant cell line (Howell et al., 1983), were grown in Ham's F12K media with 10% fetal bovine serum, 10 mM L-glutamine, and antibiotic-antimycotic solution at 37° C in room air, 5% CO_2.

Experiments with VA cells and LA9 cells were all performed with confluent 100 mm tissue culture plates.

Polymerase Chain Reaction (PCR)

The PCR reaction contained: DNA template (10-20 ng), 20 mM Tris-HCl pH 8.0, 50 mM KCl, 1.5 mM $MgCl_2$, 0.2 mM of each dNTP, 100 pmol of each oligonucleotide primer (oligonucleotide primers for PCR were obtained deprotected, desalted, and dephosphorylated) in a total volume of 99.5 µl covered with 60 µl of mineral oil. This mixture was heated for 5 minutes to allow denaturation of the template and 0.5 µl (2.5 U) of Taq DNA Polymerase were added after 3 minutes of this time. The PCR was run in a Perkin Elmer 480 thermocycler (Perkin Elmer Corporation, Norwalk, CT) for 25 cycles, 1 minute and 30 seconds at 94°C for denaturation, 30 seconds at 55-65°C for annealing, and 1 minute at 72°C for extension. After 25 cycles, samples were incubated at 72°C for 10 minutes to allow complete extension and addition of an extra deoxyadenosine nucleotide in each fragment by Taq DNA polymerase and refrigerated at 4°C. Mineral oil was extracted by the addition of 120 µl of chloroform:isoamyl alcohol (IAA), vortexing, and centrifugation for 5 minutes at 13,000 × g at room temperature. The aqueous phase was transferred to a new tube and 10 µl of the PCR reaction plus 1/6 volume of bromophenol blue/xylene cyanol/Ficoll mixture was loaded on a 1-2% Seakem HGT agarose gel containing ethidium bromide (0.1 mg/ml), 40 mM Tris-acetate, 20 mM acetic acid, 1 mM EDTA and run with TAE buffer for 40-60 minutes at 80-100 volts.

The DNA templates for the PCR used to produce the *MnSOD* genomic fragments in the enhancer deletion analyses were plasmids containing restriction-digested fragments from the original genomic clones (Dougall, 1990).

TA Cloning of PCR Products

Taq DNA polymerase has a nontemplate-dependent activity, which adds a single deoxyadenosine (A) to the 3' ends of PCR products. The linearized vector, pCR2.1, supplied in the TA Cloning kit (Invitrogen, Carlsbad, CA), has a single 3' deoxythymidine (T) residue. This allows PCR inserts to ligate efficiently with those vectors. To ligate the PCR product in the TA cloning vector, 1 µl of fresh PCR reaction was incubated with 2 µl of the pCR2.1 vector (50 ng in 10 mM Tris-HCl, 1 mM EDTA, pH 7.5), 1 µl of 10X T4 DNA ligase buffer (60 mM Tris-HCl, pH 7.5, 60 mM $MgCl_2$, 50 mM NaCl, 1 mg/ml bovine serum albumin, 70 mM β-mercaptoethanol, 1 mM ATP, 20 mM dithithreitol, 10 mM spermidine), 5 µl of sterile ddH_2O, and 1 µl of T4 DNA ligase (4 U) for 16 hours at 16°C.

Two µl of the ligation reaction were used to transform 50 ml of *E. coli* competent cells, INVαF' strain, in the presence of 2 ml of 0.5 M β-mercaptoethanol, for 30 minutes, on ice. The transformation reaction was then heat shocked for 45 seconds at 42°C and 450 µl of SOC medium (2% tryptone, 0.5% yeast extract, 10 mM NaCl, 2.5 mM KCl, 10 mM $MgCl_2$, 20 mM glucose, pH 7.0) were added. This mixture was incubated at 37°C for one hour in a rotary shaker at 225 rpm. After this time, 100 µl of the bacteria solution were plated using a glass spreader on YT (1.6% bacto-tryptone, 1% yeast extract, 0.5% NaCl, pH 7.0) agar plate (1.5% Bacto-agar added), supplemented with 50 µg/ml of ampicillin and covered with 20 µl of 5-Bromo-4-Chloro-3-indolyl-β-D-galactoside (X-gal) (40 mg/ml), and incubated at 37°C overnight. X-gal is a substrate for β-galactosidase, and when this gene is present in the vector, β-galactosidase metabolizes X-gal, a blue product is formed and the colony becomes blue. If an insert is present in the

plasmid, the β-galactosidase gene is disrupted, X-gal is not metabolized, and the colony remains white.

Reporter Vector Cloning

A 4.5 kb EcoR I/Eag I fragment of 5' non-coding sequence was isolated from the 17 kb *MnSOD* genomic clone (Figure 3-1) and the 5' overhang ends filled in using the large fragment of E. coli DNA polymerase I (Klenow fragment). The resulting blunt-end Eco/Eag fragment was cloned into the Hinc II polylinker site in a promoterless, pUC 12-based human growth hormone expression vector, pØGH, (Selden et al., 1986), creating a 9.3 kb plasmid referred to as Eco/E GH (Figure 3-10). The unique restriction enzyme site, *Hind*III, was utilized to delete a 2.0 Kb portion of the *MnSOD* Eco/E sequence, creating the vector, Hind/E (Kuo et al., 1999, Figure 3-10). To test for non-specific effects of the inflammatory mediators on hGH expression, we used an hGH expression vector that contained the herpes simplex thymidine kinase minimal promoter, pTKGH (Selden et al., 1986).

To identify possible regulatory elements in the remainder of *MnSOD* that might interact with the 5' promoter, we cloned an internal 6.1 kb Hind III fragment (+1180 to +7312) from the rat genomic clone into the *Hind*III site of the Hind/E GH vector, creating a 13.45 kb vector (Figure 3-1). The same Hind III fragment was cloned into Hind/E GH in the opposite orientation. To begin to localize observed enhancer effects, we removed the Hind III/Hpa I fragment (+1180 to +5046) and the Hpa I/Hind III fragment (+5046 to +7312) from the Hind III fragment in both orientations creating enhancer deletions of 3.8 Kb or 2.3 Kb in the Hind/E GH construct (Figure 3-3). To clarify the position of the enhancer within the 3.8 kb fragment, serial 3' and 5' deletions of the area were performed

by creating PCR products (Figure 3-3) which were subsequently cloned into the Hind/E GH vector at the *Hind*III site or *Nde*I site. Oligonucleotides flanking the regions of interest were designed containing either *Hind*III or *Nde*I sites for convenient ligation into the restriction sites. To test whether the enhancer activity was specific to the MnSOD promoter, we used the plasmid, TKGH, which contains a heterologous, TATA-containing, non-GC-rich promoter. The 6.1 kb Hind III *MnSOD* genomic fragment (+1180 to +7312) was cloned into the *Hind*III site (Figure 3-9) in the TKGH polylinker in both orientations. To evaluate the interaction of the promoter with the enhancer fragment, the 919 bp (Figure 3-3) fragment of *MnSOD* containing the entire enhancer region was ligated into the *Nde*I site of the promoter deletion constructs (Figure 3-10).

Comparison of the rat enhancer sequence with the analogous region in human *MnSOD* revealed a high degree of homology in intron 2. PCR amplification of a 466 bp fragment (+2410 to +2875, human manganese SOD, accession S77127) from human genomic DNA with primers, 5' CGTTAGTGGTTTGCACAAGGAAGATAATCG 3' and 5' GGCTCTGATTCCACAAGTAAAGGACTG 3', to create a fragment, which was inserted into *Nde*I site of the TKGH vector in both orientations.

Plasmid Purification

For small scale plasmid isolation the QIAprep Spin miniprep from Qiagen was used. A single bacterial colony from YT agar plates with ampicillin was used to inoculate 5 ml of YT media (1.6% bacto-tryptone, 1% yeast extract, 0.5% NaCl, pH 7.0) supplemented with 50 μg/ml of ampicillin and grown overnight at 37°C in a rotary water bath shaker. Plasmids were extracted using the QIAprep Spin Miniprep kit following the manufacturer's protocol. Bacteria from 1.5 ml of YT culture were collected by

centrifugation at 13,000 × g for 5 minutes, resuspended in 250 µl of resuspension buffer (50 mM Tris-HCl, pH 8.0, 10 mM EDTA, 100 µg/ml RNase), lysed with 250 µl of lysis buffer (200 mM NaOH, 1% SDS), neutralized and adjusted to high-salt binding conditions with 350 µl of neutralization buffer (3 M potassium acetate, pH 5.5), and centrifuged for 10 minutes at 13,000 × g, at 4°C. The supernatant was applied to a QIAprep silica-gel membrane column. A vacuum manifold was used for the following steps. First, the supernatant was drawn through the column using the vacuum manifold. The column was washed once with 500 µl wash buffer (10 mM Tris-HCl, 80 % ethanol) containing chaotrophic salts and once with 750 µl wash buffer (10 mM Tris-HCl, 80 % ethanol). The column was then centrifuged at 13,000 × g for 2 minutes at room temperature. The plasmid DNA was eluted from the column with addition of 100 µl of TE buffer (50 mM Tris-HCl, pH 8.0, 10 mM EDTA), and centrifugation at 13,000 × g for one minute at room temperature into a clean, DNase-free eppendorf tube.

For large, scale plasmid isolation a QIAGEN plasmid maxi kit was used. One ml of a single colony overnight liquid culture (5 ml YT/ampicillin) was inoculated in 50 ml (high copy plasmid) of YT media supplemented with 50 µg/ml of ampicillin, and grown overnight at 37°C in a rotary water bath shaker. Bacteria were collected by centrifugation (4,000 × g, 15 minutes, 4°C), pellets were resuspended in 10 ml of resuspension buffer (50 mM Tris-HCl, pH 8.0, 10 mM EDTA, 100 µg/ml RNase), lysed with 10 ml of lysis buffer (200 mM NaOH, 1% SDS) and incubated for 5 minutes at room temperature, neutralized by addition of chilled (4°C) neutralization buffer (3 M potassium acetate, pH 5.5), incubated on ice for 20 minutes, and centrifuged at 16,000 × g for 30 minutes at 4°C. The supernatant was removed from the centrifugation tube with a sterile transfer

pipette and allowed to flow through by gravity on a QIAGEN-tip 500 column, that had been previously equilibrated with 10 ml of equilibration buffer (750 mM NaCl, 50 mM MOPS, pH 7.0, 15% isopropanol, 0.15% Triton X-100). The flow-through was discarded and the column was washed twice with 30 ml of wash buffer (1 M NaCl, 50 mM 3-(N-morholino)propane sulfonic acid (MOPS), pH 7.0, 15% isopropanol) by gravity flow. Plasmid DNA was eluted from the column with 15 ml of elution buffer (1.25 M NaCl, 50 mM Tris-HCl, pH 8.5, 15% isopropanol). The DNA present in the eluate was precipitated with 0.7 volumes (10.5 ml) of isopropanol, and collected by centrifugation (16,000 × g, 30 minutes, 4°C). The pellet was washed once with 5 ml of 70% ethanol and centrifugation was repeated (16,000 × g, 30 minutes, 4°C). The final pellet was resuspended in 300-500 µl of TE buffer.

Plasmid DNA concentration was estimated by measuring the absorbance at 260 nm in a Beckman DU-64 Spectrophotometer (Beckman Instruments, Inc., Fullerton, CA), of water dilutions (1:50) from each sample. An absorbance of 1 at 260 nm corresponds to 50 mg of double-stranded DNA. The ratio between the readings taken at 260 nm and 280 nm (A_{260}/A_{280}) provided an estimate of DNA purity (1.5-2.0). Typical yield depended on the size of the plasmid, but ranged from 20-50 µg of plasmid DNA for QIAprep Spin minipreps and 400-800 µg for maxi-size preparations.

Transient Transfection of Mammalian Cells

L2 cells, a rat pulmonary epithelial-like cell line (ATCC CCL 149), were grown in Ham's modified F12K medium (GIBCO) with 10% fetal bovine serum (Flow Laboratories), ABAM (penicillin G 100 U/ml, streptomycin 0.1 mg/ml, amphotericin B 0.25 mg/ml (Sigma) and 4 mM glutamine at 37°C in room air, 5% CO_2. To control for

transfection efficiency, transfections were carried out using a batch transfection method. Cells were grown as monolayers on 150 mm tissue culture plates until 70-90% confluent. The cells were transfected with 10 mg of each expression vector using the DEAE-dextran method (Kriegler et al., 1990). After 24 h, cells from each 150 mm, batch transfected plate were trypsinized, pooled, and plated onto four separate 100 mm tissue culture plates. Inflammatory mediators were added to the medium of each plate 24 h later with final concentrations of 0.5 μg/ml Escherichia coli lipopolysaccharide (LPS, E. coli serotype 055:B5, Sigma), 10 ng/ml TNF-α, or 2 ng/ml IL-1β. Twenty-four hours later, total RNA was isolated from the cell monolayers for northern analysis.

RNA Isolation

Total cellular RNA was isolated according to the procedure described by Chomczynski and Sacchi (1987) with modifications (Visner et al, 1990). Briefly, the monolayer cells (L2 cells or VA cells), cultured as noted above, were washed once with room temperature PBS, and then 3 ml/100 mm tissue culture plate of guanidinium thiocyanate solution (4 M guanidinium thiocyanate, 25 mM sodium citrate pH 7.0, 0.5% sarcosyl, and 0.1 M 2-mercaptoethanol) were added. The homogenate was collected in a 15 ml conical polypropylene tube and extracted with 0.1 volume of 2 M sodium acetate pH 4.0, and an equal volume of water-saturated phenol. This suspension was mixed together and cooled on ice for at least 15 minutes. Before centrifugation at 3,000 × g for 20 minutes at 4°C, 0.22 volumes of chloroform/isoamyl alcohol (IAA) (49:1) were added and the mixture was shaken vigorously for 20 seconds. After centrifugation, the aqueous phase was transferred to a fresh centrifugation tube and mixed with an equal volume of isopropanol. This solution was placed at –20°C for at least 1 hour and then centrifuged at

10, 000 × g for 25 minutes at 4°C. The RNA pellet was resuspended in 500 µl of guanidinium thiocyanate solution and transferred to a 1.5 ml microfuge tube. An equal volume of isopropanol was added and the mixture was incubated for at least an hour at –20°C. RNA was collected by centrifugation at 10, 000 × g for 10 minutes at 4°C, and 400 µl of DEPC-treated water was added to the pellet and incubated at 50°C for 15 minutes. The RNA was precipitated with 0.1 volume of DEPC-treated 3 M sodium acetate pH 5.2, and 2.2 volumes of 100% ethanol, followed by incubation at –20°C for at least an hour. The RNA was collected again by centrifugation, resuspended in 300 µl of DEPC-treated water and ethanol precipitated one more time. The final pellet was dried in a Savant speed-vacuum centrifuge to remove any trace amounts of ethanol, and then resuspended in DEPC-treated water.

RNA concentration was estimated by measuring the absorbance at 260 nm in a Beckman DU-64 Spectrophotometer (Beckman Instruments, Inc., Fullerton, CA), of two water dilutions (1:20) from each sample. An absorbance of 1 at 260 nm corresponds to 40 µg of RNA. The ratio between the readings taken at 260 nm and 280 nm (A_{260}/A_{280}) provided an indication of RNA purity (1.5-2.0). Typical RNA yield for L2 cells or VA cells was 80-150 µg per 70-100% confluent 100 mm tissue culture plate.

Northern Analysis

RNA was size-fractionated for 16 hours at 40 volts on a 1% Seakem HGT agarose gel containing 6.6% formaldehyde, 40 mM MOPS pH 7.0, 10 mM sodium acetate pH 7.4, and 1 mM EDTA pH 8.0 with constant buffer recirculation. For each lane of the gel, twenty µg of total RNA were dried and resuspended in 30 ml of 12.5 M formamide, 6.6% formaldehyde, 6 mM sodium acetate pH 7.4, 0.5 mM EDTA pH 8.0, 20 mM 3-(N-

morholino)propane sulfonic acid (MOPS) pH 7.0. This RNA was dissolved and heated by incubations for 10 minutes at 50°C, then for 10 minutes at 65°C. A 5 µl aliquot of loading dye (0.4% xylene cyanol FF, 0.4% bromophenol blue, 1 mM EDTA pH 8.0, 50% glycerol, 0.3 µg/µl ethidium bromide) was added prior to loading the gel. To confirm that equal amounts of RNA had been loaded into each lane, after electrophoresis, each gel was photographed under UV light and the level of ribosomal RNA assessed by the ethidium bromide staining. Ethidium bromide was present in the loading dye and RNA could be visualized promptly under UV light after electrophoresis. The gel was then treated for 30 minutes with 50 mM NaOH, 30 minutes with 100 mM Tris-HCl pH 7.0, and twice for 25 minutes with 50 mM TBE (10 mM Tris-HCl, pH 8.0, 1 mM EDTA, pH 8.0). The RNA was electo-transferred to a positively-charged nylon membrane in 40 mM TBE for 75 minutes and then covalently cross-linked to the membrane with UV light (Church and Gilbert, 1984).

Genomic DNA Isolation

For genomic DNA isolation, L2 cells were grown in 15 cm tissue culture plates until 70-90% confluent, washed once with PBS and lysed with 3 ml lysis solution (50 mM Tris-HCl, pH 8.5, 25 mM EDTA, pH 8.0, 50 mM NaCl, 0.5% SDS, 300 µg/ml Proteinase K). The lysate was incubated overnight on a rocking platform at room temperature. After this incubation, the lysate was then extracted once with equal volume of Tris-equilibrated phenol for at least 1 hour at room temperature on a rocking platform. The phases were separated by centrifugation at 3,000 × g for 20 minutes at room temperature. The upper aqueous phase was transferred with a sterile large-bore, transfer pipette to a new tube. Then the lysate was extracted once with an equal volume of

phenol/chloroform:isoamyl alcohol (IAA) (50/49:1) and once with chloroform:IAA, with incubations of at least one hour at room temperature on a rocking platform, and centrifugations at 3,000 × g for 20 minutes at room temperature to separate the phases. After separation of the phases in the cholorform:IAA extraction, 2.5 ml of RNase A (750 U/ml) was added to the lysate, for digestion of contaminant RNA, and the mixture was incubated overnight at room temperture on a rocking platform. The lysate was extracted again, once with phenol/chloroform:IAA, and once with chloroform:IAA, as above. DNA was precipitated from the aqueous phase by addition of 120 µl 5M NaCl to final concentration of 0.2 M and 2.5 volumes (7.5 ml) of ice-cold 100% ethanol. The cotton-like DNA was collected with a sealed bent glass Pasteur pipette, washed by rinsing the DNA with 2 ml of chilled (4°C) 80% ethanol and resuspended in 300 µl of TE buffer (10 mM Tris-HCl, pH 8.0, 1 mM EDTA, pH 8.0).

Electrophoretic Mobility Shift Assay (EMSA)

EMSA were performed as previously described (Fried and Crothers, 1981) with 8 mg nuclear extract prepared from control and LPS, TNF-α, or IL-1β-treated L2 cells by high salt extraction (Andrews and Faller, 1991). Binding reactions were carried out at room temperature in 10 mM HEPES (N-[2-Hydroxyethyl]piperazine-N'-[2-ethanesulfonic acid])-KOH, pH 7.9, 100 mM KCl, 1mM dithiothreitol, 0.5 mM $MgCl_2$, 0.1 mM EDTA and 8.5% glycerol to yield a final volume of 20 µl. EMSA probes were made from cloned PCR products of the defined enhancer region between 4130 and 4491 and end-labeled by filling the recessed 3' termini of *Eco*RI digested fragments with ^{32}P-dATP using the large fragment of *E. coli* DNA polymerase I (Klenow fragment). Fragments used in EMSAs were 143 bp (+4348 to +4491), 143 bp (+4231 to +4374), 100

bp (+4231 to +4331), 95 bp (+4331 to +4426), and 103 bp (+4426 to +4529). Numbers shown in parentheses refer to sequence in the rat *MnSOD* gene (accession X56600).

***In Vivo* DMS Treatment**

L2 cells were cultured as described above in 150 mm tissue culture plates. The medium was removed by aspiration and the cells washed once with room temperature phosphate buffered saline (PBS, 10 mM sodium phosphate, pH 7.4 and 150 mM NaCl). The PBS buffer was removed and replaced with room temperature PBS containing 0.25%-0.5% demethyl sulfate (DMS, Aldrich) for 1-2 min. The PBS containing DMS was rapidly removed (30-60 seconds), and the cell monolayer washed twice with 4°C PBS to quench the DMS reaction. The cells were lysed in 5 ml of lysis solution (50 mM Tris pH 8.5, 25 mM EDTA pH 8.0, 50 mM NaCl, 0.5% SDS, 300 μg/ml Proteinase K) followed by incubation overnight at room temperature on a rocking platform. Genomic DNA was then purified by phenol/chloroform extractions. Each sample was extracted once with an equal volume of Tris-equilibrated phenol, followed by two extractions with a 24:24:1 (v/v/v) mixture of Tris-equilibrated phenol/chloroform/isoamyl alcohol, and finally by one extraction with a 24:1 (v/v) mixture of chloroform/isoamyl alcohol. Each extraction was performed for at least an hour on a rocking platform prior to collection of aqueous phase. The aqueous phase was collected each time by centrifugation at 14, 000 × g for 10 minutes at room temperature and ethanol precipitated. Samples were then treated with 100 μg/ml RNase A, organic extracted as above, ethanol precipitated and suspended in TE (10 mM Tris pH 8.0 and 1 mM EDTA). The DNA samples were digested with BamH I restriction endonuclease enzyme, and strand cleavage at modified guanine residues was achieved by treatment with 1 M piperidine (Fisher Scientific) at

90°C for 30 minutes. Naked genomic DNA was isolated and purified from cells without any DMS treatment and digested with restriction endonuclease enzyme, *BamHI* (New England Biolabs).

As a control, genomic DNA was extracted in the same way from cells incubated in Ham's F12K medium for 2 or 4 hours, but not treated with DMS. One hundred μg of this "naked" DNA was restriction digested with *BamHI*. After digestion, DNA was extracted once with pheno/chloroform:IAA, once with chloroform:IAA, and ethanol precipitated with 2.5 volumes of 100% ethanol and 2.5 M ammonium acetate incubating at –70°C for 30 minutes. DNA was collected by centrifugation at 16,000 × g for 30 minutes at 4°C, and washed twice with 80% ethanol and centrifugation at 16,000 × g for 30 minutes at 4°C. After lyophilizing, the pellet DNA was resuspended in 10 μl of sterile water. The *in vitro* DMS treatment of the naked DNA recovered from digestion of *BamHI* was done as described by Maxam and Gilbert (1980) with some modification. Naked DNA (100 μg) in 10 μl of water was added to 190 μl of DMS buffer (50 mM sodium cacodylate, 0.1 M EDTA, pH 8.0), treated for 30 seconds with 0.5 μl (0.25%) of DMS, and immediately precipitated with addition of 7.5 M ammonium acetate to the final concentration of 2.5 M, 14 μg of E. coli tRNA, and 2.5 volumes of 100% ice-cold ethanol. After incubation in a dry ice/ethanol bath for at least 5 minutes, DNA was collected by centrifugation at 13,000 × g for 30 minutes at 4°C, resuspended in 250 μl of common reagent (2.5 M ammonium acetate, 0.1 mM EDTA, pH 8.0), and precipitated again by addition of 14 μg of tRNA and 750 μl of ice-cold 100% ethanol. After incubation for 5 minutes in the dry ice/ethanol bath, DNA was collected by centrifugation at 13,000 × g, for 30 minutes at 4°C and washed twice with 80% ethanol with

centrifugation as above. After lyophilization, the final DNA pellet was resuspended in 90 µl of sterile water.

Once the DMS-modified DNA (both *in vivo*- and *in vitro*-treated samples) were precipitated and redissolved in water (approximately 70 mg in 90 ml of sterile water) as described, the DNA was mixed with 10 ml of piperidine (10 M) and incubated at 90°C for 30 minutes to cleave the DNA at the modified guanine residues (Maxam and Gilbert, 1980). DNA was then ethanol precipitated, collected by centrifugation at 13,000 × g at 4°C for 30 minutes, washed twice with 80% ethanol, lyophilized, and then resuspended and lyophilized three more times in 500 µl of sterile water. After the last lyophilization, DNA was resuspended in 20 µl of TE buffer.

Ligation-Mediated PCR (LMPCR)

LMPCR was begun by annealing 3 pmol of primer 1 to 3 µg of DMS-modified and piperidine cleaved DNA for each sample in 1 X Vent polymerase buffer (10 mM KCl, 10 mM $(NH_4)_2SO_4$, 20 mM Tris-HCl (pH 8.8), 2 mM $MgSO_4$, 0.1% Triton X-100), in a total volume of 15 ml, with denaturation at 95°C for 10 minutes followed by primer annealing at 45°C for 30 minutes. Primer 1 is the primer for the known site of the cleaved DNA and is a synthetic single stranded oligonucleotide. The first strand primers utilized for bottom strand, 5'-GGATAACTTTGGGGAGTTGGTTC-3' and 5'-GAATAATGTTAGCCGTGTCTCTGGG-3', as well as for the top strand, 5'-CCAACCTTTGGGTTCTCCAC-3'. The first strand synthesis was performed in 1 X Vent polymerase buffer with 4 mM $MgSO_4$, 0.25 mM of each dNTP, and 2 U of Vent DNA polymerase. The samples were incubated for 1 minute each at 53°C, 55 °C, 57 °C,

60 °C, 62 °C, 64 °C, 68 °C, followed by incubations for 3 minutes each at 72°C (Hornstra and Yang, 1993). Separate primer 1 for top and bottom DNA sequence were designed.

Following the first strand synthesis, a common linker was ligated to the double-stranded DMS-piperidine cleaved fragment. The linker sequences used were the same as published by Mueller and Wold (1989). The double-stranded linker is composed of two synthesized, dephosphorylated complementary oligonucleotides, a 25-mer oligonucleotide (5'-GCGGTGACCCGGGACATCTGAATT-3') annealed to an 11-mer oligonucleotide (5'-GAATTCAGATC-3'). The double stranded linker (20 pmol/ml) was prepared from these oligonucleotides by mixing 2 nmol each in 250 mM Tris-HCl, pH 7.7 (total volume of 100 ml), and heating to 95°C for 10 minutes followed by gradual cooling down to 4°C for 3 hours, in a thermocycler (Perkin Elmer 480, Applied Biosciences PE, Norwalk, CT) and incubation at 4°C overnight. After the primer extension step with primer 1, 20 µl of 4°C solution containing 50 mM dithiothreitol, 18 mM $MgCl_2$, 0.125 µg/µl nonacetylated BSA (Sigma Cat#A-7511), and 110 mM Tris-HCl, pH 7.5 (Garrity and Wold, 1992) were added, followed by addition of 25 ml of a 4°C ligation solution containing 20 mM dithithreitol, 10 mM $MgCl_2$, 0.05 µg/µl nonacetylated BSA, 3 mM ATP, 4 pmol of annealed common linker, and 4 U of T4 DNA ligase (Garrity and Wold, 1992). Ligation was performed at 16°C overnight. The T4 DNA ligase and the Vent polymerase were removed by one extraction with an equal volume of phenol/chloroform:IAA and one extraction with an equal volume of chloroform:IAA. DNA was precipitated by the addition of 7.5 M ammonium acetate to a final concentration of 2.5 M, 14 µg of tRNA, and 2.5 volumes of 100% ethanol and incubation at –70°C for 30 minutes. After precipitation, the DNA was collected by

centrifugation (13,000 × g, 30 minutes, 4°C), washed once with 80 % ethanol, and again DNA collected after centrifugation (13,000 × g, 30 minutes, 4°C), lyophilized, and resuspended in 20 ml of sterile water.

After ligation of the linker, the nested set of linear genomic DNA fragments from the region of interest were amplified by PCR using a second gene-specific oligonucleotide primer, termed primer 2 (5'-GGGGAGTTGGTTCTCTCCTTTCACTG-3' and 5'-GCCGTGTCTCTGGGTTAGCTGTATTGC-3', respectively for bottom strands and 5'-CCAACCTTTGGGTTCTCCAC-3' for the top strand, as well as the complementary primer to the 25-mer linker-primer (5'-CGCCACTGGGCCCTCTAGACTTAAG-3'). PCR conditions were the same for both DNA strands and sets of primers, as described by Hornstra and Yang (1993) with some modifications. Freshly prepared Taq DNA polymerase mix (79.4 µl) containing 1 x Taq DNA polymerase buffer (1 x 20 mM Tris-HCl, pH 8.4, 50 mM KCl, 1.75 mM $MgCl_2$, 0.25 mM each dNTP, 15 pmol primer 2, and 10 pmol 25-mer complementary linker primer were added to the common linker-ligated DNA samples. Samples were initially heated to 95°C for 5 minutes and 0.6 µl (3 U) of Taq DNA polymerase was added after the first two minutes of this period. The annealing temperatures (53-65°C) were determined experimentally to establish the conditions that yielded the best results. Samples were denatured at 95°C for 1 minute, annealed at 58°C for 2 minutes, and extended at 76°C for 3 minutes. Samples were denatured, annealed and extended in this manner for 25 cycles. In addition, with each cycle of PCR amplification, the extension time was increased by 5 seconds. After 25 cycles, samples were kept at 76°C and 5 ml of a fresh PCR incubation solution containing 2.5 mM each dNTP, 1.75 mM $MgCl_2$, 1 X

Taq DNA polymerase buffer, and 1 U of Taq DNA polymerase was added. Samples were then incubated at 76°C for 30 minutes to ensure full extension of each template strand and addition of a single deoxyadenosine nucleotide to the end of every fragment. After this incubation, samples were placed on ice, and 1 ml of 0.5 M EDTA was added to stop the reaction. The DNA was precipitated by addition of 7.5 M ammonium acetate to a final concentration of 2.5 M, 14 μg of tRNA, and 2.5 volumes of 100% ethanol, and incubation at –70°C for 30 minutes. DNA was collected by centrifugation (13,000 × g, 4°C, 30 minutes), washed twice with 80% ethanol and collected again by centrifugation (13,000 × g, 4°C, 30 minutes), lyophilized, and resuspended in 20 μl of water.

Following LMPCR amplification of the genomic DNA fragments from the region of interest, the "footprint" is visualized by genomic sequencing (Church and Gilbert, 1984). For this protocol, a 2 μl aliquot of each LMPCR sample is dried in a vacuum concentrator and redissolved in 2 μl of formamide-dye solution (98% formamide, 0.025% xylene cyanol, 0.025% bromophenol blue, and 0.5X TBE (44.5 mM Tris-base, 44.5 mM boric acid, 1 mM $Na_2EDTA\ 2H_2O$). Samples were then loaded onto a 8.3 M urea, 5% Long Ranger polyacrylamide, TBE (89 mM Tris-base, 89 mM boric acid, 2 mM EDTA) DNA sequencing gel (60 centimeters long), and size-fractionated, with TBE (89 mM Tris-base, 89 mM boric acid, 2 mM EDTA) as tank buffer, at 120 W for 4-5 hours. The PCR fragments were then electro-transferred as described in Hornstra and Yang (1993), in an electro-transfer apparatus (Harvard Biolabs, Sommerville, MA), using 40 mM TBE (40 mM Tris-base, 33.8 mM boric acid, 0.4 mM EDTA, pH 8.3) as transfer buffer, for 45 minutes, at 110 V, 2 A, to a Zetabind positively charged nylon membrane (Cuno, Meriden, CT), with UV crosslinking (Church and Gilbert, 1984). The resulting

membrane containing the electro-transferred DNA was then hybridized with a ^{32}P-radio-labeled oligonucleotide positioned internal to primer 2, called primer 3. The oligonucleotide was ^{32}P-radio-labeled as described above for oligonucleotide probes and separated from the free radiolabeled-nucleotide using the QIAquick Nucleotide Removal kit from Qiagen as follows. The T4 polynucleotide kinase labeling reaction was added to 10 volumes of Qiagen PN buffer in the kit and passed through a QIAquick column. Bound DNA was washed twice with a buffer containing 80% ethanol and eluted with 100 µl of TE buffer. The resulting autoradiograph of this preliminary gel was used as a loading control to obtain data for more adequate loading of the final gel in which the amount of each sample loaded was adjusted to obtain equal signal intensity in all lanes, and the final gel was run, in the same way, but with only two samples of each treatment.

Site-Directed Mutagenesis and Substitutions by PCR

The technique of mutagenesis by overlap extension or site-directed mutagenesis using PCR has been previously described (Ho et al., 1989). The method employs PCR as a means of creating altered DNA fragments from cloned DNA in a vector with essentially 100% efficiency and in very few steps. Two inside primers (Primer 2 and Primer 3) are designed for each mutation. For base mutation, the inside primers are mismatched to the target sequence at the mutated base. Two PCR reactions (Figure 2-1), performed as described, were run to generate the two overlapping products, one reaction using primer 3 (P3) and the 3' primer (P4) used to amplify the original wild-type 360 bp construct, and the other reaction using primer 2 (P2) and the 5' primer (P1) used to amplify the original wild-type 360 bp construct. The PCR amplicons were agarose gel-purified using the

QIAquick Gel Extraction kit to remove the original PCR primers which might interfere with the subsequent reaction. Because the mutagenesis primers are complementary to

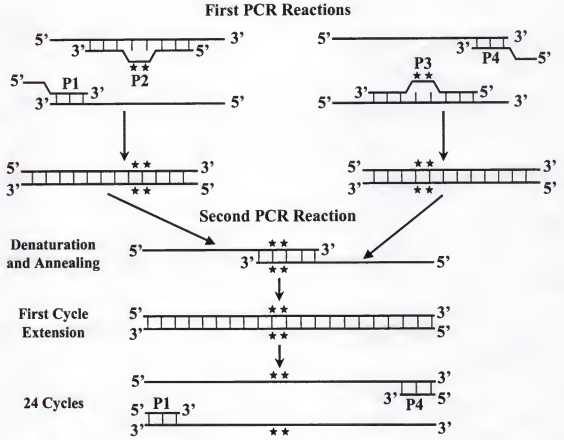

Figure 2-1. Schematic representation of PCR-based mutagenesis.

each other, the two overlapping fragments can be fused in a subsequent extension reaction. The overlapping gel-purified products (approx. 20 ng) were used as DNA templates for a second PCR reaction and the PCR reaction conditions were the same as described previously, using the 5' (P1) and 3' (P4) primers used to amplify the original wild-type 360 bp *MnSOD* enhancer fragment, which contains *Nde*I sites at both ends. In the first round of denaturation/annealing/extension of the second PCR reaction, the two PCR reaction products used as templates, which are the two overlapping parts of the final amplicon, were denatured and annealed to each other, forming the two possible heteroduplex products, with recessed 3' ends, that were subsequently extended by Vent DNA polymerase to produce a product that was the sum of the two overlapping products and containing the mutation. This product became the template for the second PCR reaction and it was amplified by 25 cycles of denaturation/annealing/extension, resulting in multiple copies of the full-length product containing the mutation.

The PCR product was cloned with the use of the PCR Script Cloning System (Stratagene), and positive colonies were identified by the presence of a 360 bp restriction fragment when the vector was digested with *Nde*I. The digested fragment was agarose gel purified using QIAquick Gel Extraction kit, and the isolated DNA fragment was cloned into the NdeI site of a linearized CIP-treated hGH vector containing the minimal *MnSOD* promoter (Kuo, unpublished data). The directionality of the mutagenized enhancer fragment was checked by PCR using primers specific to the enhancer fragment and a primer specific to the vector. Directionality and mutations were also checked by direct DNA sequencing. The final reporter gene plasmids containing these site-directed

mutant PCR fragments were grown in 50 ml DN5α *E. coli*, isolated with a Qiagen Plasmid Maxi kit and then used for transient transfections in L2 cells, as described above.

Radiolabeled Probe Synthesis

For radiolabel hybridization of UV-crosslinked RNA on positively-charged, nylon membranes, the cDNA (MnSOD, hGH, or Cathepsin B) was radio-labeled using a random primer DNA labeling system (Gibco BRL, Gaithersburg, MD) as follows. 100-500 ng of DNA in 17 μl of ddH2O were boiled for 5 minutes and 15 μl of the random primers-buffer solution (0.67 M HEPES, 0.17 M Tris-HCl, 17 mM $MgCl_2$, 33 mM 2-mercaptoethanol, 1.33 mg/ml BSA, 18 OD_{260} units/ml oligodeoxyribonucleotide primers (hexamers), pH 6.8) were added together with 2 μl of each dCTP, dTTP, and dGTP (0.5 mM in Tris-HCl (pH 7.5)), 2 μl Klenow fragment (6 U), and 10 μl of [α-^{32}P]dATP (100 μCi). The labeling process was allowed to proceed for 3-4 hours at room temperature. The un-incorporated nucleotides were removed by passing the labeling reaction over a Sephadex G-50 column using TE buffer with 100 mM NaCl as elution buffer. The probe was incubated for five minutes in boiling water before being added to the membrane and hybridization solution.

When the radiolabeled-probe was an oligonucleotide (for hybridization for *in vivo* footprinting analyses), the labeling was done by phosphorylation with bacteriophage T4 polynucleotide kinase as described in Sambrook et al (1989), with some modifications. Briefly, 30 pmol of oligonucleotide were incubated with 120 μCi of [γ-^{32}P]ATP, 70 mM Tris-HCl pH 7.6, 5 mM DTT, 10 mM $MgCl_2$, and 20 units of T4 polynucleotide kinase, in a total volume of 20 μl, for 30 minutes at 37°C. The ^{32}P-radiolabeled oligonucleotide was separated from the free radiolabeled-nucleotide, by precipitation with addition of 5

M NaCl to the final concentration of 0.2 M, 25 μg of tRNA, and 2.5 volumes of 100% ethanol, followed by incubation at –70°C for 20 minutes. The precipitated probe was collected by centrifugation at 13,000 × *g* for 30 minutes at room temperature, resuspended in 200 μl of TE buffer and added to the membrane hybridization solution after incubating in boiling water for 5 minutes.

Hybridization of Northern and Southern Blots

Membranes were pre-hybridized with 20 ml of hybridization solution (0.5 M sodium phosphate, pH 7.2, 7% SDS, 1 mM EDTA, pH 8.0, 1% BSA) for at least 20 minutes and then the probe was added after boiling for 5 minutes. After an overnight incubation at 61°C, the blots were washed 4 times for 10 minutes with each wash temperature at 65°C in a high-stringency buffer (0.04 M sodium phosphate, pH 7.2, 1 mM EDTA, pH 8.0, 1% SDS), blotted dry on Whatman filter paper #1 and exposed to film. When the probe was an oligonucleotide, the incubation overnight was at 40°C, the washing temperature was 45°C, and the high-stringency wash buffer had the Na^+ concentration adjusted to 350 mM with 5M NaCl. After washing, the membrane was subjected to autoradiography by exposure to Hyperfilm MP (Amersham-Pharmacia, Piscataway, NJ).

The exposed film was scanned using a Hewlett-Packard ScanJet 4c/T into Adobe Photoshop (Adobe Systems Incorporated, San Jose, CA) computer software for creation of the figures displayed in this dissertation made in Microsoft Office Powerpoint (Microsoft Corporaton, Redmond, WA).

CHAPTER 3
CYTOKINE-INDUCIBLE ENHANCER WITH PROMOTER ACTIVITY IN BOTH THE RAT AND HUMAN MANGANESE SUPEROXIDE DISMUTASE GENES

Introduction

The superoxide dismutases (SODs) are the first line of cellular defense against the damaging effects of superoxide anion radicals (Halliwell and Gutteridge, 1990). Manganese superoxide dismutase (MnSOD) is the most highly regulated of the three SODs (Visner et al., 1991; Dougall and Nick, 1991), being localized to mitochondria (Suzuki et al., 1993; Del Maestro and McDonald, 1989) and conferring potent cytoprotection (Shull et al., 1991; Wong and Goeddel, 1988; Wong et al., 1989; Visner et al., 1990; Eastgate et al., 1993; Akashi et al, 1995; Manganaro et al., 1995; Baker et al., 1998). Multiple studies have shown that increased cellular levels of MnSOD are cytoprotective during cellular oxidative stress (Shull et al., 1991) or inflammatory challenges, such as TNF-α-mediated apoptosis (Wong and Goeddel, 1988; Wong et al., 1989), IL-1 cytotoxicity (Visner et al., 1990), ionizing radiation (Eastgate et al., 1993; Akashi et al., 1995), and neurotoxicity (Manganaro et al., 1995; Baker et al., 1998). The role of MnSOD as a potent cytoprotective enzyme is most strikingly illustrated in three transgenic model studies. The first transgenic model involves targeted overexpression of *MnSOD* in the pulmonary epithelium of mice resulting in a decreased level of inflammation as a consequence of a hyperoxic exposure (Wispe et al., 1992). In the second study, the physiological importance of this gene is best exemplified through gene ablation where *MnSOD* knockout mice manifest severe dilated cardiac myopathy and die

within ten days of birth (Li et al., 1995). The third study shows that treatment of the *MnSOD* knockout mouse with the superoxide dismutase mimetic, manganese 5,10,15,20-tetakis (4-benzoic acid) porphyrin, rescues these mice from the systemic toxicity, but allows development of a severe neurodegenerative disorder by three weeks of age (Melov et al., 1998).

Previous investigations from this and other laboratories have established that levels of steady state MnSOD mRNA and protein increase following exposure to bacterial lipopolysaccharide (LPS), tumor necrosis factor (TNF) and interleukin-1 (IL-1) (Wong and Goeddel, 1988; Visner et al., 1990; Visner et al., 1991; Melov et al., 1998). Stimulus-dependent increases in mRNA levels are inhibited by actinomycin D (Visner et al., 1992), suggesting increased transcription of the gene, which has been confirmed by subsequent nuclear run-on studies (Hsu, 1993). Results from DNase I hypersensitive studies analyzing the chromatin structure of *MnSOD* have identified multiple regions of increased nuclease accessibility located throughout the gene as well as a stimulus-dependent alteration in chromatin structure in the 5' flanking region (Kuo et al., 1999). Furthermore, dimethyl sulfate *in vivo* footprinting studies have identified the binding sites for ten basal protein factors which interact with the promoter as well as stimulus-dependent alterations in guanine residue reactivity near the hypersensitive site found only in stimulus treated cells (Kuo et al., 1999). To complement the preceding studies on chromatin structure and *in vivo* footprinting, functional studies of the promoter were performed by analyzing deletions of the 5' flanking region. The promoter deletion data suggest that basal promoter activity requires only a very small portion of the 5' flanking region. Together these data suggest that multiple protein-DNA interactions occur during

transcription under basal conditions and that treatment with inflammatory mediators, causes an alteration in chromatin structure in the promoter region of the gene.

Not all *cis*-acting regulatory elements are located in 5' flanking regions. In fact, regulatory sequences have been identified within introns or in distant 3' flanking sequences of the human and mouse immunoglobulin kappa gene (Queen and Baltimore, 1983; Judd and Max, 1992), platelet-derived growth factor gene (Takimoto and Kuramoto, 1993), alcohol dehydrogenase-1-S (Callis et al., 1987) and collagen genes (Simkevich et al., 1992). To identify regions of *MnSOD* that regulate basal and stimulated expression, our present study utilized deletion analysis of rat *MnSOD* (Hurt et al., 1992) coupled with transient transfection studies in a rat lung epithelial cell line. Measuring mRNA expression levels of the human growth hormone reporter gene, we have localized a complex enhancer element within intron 2 of the rat and a homologous region in intron 2 of the human *MnSOD*. Most interestingly, this regulatory element possesses the ability to promote cytokine-inducible transcription independent of a promoter sequence.

Results

An Inducible *Cis*-Acting Enhancer Element Exists within *MnSOD*

Previous results of steady-state MnSOD mRNA levels in rat pulmonary epithelial and endothelial cells demonstrated dramatic induction with inflammatory mediators (Visner et al., 1991). In addition, nuclear run-on experiments showed that stimulus-dependent MnSOD expression is at least in part a consequence of *de novo* transcription (Hsu, 1993). *MnSOD* promoter deletion analysis demonstrated levels of stimulus-dependent *MnSOD* expression that were far lower than that seen with the endogenous

steady-state mRNA. The vector constructs used in the analysis contained only 5' flanking sequence, incorporating only one of the seven DNase I hypersensitive sites within *MnSOD* (Kuo et al., 1999). To determine whether the remaining DNase I hypersensitive sites within MnSOD contained regulatory function, we created hGH expression vectors that combine both the MnSOD promoter (a 2.5 Kb *Hind*III to *Eag*I fragment) and a 6.1 kb *Hind*III fragment, containing the remaining DNase I hypersensitive sites (Figure 3-1). Expression of *hGH* in cells transfected with these vectors was compared in the same experiments to expression of *hGH* in cells transfected with the vector construct, Hind/E GH, containing only the 5' promoter fragment.

Of note, the data displayed in Fig. 3-2 and all subsequent figures use northern analysis to directly assess transcription rates from the transfected reporter constructs. This is distinct from studies which assay reporter protein levels or enzymatic activity that must take into consideration potential effects of stimuli on translation and post-translational events.

As shown in Fig. 3-2A, LPS treatment caused a dramatic enhancement of steady-state mRNA expression as a result of adding the internal MnSOD genomic fragment, in a manner independent of fragment orientation. The same result was obtained when transfected cells were stimulated with TNF-α or IL-1β (data not shown). Furthermore, cleavage of the 6.1 kb *Hind*III fragment by making use of the unique *Hpa*I site demonstrated that the *cis*-acting element responsible for the inducible activity was localized to the 5' 3.8 kb portion of the original *Hind*III fragment (Figure 3-2B). Again, orientation did not influence the inducible activity in response to inflammatory

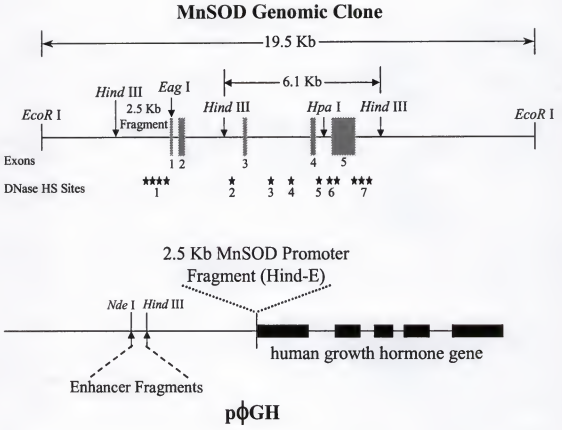

Figure 3-1. Schematic representations and restriction maps of the *MnSOD* genomic clone and the expression vectors constructed to assess potential enhancer activity. The restriction enzyme sites are indicated above the sequence (e.g., *Hind*III). The expression vectors contain the 6.1 kb *Hind*III fragment from positions +1107 to +7238 of *MnSOD*, with DNase-I hypersensitive sites 2-7 (*; Kuo et al., 1999) in either the 5'-to-3' or the 3'-to-5' orientation. In addition, each expression vector contains the *MnSOD* 5' promoter sequence from the *Hind*III site to the *Eag*I site (Hind-E). The *Hind*III fragment, from positions +1107 to +7238 of *MnSOD*, has been cut at position +4938 by *Hpa*I digestion creating the 3.8 kb and 2.3 kb fragments. The *Hind*III (+1107) to *Hpa*I (+4938) fragment contains hypersensitive sites 2, 3, and 4 (*; Kuo et al., 1999). The *Hpa*I (+4938) to *Hind*III (+7238) fragment contains hypersensitive sites 5, 6, and 7. These two fragments were tested in in transient transfections as was the 6.1 kb *Hind*III fragment. The restriction sites (*Hind*III and *Nde*I) into which the enhancer deletions were ligated are denoted on the hGH vector, which also contains the *MnSOD* promoter (Hind-E). Reproduced with permission from Rogers et al. (2000), Biochem. J., 347, 233-242. © Biochemical Society.

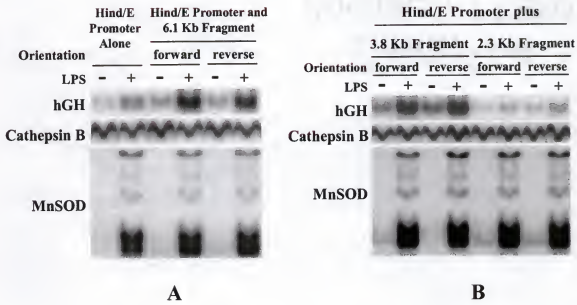

Figure 3-2. hGH mRNA levels after transfection in rat lung epithelial cells with vectors containing the internal *Hind*III fragment of *MnSOD* coupled to the promoter versus *MnSOD* promoter alone. Northern analysis was done using radiolabeled probes synthesized from hGH, MnSOD and cathepsin B cDNAs as described in the Methods section. hGH mRNA expression in rat lung epithelial cells transfected with vectors containing either the 3.8 kb or the 2.3 kb fragments which are deletions of the internal *Hind*III fragment of *MnSOD*. Reproduced with permission from Rogers et al. (2000), Biochem. J., 347, 233-242. © Biochemical Society.

mediators, thus indicating that the element could partially satisfy the definition of an enhancer.

The *MnSOD* Inducible Enhancer Element Is Located within Intron 2

To further localize the inducible *cis*-acting element within the 3.8 kb region, a set of serial deletion fragments spanning this region were amplified by PCR using complementary oligonucleotides and inserted into the *MnSOD* promoter vector, Hind-E GH. Deletions of the fragment from the 5' end and from the 3' end (Fig. 3-3) were generated in this manner. The inducible enhancer activity was evaluated by transient transfections into L2 cells using northern analysis. Based on the 3' deletions of the 3.8 kb *Hind*III-*Hpa*I fragment, the enhancer activity was localized to a region of approximately 450 bp in the 5' end of this 3.8 Kb fragment (Fig. 3-4). This position coincides extremely well with DNase hypersensitive site 2 (Kuo et al., 1999) located near the intron 2-exon 3 boundary.

In an effort to localize the enhancer more precisely, 5' deletions were also constructed as shown in Figure 3-5. Multiple 3' and 5' deletions containing the enhancer fragment demonstrate inducible activity comparable to the steady-state mRNA levels of the endogenous gene. Interestingly, the 338 and 227 bp deletions show reduced enhancer activity relative to the 455 bp fragment as shown in figure 3-5B, thus further delineating the enhancer activity regulated by LPS, TNF-α, and IL-1β to within a 200 to 300 bp region near the 3' end of intron 2.

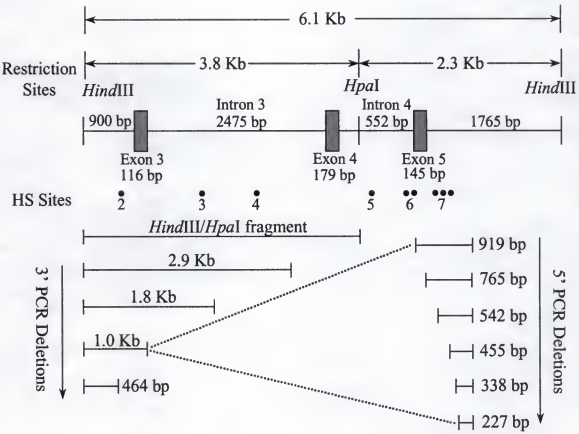

Figure 3-3. Deletions of the 3.8 kb enhancer fragment. Seriel deletions from both the 5' and 3' ends of the 3.8 kb fragment were created by PCR amplification and ligated into either the *Hind*III site or the *Nde*I site of the Hind/E GH vector (see Figure 3-1). Reproduced with permission from Rogers et al. (2000), Biochem. J., 347, 233-242. © Biochemical Society.

Figure 3-4. Northern analysis of transient transfections of the 3' PCR deletions of the 3.8 kb enhancer fragment localized the inducible activity to the 464 bp/1.0 kb fragment. Reproduced with permission from Rogers et al. (2000), Biochem. J., 347, 233-242. © Biochemical Society.

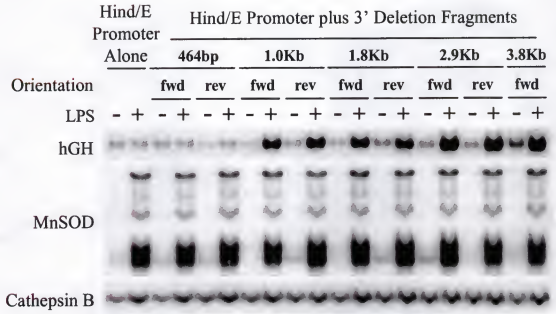
Hind/E Promoter Alone
Hind/E Promoter plus 3' Deletion Fragments
464bp
1.0Kb
1.8Kb
2.9Kb
3.8Kb
Orientation
fwd
rev
LPS
hGH
MnSOD
Cathepsin B

A

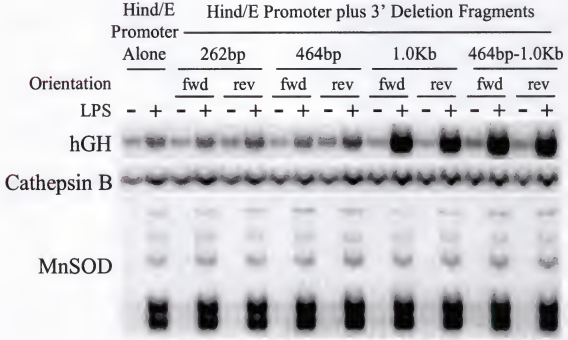
Hind/E Promoter Alone
Hind/E Promoter plus 3' Deletion Fragments
262bp
464bp
1.0Kb
464bp-1.0Kb
Orientation
fwd
rev
LPS
hGH
Cathepsin B
MnSOD

B

Figure 3-5. Northern analysis of transient transfections of the 5' PCR deletions of the 3.8 kb enhancer fragment localized the inducible activity to an area between the 455 bp and the 227 bp fragments in the 3' end of the 1.0 kb PCR fragment. Reproduced with permission from Rogers et al. (2000), Biochem. J., 347, 233-242. © Biochemical Society.

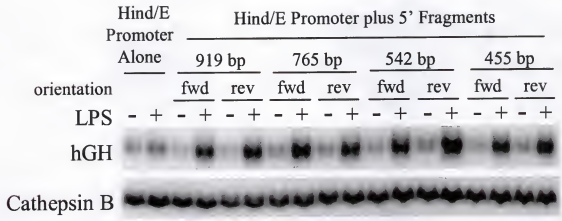
Hind/E Promoter Alone
Hind/E Promoter plus 5' Fragments
919 bp
765 bp
542 bp
455 bp
orientation
fwd
rev
LPS
hGH
Cathepsin B

A

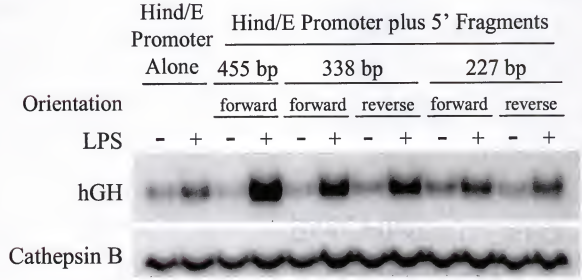
Hind/E Promoter Alone
Hind/E Promoter plus 5' Fragments
455 bp
338 bp
227 bp
Orientation
forward
forward
reverse
forward
reverse
LPS
hGH
Cathepsin B

B

The Enhancer Is Likely Composed of A Complex Set of Interacting Elements

To further localize the enhancer within the 3' end of intron 2, additional deletion constructs were created (Fig. 3-6). PCR amplification was used to generate a 260 bp fragment spanning the region between the two 5' deletions shown in Figure 3-3 (455 bp and 227 bp) as well as two 143 bp fragments which overlap each other within the 260 bp fragment (Fig. 3-6). The ability of these fragments to cause inducible expression was evaluated by transient transfection and northern analysis. The 260 bp fragment reproduced the enhancer activity seen with the larger, 919 bp fragment (Fig. 3-7). In addition, response to all the inflammatory mediators (LPS, TNF-α, and IL-1β) was maintained. Interestingly, the two overlapping 143 bp fragments show reproducibly diminished enhancer activity as compared to the 260 bp fragment (Fig. 3-7). These results are consistent with the previous deletion analyses in Figure 3-5, which showed partial enhancer activity in the 338 bp fragment compared to the 455 bp fragment and loss of activity with the 227 bp fragment. Together the results summarized in Figures 3-5 and 3-7, demonstrate that the 260 bp fragment delineates the minimum functional boundaries of the enhancer along with the complexity and interactive nature of this important regulatory sequence, as displayed by the retention of enhancer activity in the 143 bp fragments relative to the promoter alone.

To further assess the complexity of the enhancer element, electrophoretic mobility shift assays (EMSA) were performed with nuclear extracts from control and treated (LPS, TNF-α, IL-1β) cells. Figure 3D illustrates the different protein binding patterns between treated and control nuclear extracts as well as the different patterns of protein binding between the two functional DNA fragments of the enhancer element.

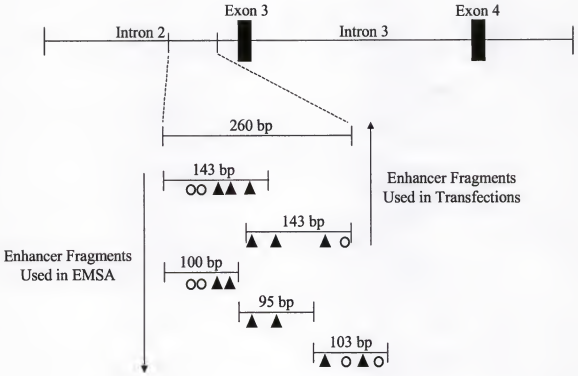

Figure 3-6. Schematic of the enhancer region in intron 2. A 260 bp PCR fragment of the enhancer region totally contained within intron 2 and two overlapping 143 bp PCR fragments encompassing the 260 bp region were created and ligated into the NdeI site of the Hind/E GH vector (see Fig. 3-1) for transient transfection in rat epithelial cells and northern analysis. In addition to the 143 bp fragments, three other fragments (100, 95 and 103 bp) were created by PCR amplification for EMSA. Putative constitutive and inducible protein-binding sites are illustrated by open circles and filled triangles, respectively. Reproduced with permission from Rogers et al. (2000), Biochem. J., 347, 233-242. © Biochemical Society.

Figure 3-7. A. Northern analysis of transient transfections of the 919 bp (see Fig. 3-6) or the 260 bp fragment (both orientations) in the Hind/E GH vectors in control, LPS, TNF-α, and IL-1β-stimulated rat pulmonary epithelial cells. B. Northern analysis of transient transfections of the 260 bp fragment and 143 bp fragments in the Hind/E GH vectors in control and LPS-stimulated rat pulmonary epithelial cells. Reproduced with permission from Rogers et al. (2000), Biochem. J., 347, 233-242. © Biochemical Society.

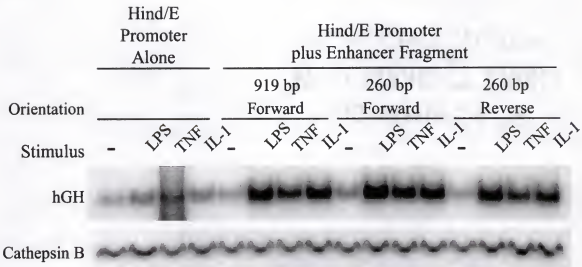
Hind/E
Promoter
Alone
Hind/E Promoter
plus Enhancer Fragment
919 bp
Forward
260 bp
Forward
260 bp
Reverse
Orientation
Stimulus
-
LPS
TNF
IL-1
hGH
Cathepsin B

A

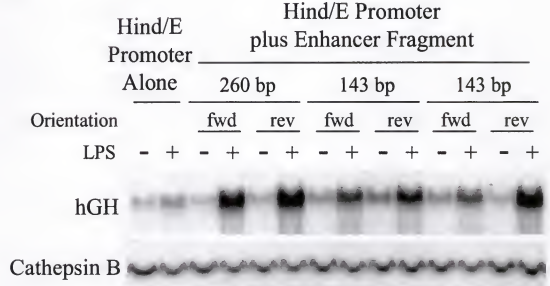
Hind/E
Promoter
Alone
Hind/E Promoter
plus Enhancer Fragment
260 bp
143 bp
143 bp
Orientation
fwd
rev
LPS
- + - + - + - + - + - + - +
hGH
Cathepsin B

B

Figure 3-8. EMSA of the two 143 bp, as well as, the 100, 95 and 103 bp fragments using nuclear extracts from untreated cells and cells treated with LPS, TNF-α, and IL-1β. Open circles refer to putative constitutive protein binding and filled triangles refer to putative inducible protein binding. Reproduced with permission from Rogers et al. (2000), Biochem. J., 347, 233-242. © Biochemical Society.

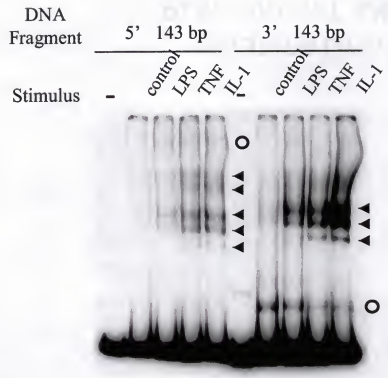
DNA Fragment
5' 143 bp
3' 143 bp
Stimulus
-
control
LPS
TNF
IL-1
control
LPS
TNF
IL-1

A

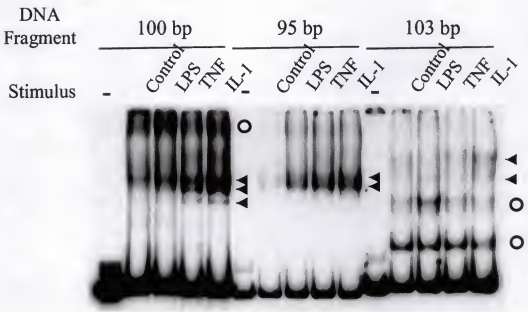
DNA Fragment
100 bp
95 bp
103 bp
Stimulus
-
Control
LPS
TNF
IL-1
Control
LPS
TNF
IL-1
Control
LPS
TNF
IL-1

B

Constitutive protein binding is observed in the 3' 143 bp fragment, but several inducible binding proteins can be appreciated in both fragments. In an attempt to further localize the protein binding sites, smaller fragments of the involved region were generated by PCR and evaluated by EMSA (Fig. 3-8). Once again, constitutive protein binding was observed in two of the fragments (100 bp and 103 bp). However, as with the 143 bp fragment, inducible protein binding was also observed in two of the smaller fragments (100 bp and 95 bp), most notably in the 95 bp fragment with a dramatic difference in binding between control and stimulated nuclear extracts. Further localization of protein binding was attempted with 50 bp and 30 bp fragments from this region, however, I was unable to obtain protein-DNA interactions, which displayed any stimulus-specific pattern (Rogers, data not shown). Unlike the results with the larger fragments (Fig. 3-8 A and B), EMSA with the smaller fragments (50 bp and 30 bp) showed only constitutive binding patterns. I believe that multiple protein-protein interactions are likely a prerequisite for the stimulus-specific DNA binding pattern, thus explaining the loss of stimulus-specific protein-DNA interaction in the smaller deletions of this complex regulatory element.

The Inducible Enhancer Elements within Rat and Human *MnSOD* Can Act with a Heterologous Promoter

To determine whether the *MnSOD* enhancer could function with a heterologous promoter, the enhancer fragment was cloned in both orientations into the TKGH expression vector. The herpes virus thymidine kinase (TK) promoter in this vector is a 200 bp minimal, TATA-containing promoter, quite dissimilar to the GC-rich, TATA- and CAAT-less *MnSOD* promoter. Results of transient transfections and northern analysis

Figure 3-9. A. Interaction of the 6.1 kb *MnSOD* fragment with the heterologous herpes-simplex TK promoter in the pTKGH expression vector. Expression vectors, pTKGH alone and pTKGH containing the 6.1 kb enhancer (both orientations), were constructed and a comparison of hGH mRNA levels in transiently transfected rat lung epithelial cells treated with LPS, TNF-α, or IL-1β was made. Northern analysis was done using radiolabeled probes from hGH, MnSOD and cathepsin B cDNAs. B. Comparison of the rat and human enhancer regions in the pTKGH vector. A 553 bp region encompassing the rat enhancer as well as the analogous region of the human *MnSOD* (466 bp fragment) were amplified by PCR and cloned into the *Hind*III site of the pTKGH vector. Northern analysis of transient transfections in rat pulmonary epithelial cells shown here and described in the Methods section. Reproduced with permission from Rogers et al. (2000), Biochem. J., 347, 233-242. © Biochemical Society.

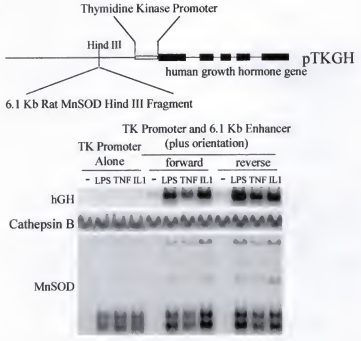
Thymidine Kinase Promoter
Hind III
pTKGH
human growth hormone gene
6.1 Kb Rat MnSOD Hind III Fragment
TK Promoter and 6.1 Kb Enhancer
(plus orientation)
TK Promoter
Alone
forward
reverse
- LPS TNF IL1 - LPS TNF IL1 - LPS TNF IL1
hGH
Cathepsin B
MnSOD

A

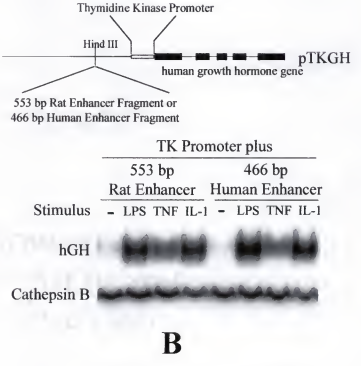
Thymidine Kinase Promoter
Hind III
pTKGH
human growth hormone gene
553 bp Rat Enhancer Fragment or
466 bp Human Enhancer Fragment
TK Promoter plus
553 bp
Rat Enhancer
466 bp
Human Enhancer
Stimulus - LPS TNF IL-1 - LPS TNF IL-1
hGH
Cathepsin B

B

(Fig. 3-9) demonstrated that the enhancer element could cooperate with the minimal TK promoter and dramatically increase the transcriptional activity of the hGH reporter gene in response to LPS, TNF-α, and IL-1β. The element functioned equally well in both orientations and interestingly was able to orchestrate reporter induction to as much as 45 fold above baseline. The ability of this element to enhance transcriptional activity of both the endogenous and a heterologous promoter in an orientation-independent and position-independent manner further qualifies it as an enhancer element.

Given the potency of this enhancer element, we compared the sequence of intron 2 in the rat gene with the corresponding region in the human *MnSOD* locus and found a high level of homology. In order to evaluate the functional significance of this region, a 553 bp fragment of the rat enhancer and an analogous 466 bp region of intron 2 of human *MnSOD* were inserted into Nde I site of the TKGH vector. The ability of the fragments to cause inducible enhancer activity was assessed by transient transfections and northern analysis. Both the rat and the human fragments caused essentially identical inducible expression in response to LPS, TNF-α and IL-1β (Fig. 3-9), indicating that this region of human intron 2 likely acts as an enhancer in the endogenous gene and that the enhancer activity itself is well conserved between species. We have also demonstrated that the rat and human enhancer can function equally as well in human cell lines (data not shown).

Evaluation of Promoter-Enhancer Interactions

We have demonstrated by *in vivo* footprinting that the *MnSOD* promoter contains 10 potential basal protein-binding sites (Kuo et al., 1999). These sites are illustrated in Figure 3-10 relative to the restriction sites that were employed for the promoter deletion analysis. To define the areas within the promoter required for interaction with the

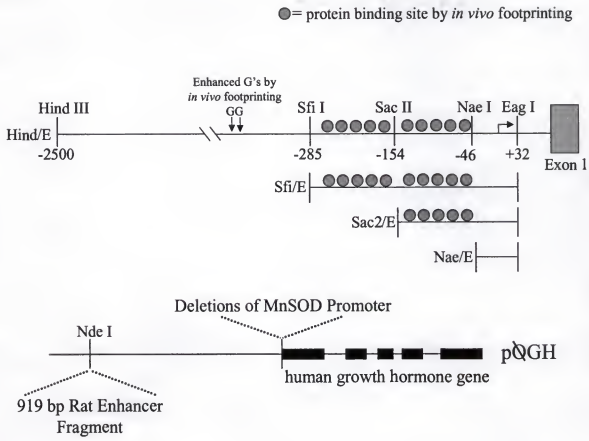

Figure 3-10. *MnSOD* promoter deletions summarizing the protein binding sites found by *in vitro* footprinting (Kuo et al., 1999). The 919 bp fragment encompassing the entire enhancer was ligated into the *Nde*I site of the hGH vector with the respective *MnSOD* promoter deletions. Reproduced with permission from Rogers et al. (2000), Biochem. J., 347, 233-242. © Biochemical Society.

Figure 3-11. A. Northern analysis following transient transfections of promoter deletion constructucts (Hind/E and Sfi/E containing the 919 bp enhancer fragment) into rat pulmonary epithelial cells. B. Northern analysis following transient transfections of promoter deletion constructs (Hind/E, Sac/E, and Nae/E containing the 919 bp enhancer fragment) into rat pulmonary epithelial cells. Reproduced with permission from Rogers et al. (2000), Biochem. J., 347, 233-242. © Biochemical Society.

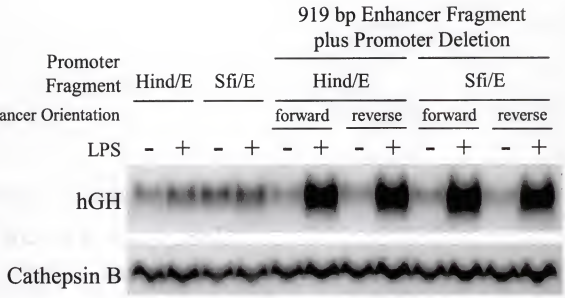
919 bp Enhancer Fragment
plus Promoter Deletion
Promoter
Fragment
Hind/E
Sfi/E
Hind/E
Sfi/E
Enhancer Orientation
forward
reverse
forward
reverse
LPS
- + - + - + - + - + - +
hGH
Cathepsin B

A

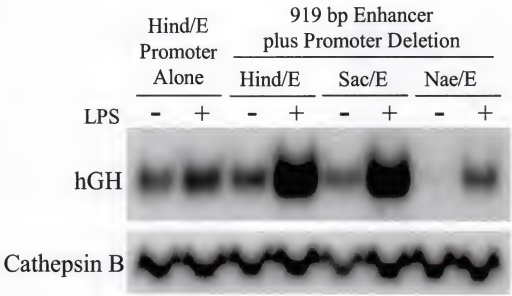
Hind/E
Promoter
Alone
919 bp Enhancer
plus Promoter Deletion
Hind/E
Sac/E
Nae/E
LPS
- + - + - + - +
hGH
Cathepsin B

B

Figure 3-12. A. Schematic of the promoter-less human growth hormone vector (pϕGH) and the position of the human 466 bp enhancer fragment. Northern analysis of the 466 bp human enhancer in pϕGH and pTKGH constructs transiently transfected into control and treated (LPS, TNF-α, and IL-1β) rat pulmonary epithelial cells. B. Schematic of the promoter-less hGH vector (pϕGH) and the position of the 260, 553, or 746 bp enhancer fragments. Northern analysis of the rat enhancer fragments (260, 553, and 746 bp) in pϕGH constructs transiently transfected into control and treated (LPS, TNF-α, and IL-1β) rat pulmonary epithelial cells. Reproduced with permission from Rogers et al. (2000), Biochem. J., 347, 233-242. © Biochemical Society.

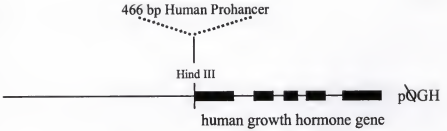
466 bp Human Prohancer
Hind III
pΔGH
human growth hormone gene

A

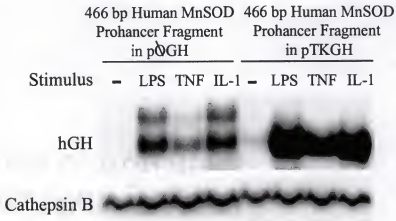
466 bp Human MnSOD Prohancer Fragment in pΔGH
466 bp Human MnSOD Prohancer Fragment in pTKGH
Stimulus - LPS TNF IL-1 - LPS TNF IL-1
hGH
Cathepsin B

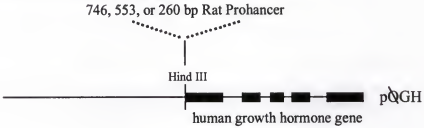
746, 553, or 260 bp Rat Prohancer
Hind III
pΔGH
human growth hormone gene

B

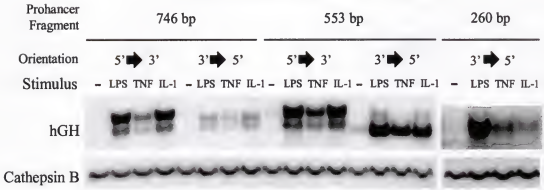
Rat Prohancer Fragments in pΔGH
Prohancer Fragment
746 bp
553 bp
260 bp
Orientation
5' 3'
3' 5'
5' 3'
3' 5'
3' 5'
Stimulus - LPS TNF IL-1 - LPS TNF IL-1 - LPS TNF IL-1 - LPS TNF IL-1 - LPS TNF IL-1
hGH
Cathepsin B

enhancer element, the previous promoter deletion constructs (Kuo et al., 1999) were coupled with a 919 bp enhancer fragment (Fig. 3-10). Transient transfection and northern analysis were used to evaluate inducible activity for these vector constructs. Of interest, the first five binding sites could be deleted without any detectable decrease in inducible activity (Fig. 3-11A). It was not until the remaining five basal binding sites were eliminated that the level of induction decreased (Fig. 3-11B) with almost complete loss of basal activity. Interestingly, LPS-inducible transcription could still occur when all promoter protein-binding sites were deleted, but only when the vector construct contained the enhancer fragment (Fig. 3-11B). However, in the absence of the enhancer element, deletion of the same promoter region, (construct Nae/E, 18), eliminated any transcription, thus, indicating that the enhancer element contained DNA sequence potentially capable of independently promoting transcription in a stimulus-regulated manner.

The Rat and Human Enhancer Elements Contain Inducible Promoter Activity

With the results of the previous experiment (Figure 3-11), we postulated that the enhancer element might exhibit stimulus-dependent promoter activity in the absence of a true promoter. Since the Nae/E GH construct did contain 77 bp from the 5' flanking region of the *MnSOD* promoter, the rat and the human enhancer elements were inserted into the promoter-less *hGH* vector (pϕGH) (Figure 3-12A). Figure 3-12A shows the results of the 466 bp human *MnSOD* enhancer fragment in the presence and absence of the TK promoter. Inducible transcription was observed with LPS, TNF-α and IL-1β, but at lower levels than when the fragment was inserted into the pTKGH vector. Interestingly, two transcripts, one the correct size and one approximately 200 to 300 bp larger, were seen when the enhancer fragment acted as its own promoter. When the 553

bp and 746 bp rat enhancer fragments were tested in the promoter-less hGH vector (pϕGH), similar results to the human fragment were obtained, in that, two different-sized transcripts were observed (Figure 3-12A and B). Of note, however, when either the 553 bp or the 746 bp enhancer fragment was inserted into pϕGH in the 3' to 5' orientation, the correct-sized transcript predominated. This result would indicate that the enhancer can indeed act as a promoter, but its orientation and position relative to the start of transcription are important. To determine if the preceding hypothesis was correct, pϕGH vector constructs containing the 260 bp enhancer fragment were created. As can be seen in Figure 6B, when the 260 bp enhancer fragment acting as a promoter was inserted into the pϕGH vector in the 3' to 5' orientation, a single stimulus-responsive transcript resulted.

Discussion

As a cellular antioxidant, mitochondrial *MnSOD* has been consistently shown to be an effective cytoprotective enzyme. *MnSOD* expression is highly regulated in response to a variety of pro-inflammatory mediators in many cell types. In rat lung epithelial cells, the inflammatory mediators, LPS, TNF-α and IL-1β, each cause *MnSOD* steady-state mRNA levels to increase 10 to 20 fold, which has been shown in nuclear run-on studies (Hsu,1993) to be partly due to increased transcription of the gene. A survey of the entire *MnSOD* locus for sites of possible protein-DNA interaction using DNase I hypersensitive site analysis revealed increased nuclease accessibility at sites in the 5' proximal promoter region and 6 other sites located within the gene (Kuo et al., 1999). The present experiments further expand our understanding of the molecular

mechanisms regulating basal and induced expression of *MnSOD* by identifying an enhancer region within the rat and human *MnSOD*.

The 5' flanking sequence of *MnSOD* is characterized by a GC-rich island, lacking a TATA- and CAAT-box for initiation of transcription. *In vivo* footprinting studies have defined protein binding sites for 10 basal transciption factors within 500 bp of the transcriptional start site (Kuo et al., 1999). Promoter deletion analysis identified essential *cis*-acting sequences located within 157 bp of the transcriptional start site (Kuo et al., 1999). This region of the promoter includes 5 of the basal protein binding sites and is capable of supporting basal and stimulated (LPS, TNF-α and IL-1β) expression. However, protein and mRNA levels of the *hGH* reporter were only induced 2 to 3 fold in transient transfection studies using vectors containing from 4.5 to 0.16 kb of the MnSOD promoter region alone (Kuo et al., 1999). Examination of the *MnSOD* promoter for known transcription factor consensus sequences by computer analysis revealed an NF-κB sequence at –353 as well as Sp1 and gut-enriched Krüppel-like factor (GKLF) (Shields and Yang, 1998; Zhang et al., 1998) sites corresponding to binding sites I-V. As previously shown, the NF-κB site is not occupied based on *in vivo* footprinting data and is not important for enhancer function (Fig. 3-11A). On the other hand guanine contacts from *in vitro* footprinting with purified Sp1 and GKLF strongly implicates these proteins with the *in vivo* contacts observed at sites I-V. However, previous data (Kuo et al., 1999) and Figure 3-11A seem to indicate that based on transient transfection studies the potential Sp1 and GKLF sites (I-V) are not essential for basal or enhancer-dependent gene expression (using LPS, TNF-α, and IL-1β as stimulants). These data may be reconciled by appreciating that constitutive Sp1 and/or GKLF binding to sites I-V might

be necessary for other stimuli known to induce INF-γ (Harris et al., 1991; Valentine and Nick, 1992), phorbol ester (Fujii and Taniguchi, 1991) or inhibit (glucocorticoids (Dougall and Nick, 1991)) *MnSOD* expression. Alternatively, it should be noted that the functional data was obtained by transient transfection of plasmid reporter gene DNA into mammalian cells. Consequently, it is very possible that the plasmid DNA does not form proper chromatin structures following transfection. Appropriate chromatin structure is likely crucial for the correct alignment of DNA sequence important for the promoter/enhancer interactions. Therefore, we must consider this as a possible explanation for the data shown in Figure 3-11B. The data in Figure 3-11B does, however, strongly implicate the functional importance of binding sites VI-X to both basal and enhancer/stimulus-specific expression. The pNae/Eag GH vector was not sufficient to drive either basal or stimulated expression (Kuo et al., 1999), suggesting that a minimal promoter sequence for transcriptional initiation was no longer present.

The observed induction of the reporter gene from the 5' *MnSOD* promoter was much lower than endogenous *MnSOD* expression following treatment with inflammatory mediators (Kuo et al., 1999). These data and the presence of DNase I hypersensitive sites within the gene suggested that regulatory elements might exist outside the 5' flanking sequence. Results from transfections with vectors combining both the 5' promoter region and the internal 6.1 kb fragment (containing the remainder of the DNase I hypersensitive sites) confirmed that genomic sequences 3' to the transcriptional start site contain enhancer activity. Most importantly, this region contains adequate enhancer activity to mimic endogenous, stimulus-dependent transcription levels. Deletion analysis of this region localized this activity to a 260 bp area within intron 2, which contains DNase I

hypersensitive site 2. When this 260 bp region is divided into two 143 bp fragments, we found that each of these fragments independently retained inducible activity, albeit at a lower level. Moreover, based on EMSA these same 143 bp fragments were able to bind both constitutive nuclear factors as well as a number of factors specific to extracts from induced cells. However, attempts to further delineate the enhancer by EMSA using DNA fragments less than 50 bp (Rogers, unpublished data) led to the elimination of stimulus-specific in vitro binding, further demonstrating the complexity of this enhancer and implying that protein-protein interactions may be critical to the formation of specific protein-DNA complexes between the promoter and enhancer. Therefore, we believe that this enhancer is composed of a set of complex, interacting elements involved in the inducible expression of *MnSOD*. Contrary to the published characterization of the murine gene (Jones et al., 1995 and 1997), our data would indicate that separate elements within this enhancer region retain an ability to induce *MnSOD* transcriptional activity, but that small (25-30 bp) individual elements cannot act independently to confer the same inducible levels seen in the endogenous gene.

Our results demonstrate that this enhancer element requires a portion of the *MnSOD* promoter to achieve levels of induction analogous to steady-state northern analysis. Using portions of the promoter coupled with the enhancer, we demonstrated the requirement for sequences from -154 to the start of transcription, which include protein-binding sites VI-X defined by *in vivo* footprinting (Kuo et al., 1999). Given the functional connection between the enhancer and the *MnSOD* promoter, we postulate that the enhancer may interact with the promoter through a mechanism involving DNA bending (Ptashne, 1986). As support for this hypothesis, we have performed co-

transfection experiments with the promoter and enhancer on separate plasmids and found under these conditions that inducible transcription could not be achieved (Rogers, data not shown). This substantiates the argument that the *MnSOD* promoter and enhancer must reside within a contiguous region of DNA. Therefore regulatory elements most likely physically interact through DNA bending (Ptashne, 1986) and possibly involving an alteration in chromatin structure in the promoter as defined by Kuo et al., 1999.

Of particular interest is the existence of a homologous functional enhancer element in human *MnSOD* (Fig. 3-10), which responds to the same inflammatory mediators as the rat enhancer in both rat and human cells (data not shown). In addition, another unique characteristic of the rat and human enhancer element is its ability to drive transcription independent of a classical promoter (Figures 3-12A and B). As an independent promoter/regulatory element, this sequence has the capacity to promote stimulus-dependent transcription with negligible basal levels. Previous work in our laboratory explored the possibility of an alternative promoter or differential mRNA splicing as a cause for the multiple transcripts in the rat. Using primer extension and ^{32}P-labeled cDNA and genomic fragments as hybridization probes, it was determined that alternative polyadenylation was the likely cause for the multiple transcripts seen in the rat *MnSOD* (Hurt et al., 1992). Understanding the regulation of this enhancer region will be important since it seems to be exquisitely responsive to acute cytokine mediators and, if similar motifs are found in other genes, may exist as a regulatory unit that serves as a general inflammatory response element. Current efforts are underway to further characterize the enhancer by DMS *in vivo* footprinting and mutagenesis for functional transfection studies.

CHAPTER 4
IN VIVO FOOTPRINTING AND MUTAGENESIS OF THE RAT MANGANESE SUPEROXIDE DISMUTASE ENHANCER

Introduction

Gene activation in response to extracellular signals, infection by pathogens, or environmental stresses requires highly integrated signal transduction pathways that direct the transcriptional machinery to the appropriate set of genes. A crucial issue in understanding inducible gene regulation is how a relatively small number of different transcription factors is used to achieve the high level of specificity required to control complex patterns of gene expression (Maniatis et al., 1987; McKnight and Yamamoto, 1992). The answer probably lies in the correct combination of transcription factors aligning on the regulatory region to cause gene activation. Most genes are regulated by multiple transcriptional activator proteins, each of which plays a role in controlling the transcription of a variety of genes with different expression patterns. The expression of a given gene depends, however, on the simultaneous interaction of a specific combination of regulatory proteins with the control DNA elements. Indeed, most transcription enhancers contain distinct sets of transcription factor-binding sites, and variations in the arrangement of binding sites provide the potential to create unique nucleoprotein complexes. Cooperative interactions between the proteins in these complexes can lead to a high level of specificity in gene activation and to a high level of transcriptional synergy.

Perhaps one of the best examples of combinatorial interactions among distinct regulatory elements is provided by the interferon-β (IFNβ) gene (Maniatis et al., 1992; Tijan and Maniatis, 1994). The IFNβ gene is activated in response to virus infection, and the transcription factors required for activating the IFNβ gene have been identified. Detailed studies of this promoter revealed a highly compact and remarkably complex organization of regulatory sequences containing four positive regulatory domains. None of these domains function on their own, but two or more copies of any one of them can act as a virus-inducible enhancer. However, the synthetic enhancers display varying levels of basal activity, are less inducible than a natural enhancer, and can respond to inducers other than virus infection. Thus, the specificity and activity of the natural intact enhancer are distinct from those of the independent enhancer elements. The activation of at least some natural enhancers appears to result from the precise arrangement of transcription factors on DNA, resulting in the formation of a highly specific three-dimensional nucleo-protein complex (stereospecific enhancer complex; Grosschedl, 1995).

Transcriptional activator proteins have been shown to synergize with each other *in vitro* using synthetic enhancers containing multiple activator binding sites (McKnight and Yamamoto, 1992; Tijian and Maniatis, 1994). In some cases, the observed transcriptional synergy could be explained, at least in part, by cooperative binding of the activators to their sites. However, in other cases, the transcriptional synergy could be observed at concentrations of activator in which the binding sites are fully occupied (Carey et al., 1990; Lin et al., 1990). The most straightforward explanation for this synergy is that activators recruit the general transcription apparatus to nearby promoters,

and the transcriptional synergy is a consequence of multiple interactions between the activators and components of the transcription apparatus (Ptashne and Gann, 1997). This recruitment could involve the stepwise association of general transcription factors with the promoter (Orphanides et al., 1996; Roeder, 1996), interactions between activators and specific TATA box binding protein (TBP) associated factors (or TAFs) in the TFIID complex (Sauer et al., 1995), or interactions between activators and components of the RNA polymerase II holoenzyme (Koleske and Young, 1995). The best example of a functional enhancer where the assembly of a protein-DNA complex is required for the inducible transcription seen at the endogenous levels is the IFNβ gene enhancer (Kim and Maniatis, 1997).

In this study, I have used DMS *in vivo* footprinting to identify potential protein-DNA interactions in the *MnSOD* enhancer element previously delineated by deletion analysis and transient transfections. In addition, after identification of putative binding sites, mutagenesis of the potential binding sites was used to verify whether the DNA elements were crucial for the inducible *MnSOD* enhancer in a functional transient transfection assay system.

Results

Multiple Potential Protein Binding Sites Exist within the *MnSOD* Enhancer

Using the technique of dimethyl sulfate (DMS) *in vivo* footprinting as the molecular probe coupled with ligation-mediated polymerase chain reaction (LMPCR), it is possible to identify *cis*-acting DNA elements at single nucleotide resolution and thus display the *in vivo* protein-DNA contacts. As a small hydrophobic molecule, the

chemical DMS can enter intact cells and react predominantly by methylating the N-7 atom of guanine and, to a lesser extent, the N-3 atom of adenine in duplexed DNA. Amino acid side chains of *trans*-acting factors, which contact guanine residues, can protect these bases from methylation by DMS. Alternatively, amino acid side chains can create a hydrophobic pocket around specific guanine residues, which increases the DMS solubility and results in enhanced reactivity. Ultimately, protein side chains produce a footprint composed of protections and/or enhancements which appear as diminished or more intense bands as compared to the corresponding band in the naked DNA guanine ladder on the final sequencing gel autoradiograph (Nick and Gilbert, 1985).

Previous work from this laboratory has established the timing of experimental conditions when cell cultures are treated with inflammatory stimuli prior to DMS (Kuo, 1998). Kinetics of transcription factor binding is stable and comparable between control and stimulus-treated samples. Those experiments demonstrated that protein-DNA contacts were detectable as early as 0.5 hr and as late as 8 hr after addition of stimulus. For the experiments in this thesis, time points of 2 and 4 hrs were chosen for DMS treatment after addition of stimulus (LPS, TNF-α, IL-1β).

Illustrated in Figure 4-1 is an autoradiograph of DMS *in vivo* footprinting and LMPCR results of both control and treated samples. Several guanine and adenine residues exhibited altered DMS reactivity, which appeared as diminished or enhanced hybidization signals relative to *in vitro* DMS-treated DNA lanes. The existence of several potential protein binding sites are postulated to account for patterns uncovered by *in vivo* footprinting. Figure 4-2 summarizes the putative protein-DNA contacts

Figure 4-1. Autoradiograph of DMS *in vivo* footprinting of enhancer region of *MnSOD*. Lanes are as follows: G, naked DNA from L2 cells treated with DMS; C, control L2 cells treated in vivo with DMS; T, TNF-α-treated L2 cells for 2 hours prior to *in vivo* treatment with DMS; I, IL-1β-treated L2 cells for 2 hours prior to *in vivo* treatment with DMS. Open triangles refer to inducible protected sites; and closed triangles refer to inducible enhanced sites. Site numbers 1-4 refer to regions where putative protein-binding may occur on the enhancer element. Sequence refers to bottom strand.

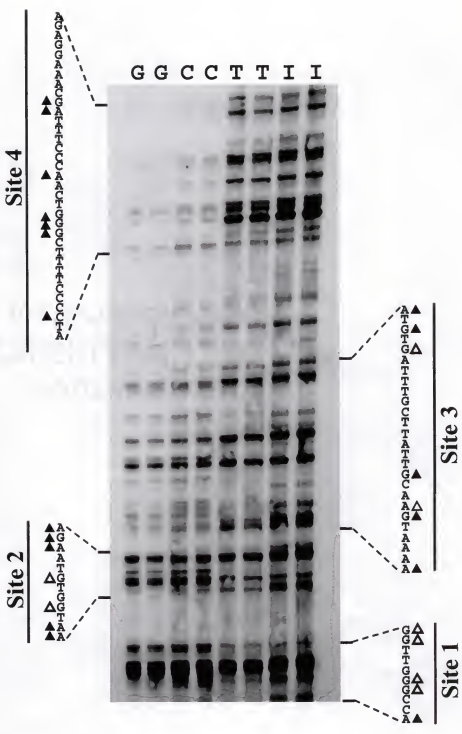
G G C C T T I I
Site 4
Site 2
Site 3
Site 1

Figure 4-2. Sequence comparison of rat, human and mouse *MnSOD* enhancer regions of intron 2. Open triangles refer to inducible protected sites; and closed triangles refer to inducible enhanced sites. Site numbers 1-4 refer to regions where putative protein-binding may occur on the enhancer element of the rat MnSOD gene. C/EBP-2 refers to putative transcription factor binding site in the mouse *MnSOD* enhancer by consensus sequence analysis and DMS *in vivo* footprinting. Arrows with numbers refer to boundaries of smallest regions of the rat MnSOD enhancer tested in transient transfection assays.

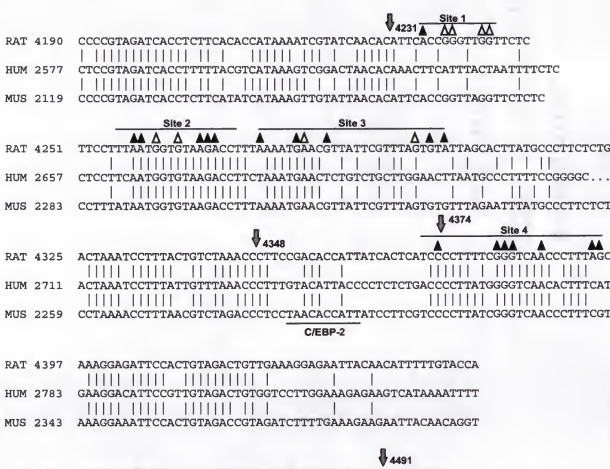
4231
Site 1
RAT 4190 CCCCGTAGATCACCTCTTCACACCATAAAATCGTATCAACACATTCACCGGGTTGGTTCTC
HUM 2577 CTCCGTAGATCACCTTTTTACGTCATAAAGTCGGACTAACACAAACTTCATTTACTAATTTTCTC
MUS 2119 CCCCGTAGATCACCTCTTCATATCATAAAGTTGTATTAACACATTCACCGGTTAGGTTCTCTC
Site 2
Site 3
RAT 4251 TTCCTTTAATGGTGTAAGACCTTTAAAATGAACGTTATTCGTTTAGTGTATTAGCACTTATGCCCTTCTCTGAG
HUM 2657 CTCCTTCAATGGTGTAAGACCTTCTAAATGAACTCTGTCTGCTTGGAACTTAATGCCCTTTTCCGGGGC.....
MUS 2283 CCTTTATAATGGTGTAAGACCTTTAAAATGAACGTTATTCGTTTAGTGTGTTTAGAATTTATGCCCTTCTCTGAC
4374
Site 4
4348
RAT 4325 ACTAAATCCTTTACTGTCTAAACCCTTCCGACACCATTATCACTCATCCCCTTTTCGGGTCAACCCTTTAGC
HUM 2711 ACTAAATCCTTTATTGTTTAAACCCTTTGTACATTACCCCCTCTCTGACCCCCTTATGGGGTCAACACTTTCAT
MUS 2259 CCTAAAACCTTTAACGTCTAGACCCTCCTAACACCATTATCCTTCGTCCCCTTATCGGGTCAACCCTTTCGT
C/EBP-2
RAT 4397 AAAGGAGATTCCACTGTAGACTGTTGAAAGGAGAATTACAACATTTTTGTACCA
HUM 2783 GAAGGACATTCCGTTGTAGACTGTGGTCCTTGGAAAGAGAAGTCATAAAATTTT
MUS 2343 AAAGGAAATTCCACTGTAGACCGTAGATCTTTTGAAAGAAGAATTACAACAGGT
4491
RAT 4451 CTAAAGTTGGGAAGGCACCTCTGTCTCGACATAAACAAATCACTTACGAC
HUM 2837 TGTTGAATTAAAGTCAGGAAATGAACACCTTAGTCTCGGAATGAATACAT
MUS 2397 CTGTAGAACTAACATTAGGAAGACACCTCGGTCTCGAAACGAAATTCCAC

being numbered sites 1 through site 4 over a region of approximately 150 to 200 bp.

Mutagenesis of Putative DNA Binding Sites Alters Inducible *MnSOD* Expression

Knowing the results of the DMS *in vivo* footprinting, mutagenesis of the enhanced or protected nucleotides within the *MnSOD* enhancer region was performed using PCR amplification. Mutations achieved were verified by sequencing. Figure 4-2 shows a comparison between the rat, human and murine sequences in intron 2 of each gene. The sites that were shown to be enhanced or protected in the rat intron 2 enhancer region are depicted as well as the *in vivo* footprinting sites found in the murine intron 2 enhancer region (Jones et al., 1997). The mutations within each of the 4 sites that were created in the hGH reporter vectors used in the mutagenesis studies are shown in figure 4-3. Figures 4-4 and 4-5 demonstrate the results of northern analysis of transient transfections of L2 cells with the wild type (WT), control, and mutated binding sites 1-4. The results in both Figures 4-4 and 4-5 would suggest that the mutations made in site 2 seem to affect the level of inducible transcription to extent much greater than the other site mutations. As way of control, the mutations made in the consensus sequence of C/EBP, referred to as C/EBP-2, does not seem to change the level of inducible expression. Also mutagenesis of the individual sites in Site 4 (4a and 4b) did not influence the level of inducible transcription until the two site mutations were combined into one vector construct.

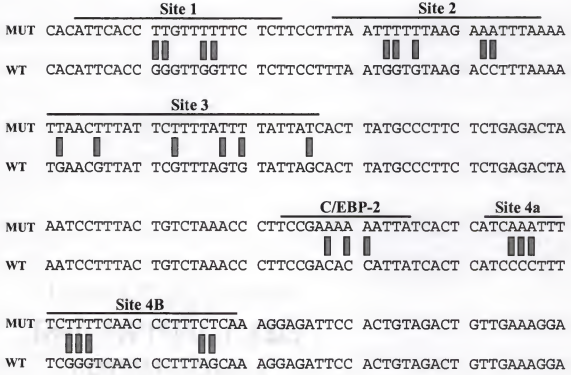
Site 1
Site 2
MUT CACATTCACC TTGTTTTTTC TCTTCCTTTA ATTTTTTAAG AAATTTAAAA
WT CACATTCACC GGGTTGGTTC TCTTCCTTTA ATGGTGTAAG ACCTTTAAAA
Site 3
MUT TTAACTTTAT TCTTTTATTT TATTATCACT TATGCCCTTC TCTGAGACTA
WT TGAACGTTAT TCGTTTAGTG TATTAGCACT TATGCCCTTC TCTGAGACTA
C/EBP-2
Site 4a
MUT AATCCTTTAC TGTCTAAACC CTTCCGAAAA AATTATCACT CATCAAATTT
WT AATCCTTTAC TGTCTAAACC CTTCCGACAC CATTATCACT CATCCCCTTT
Site 4B
MUT TCTTTTCAAC CCTTTCTCAA AGGAGATTCC ACTGTAGACT GTTGAAAGGA
WT TCGGGTCAAC CCTTTAGCAA AGGAGATTCC ACTGTAGACT GTTGAAAGGA

Figure 4-3. The sequence of the rat *MnSOD* intronic enhancer region displaying the putative protein-DNA binding sites and the mutations made in each site for construction of hGH reporter vectors and transient transfection into L2 pulmonary epithelial cells. Rectangles mark the mutated base pairs with the sequence for the wild type (WT) *MnSOD* enhancer on the bottom and the mutated sequence on top.

Figure 4-4. Northern analysis of transient transfections of wild-type (WT) and mutated binding site enhancer elements in hGH vector. WT refers to the unchanged rat 360 bp enhancer fragment, control refers to the mutated C/EBP-2 site in the 360 bp fragment, Site 2 refers to the Site 2 mutation in the 360 bp fragment, Site 4a and 4b refer to the site 4a and 4b mutations in the 360 bp enhancer fragment. The upper panel shows cells that were stimulated with TNF-α for 8 hours prior to isolation of RNA and the lower panel shows cells that were stimulated with IL-1β for 8 hours prior to RNA isolation. In all vectors in both panels the enhancer fragment was in a 5'-3' orientation. hGH refers to the reporter gene product in each vector. Cathepsin B was used as a RNA loading control.

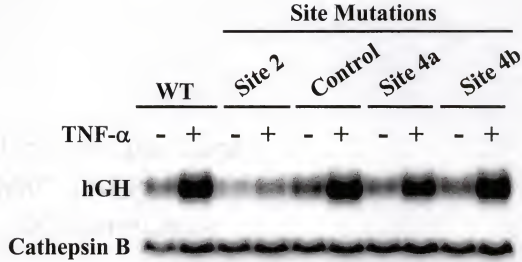
Site Mutations
WT
Site 2
Control
Site 4a
Site 4b
TNF-α - + - + - + - + - +
hGH
Cathepsin B

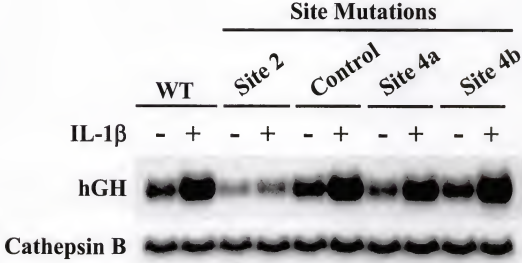
Site Mutations
WT
Site 2
Control
Site 4a
Site 4b
IL-1β - + - + - + - + - +
hGH
Cathepsin B

Figure 4-5. Northern analysis of transient transfections of wild-type (WT) and mutated binding site enhancer elements in hGH vector. WT refers to the unchanged rat 360 bp enhancer fragment, Site 2 refers to the Site 2 mutation in the 360 bp fragment, Site 4 refers to the combination of mutations in sites 4a and 4b in the 360 bp enhancer fragment. The upper panel shows cells that were stimulated with lipopolysacharride (LPS) for 8 hours prior to isolation of RNA. The middle panel shows cells that were stimulated with TNF-α for 8 hours prior to isolation of RNA. The lower panel shows cells that were stimulated with IL-1β for 8 hours prior to RNA isolation. hGH refers to the reporter gene product in each vector.

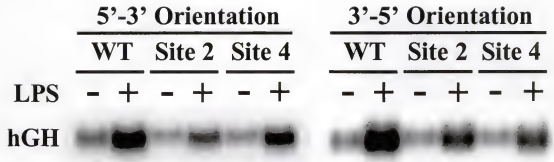
5'-3' Orientation
3'-5' Orientation
WT
Site 2
Site 4
WT
Site 2
Site 4
LPS
- + - + - +
- + - + - +
hGH

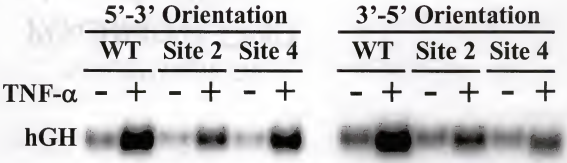
5'-3' Orientation
3'-5' Orientation
WT
Site 2
Site 4
WT
Site 2
Site 4
TNF-α
- + - + - +
- + - + - +
hGH

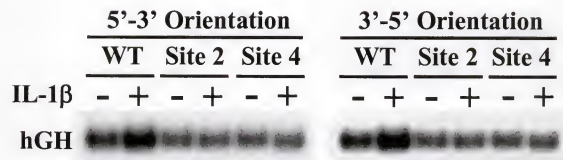
5'-3' Orientation
3'-5' Orientation
WT
Site 2
Site 4
WT
Site 2
Site 4
IL-1β
- + - + - +
- + - + - +
hGH

Discussion

A number of eukaryotic genes with complex enhancer elements exist in the literature, such as β-interferon (Kim and Maniatis, 1997, Merika et al., 1998), T-cell receptor α (Giese et al., 1995; Mayall et al., 1997), interleukin-4 (Henkel and Brown, 1994; Ranganath et al., 1998), and urokinase (De Cesare et al., 1995; De Cesare et al., 1997). Within the cell, multiple factors not only participate in the initiation of transcription but also share an active role in the regulation of gene expression. In addition, from the data available on eukaryotic transcription, it is clear that the mechanisms by which transcription is regulated are tremendously complex.

The data shown here in this chapter would agree with findings of other investigators regarding the complex transcription factor binding patterns in inducible enhancer elements. Perhaps the most studied eukaryotic enhancer element, the β-interferon enhancer, demonstrates the combinatorial complexity of inducible enhancers. *In vitro*, it requires the binding of five different DNA binding proteins in order to simulate the *in vivo* levels of inducible gene expression. The *MnSOD* enhancer element likely requires a similar complex combination of DNA binding proteins to simulate the *in vivo* levels of inducible expression. The *in vivo* footprinting data would suggest that multiple proteins bind within the enhancer element (Figure 4-1). From the enhancer mutagenesis experiments, I would propose that interaction of the enhancer element with multiple DNA binding proteins is necessary to achieve the inducible expression seen *in vivo*. Mutations created within the enhancer at site 2 appear to disrupt the inducible levels of transcription as compared to the wild-type (WT) vector (Figures 4-4 and 4-5).

A protein binding at the putative site 2 may be found in further experiments to be a crucial member of the protein DNA enhancer complex. Also, when mutations were made individually at sites 4a and 4b, no significant reduction in inducible gene expression was seen (Figure 4-4). When the mutated sites were combined in a single vector, a reduction in the amount of inducible expression was observed, not unlike that seen in the deletion experiments of chapter 3 (Figures 3-5B and 3-7B). So there may be another putative protein that is integral to the inducible activity of the enhancer. This additional data lends further support for the hypothesis that this is a complex enhancer with interacting elements.

Many more experiments will need to be done with this regulatory element. More *in vivo* footprinting data, will be necessary to get a clear picture of the proteins binding to both strands of the enhancer element. Perhaps a different technique of footprinting, such as DNase I footprinting, may delineate the protein boundaries better than DMS footprinting since the GC ratio of this region of the *MnSOD* gene is only about 40% compared to the promoter which is over 70% GC-rich. Further combinations of mutagenesis combined with transient transfections may answer the questions regarding the cooperativity of the proteins binding in this regulatory region. Perhaps, rather than mutagenesis, simply altering the phasing by inserting DNA (6 bp) in key regions between putative binding sites may be enough to disrupt the protein complex formation. Finally, cloning the factors binding to the important putative binding sites within the enhancer will be necessary to allow evaluation of the inducible transcriptional regulation in an *in vitro* system.

CHAPTER 5
REACTIVE OXYGEN SPECIES AND MITOCHONDRIA-TO-NUCLEUS SIGNALING

Introduction

Manganese superoxide dismutase (MnSOD), a vital anti-oxidant enzyme localized to the mitochondrial matrix, catalyzes the dismutation of superoxide anions ($O_2^{\cdot-}$) to hydrogen peroxide (H_2O_2). In aerobic cells, the mitochondrial electron transport chain is probably the most abundant source of $O_2^{\cdot-}$. At atmospheric oxygen concentrations, it is estimated that between 1 to 3% of the O_2 reduced in the mitochondrial electron transport chain during ATP production may form $O_2^{\cdot-}$(Chance et al., 1979; Beyer, 1990; Nohl et al., 1996). Although $O_2^{\cdot-}$and other reactive oxygen species (ROS) are byproducts of normal respiration, imbalance or loss of cellular homeostasis results in oxidative stress, causing damage to cellular components - lipid membranes, proteins, and nucleic acids (Freeman and Crapo, 1982; Fridovich, 1986). *MnSOD* acts as the first line of cellular defense to detoxify these $O_2^{\cdot-}$(Fridovich, 1975). Various inflammatory mediators (TNF-α, IL-1 β, IL-6 and LPS) in multiple tissues have been demonstrated to elicit dramatic elevations of both the messenger RNA and protein levels of MnSOD (Visner et al., 1990; Dougall and Nick, 1991; Visner et al., 1991; Valentine and Nick, 1992; Visner et al., 1992; Eastgate et al., 1993). The increased levels of *MnSOD* have been shown to be cytoprotective (Wong and Goeddel, 1988; Wong et al., 1989; Warner et al., 1991; Wispe et al., 1992). However, the signaling

pathways responsible for *MnSOD* expression are numerous and are still far from being fully elucidated.

Elaborate intercommunications take place between the nucleus and mitochondria coordinating not only mitochondrial gene expression and genome maintenance, but also nuclear gene expression (Poyton and McEwen, 1996). The classic view has been that mitochondria simply function as organelles responding to changes in energy demand. However, recent data would suggest a more complex picture where mitochondria also function as active signaling organelles in a number of important intracellular pathways (Surpin and Chory, 1997; Ichas and Mazat, 1998; Mignotte and Vayssiere, 1998; Chandel and Schumacker, 1999). An example of such a complex signaling pathway would be the role that mitochondria play in regulating cellular apoptosis initiated by TNF-α at membrane receptors (Duriez et al., 2000).

It is well documented that TNF-α binding to membrane receptors triggers complex signal transduction cascades (Feng et al., 1995; Warner et al., 1996; De Keulenaer et al., 2000), some of which result in excess ROS production in the mitochondria (Schulze-Osthoff, 1992; Schulze-Osthoff, 1993). The cytocidal-effect of these ROS is either direct or necessary for downstream signaling events leading to cell death. The crucial toxic role of ROS was demonstrated by the inhibition of mitochondrial electron transport at specific sites, which differentially interferes with TNF-α-mediated cytotoxicity (Schulze-Osthoff, 1992) and by the correlation between sensitivity to TNF-α cytotoxicity and mitochondrial activity in the cell (Schulze-Osthoff, 1993). Pharmacological experiments revealed that the mitochondrial respiratory chain is the major source of TNF-α-induced ROS (Schulze-Osthoff, 1992; Schulze-Osthoff,

1993; Goossens et al., 1996). Antioxidants inhibit various actions of TNF-α (transcription factor activation, gene expression, and cytotoxicity), and exogenously added ROS mimic its biological action (Kinnula et al., 1998; Arai et al., 1998; Gottlieb et al., 2000). Our data would agree with the literature regarding ROS and TNF-α.

Since the superoxide radical, a central ROS, is the substrate for *MnSOD*, it would lead to reason that the level of intracellular ROS might regulate *MnSOD* transcription. In this dissertation, I show that inhibition of mitochondrial electron transport results in the loss of TNF-α-stimulated *MnSOD* expression, most likely due to the loss of mitochondria-to-nucleus signaling with ROS acting as the second-messenger in the signal transduction pathway. In addition, I demonstrate that although inflammatory mediators (TNF-α, IL-1β, and LPS) may elicit similar inducible mRNA levels of *MnSOD*, the signaling pathways leading to this expression are very different.

Results

Mitochondrial Electron Transport Inhibitors Modulate TNF-α-Induced Expression of *MnSOD* in Pulmonary Epithelial Cells.

Previous analysis of the effects of mitochondrial electron transport chain inhibitors showed that, depending on the inhibitor's site of action, the cytotoxicity of TNF-α was either increased or decreased (Schulze-Osthoff, 1992). A schematic of the mitochondrial respiratory chain is shown in Fig. 5-1A. Based on earlier experiments demonstrating stimulated expression of *MnSOD* mRNA following treatment of a rat pulmonary epithelial-like cell line (L2 cells) with inflammatory mediators (Visner et al., 1990; Visner et al., 1991), I initiated studies to evaluate the effect of TNF-α on *MnSOD* expression in cells also treated with mitochondrial respiratory chain inhibitors.

Figure 5-1. A. Simplified scheme of the respiratory chain showing sites of substrate entry, inhibitor action, and potential sites of superoxide anion formation. Cyt, cytochrome; UQ, ubiquinone; Fe-S, iron sulfur center; HQNO, 2-heptyl-4-hydroxyquinoline N-oxide. B. Northern analysis of RNA from pulmonary epithelial cells exposed to TNF-α and/or mitochondrial inhibitors. Inhibition of TNF-α-stimulated induction of MnSOD by amobarbital (50 and 400 mM) and antimycin A (12.5 and 50 mM) in rat pulmonary epithelial cells (L2 cells) either untreated or treated with mitochondrial inhibitors alone or in combination with TNF-a (10 ng/ml) or with TNF-α alone. Control lanes 2 and 3 contain 0.1 and 0.5% ethanol, which were used as the solvent for all inhibitors not soluble in water.

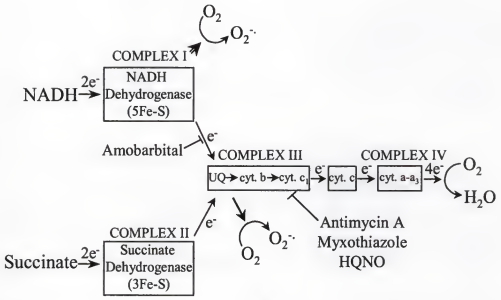
O_2
$O_2^{\cdot-}$
COMPLEX I
NADH
2e⁻
NADH Dehydrogenase (5Fe-S)
e⁻
Amobarbital
COMPLEX III
UQ → cyt. b → cyt. c_1
e⁻
cyt. c
e⁻
COMPLEX IV
cyt. a-a_3
4e⁻
O_2
H_2O
COMPLEX II
Succinate
2e⁻
Succinate Dehydrogenase (3Fe-S)
e⁻
$O_2^{\cdot-}$
O_2
Antimycin A
Myxothiazole
HQNO

A

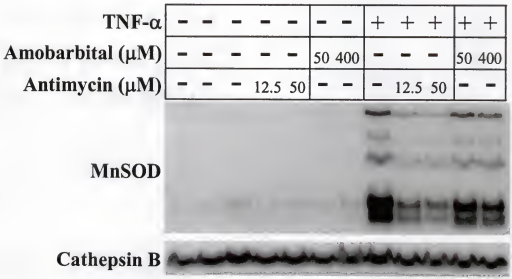
TNF-α
Amobarbital (μM)
Antimycin (μM)
MnSOD
Cathepsin B

B

Fig. 5-1B illustrates the effects of treatment of L2 cells with antimycin A or amobarbital, and/or TNF-α. The control samples exhibit a low constitutive level of expression of *MnSOD* mRNA. Addition of antimycin A or amobarbital at increasing concentrations (Schulze-Osthoff, 1992) did not affect this constitutive *MnSOD* mRNA expression. Maximal induction of *MnSOD* mRNA levels with TNF-α occurs after 8 hours, and thus this time point was selected for isolation of RNA for northern analysis. Co-treatment with TNF-α and antimycin A simultaneously caused a marked decrease in *MnSOD* mRNA expression at both concentrations of antimycin A (Schulze-Osthoff, 1992). Amobarbital, which blocks electron transfer through complex I (Fig. 5-1A), had minimal effect on TNF-α-induced expression of *MnSOD* mRNA compared to antimycin A. Microscopic examination at 8 hours showed no apparent difference in the cellular viability between control and treated cells.

Antimycin A Strongly Decreases TNF-α-Inducible *MnSOD* Expression in Pulmonary Endothelial Cells.

With the results shown in Fig. 5-1B, we proceeded to evaluate the cellular specificity of the mitochondrial inhibitor, antimycin A, studying its effects on another cell type, the rat pulmonary artery endothelial cell line (VA cells, Visner et al., 1992). Observing that the two concentrations of antimycin A used in the pulmonary epithelial cell experiments (Fig. 5-1B) gave similar results in the inhibition of TNF-α-stimulated *MnSOD* mRNA levels and based on that fact that much lower concentrations of antimycin A are effective at inhibiting mitochondrial electron transport, we tested

Figure 5-2. A. Northern analysis of RNA from pulmonary artery endothelial cells exposed to TNF-α and/or antimycin A. Inhibition of TNF-α-stimulated induction of MnSOD by antimycin A in rat pulmonary endothelial cells (VA cells) either untreated or treated with increasing concentrations of antimycin A alone or in combination with TNF-α (10 ng/ml) or with TNF-α alone. B. Northern analysis of RNA from pulmonary artery endothelial cells exposed to TNF-α and myxothiazole. Inhibition of TNF-α-stimulated induction of MnSOD in rat pulmonary endothelial cells (VA cells) either untreated or treated with increasing concentrations of myxothiazole alone or in combination with TNF-α (10 ng/ml) or TNF-α alone.

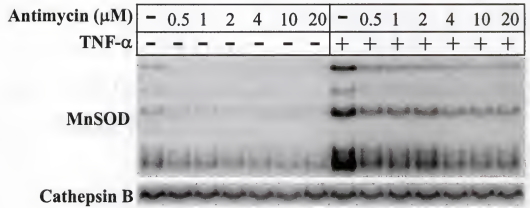
Antimycin (μM) - 0.5 1 2 4 10 20 - 0.5 1 2 4 10 20
TNF-α - - - - - - - + + + + + + +
MnSOD
Cathepsin B

A

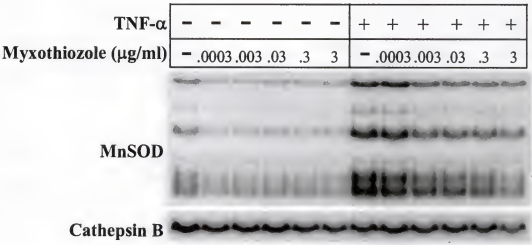
TNF-α - - - - - - + + + + + +
Myxothiozole (μg/ml) - .0003 .003 .03 .3 3 - .0003 .003 .03 .3 3
MnSOD
Cathepsin B

B

concentrations from 0.5 to 20 μM to find the optimum inhibitory concentration in the VA cells. Fig. 5-2A illustrates the effects of increasing concentrations of antimycin A on *MnSOD* mRNA levels. The maximal inhibition was achieved at a concentration of 4 μM. Using this concentration of antimycin A, I tested the effect on TNF-α-stimulated expression over 24 hours. The maximal inhibition appears to occur between 8 to 12 hours when both TNF-α and antimycin A are added simultaneously (data not shown). Furthermore, the sequence of addition of TNF-α or antimycin A to the cells was important for the TNF-α-stimulated expression of *MnSOD* mRNA. If TNF-α was added as little as 15 minutes prior to antimycin A, the diminution of the inducible expression was dramatically reduced (data not shown). Other investigators have found that pretreatment of L929 cells with mitochondrial inhibitors resulted in a significant decrease in binding of TNF to cell surface receptors (Sanchez-Alcazar et al., 1995). Thus, all the cell treatments in these experiments were done simultaneously.

Treatment of both pulmonary epithelial and endothelial cells with the complex III inhibitor, antimycin A, showed dramatic inhibition of TNF-α-induction of *MnSOD* mRNA. With this in mind, I decided to test whether another complex III inhibitor would give similar results. The inhibitors, antimycin A and myxothiazol, both block electron transport at the cytochrome b_1-c segment of the mitochondrial respiratory chain, but at different binding sites (Thierbach and Reichenbach, 1981; Iwata et al., 1998). Fig. 5-2B shows the effects of increasing concentrations of myxothiazol on TNF-α-stimulated expression of *MnSOD* mRNA. The extent of inhibition by myxothiazol is very similar to the pattern observed for antimycin A, which might be expected considering the proximity of the binding of antimycin and myxothiazole in the cytochrome b_1-c crystal structure

(Iwata et al., 1998). Interestingly, the inhibition of gene expression by these electron transport inhibitors is exquisitely specific since 2-heptyl-4-hydroxyquinoline N-oxide (HQNO), which also inhibits complex III, but at a different site, does not alter TNF induction of *MnSOD* (data not shown). These results would suggest that inhibition of mitochondrial electron transport at complex III alters production of ROS that can act in retrograde communication with the nucleus.

The Signaling Pathway for TNF-α Is Different from the Pathways for LPS- or IL-1-Stimulated Expression of *MnSOD*.

Previously, it has been shown that both lipopolysaccaride (LPS) and interleukin-1 (IL-1) also induce expression of *MnSOD* in both pulmonary epithelial and endothelial cells (Visner et al., 1990; Visner et al., 1992). Maximal induction occurs at 8 to 12 hours similar to TNF-α. To evaluate whether signaling pathways for all three inflammatory mediators were similar when mitochondrial respiration is inhibited with antimycin A, I examined the effect that increasing concentrations of antimycin A had on the LPS- and IL-1-stimulated expression of *MnSOD* in VA cells (Fig. 5-3A). Only at the highest concentration of antimycin A did the level of stimulated expression of *MnSOD* vary even slightly from LPS or IL-1 alone. This would suggest that the intracellular signaling pathway of TNF-α is different from that of LPS or IL-1.

TNF-α-stimulated expression of *MnSOD* is unaffected by antimycin A in a resistant fibroblast cell line. To demonstrate that the effects of antimycin A are directly associated with mitochondrial inhibition and not due to other possible side effects, I obtained an antimycin-resistant mouse fibroblast mutant cell line, LA9 (Howell et al., 1983). In this mutant, the rate of respiration is normal, but electron transport through the

Figure 5-3. A. Northern analysis of RNA from pulmonary artery endothelial cells exposed to lipopolysaccaride (LPS) or interleukin-1 and/or antimycin A. Inhibition of LPS- and IL-1-stimulated induction of MnSOD in rat pulmonary endothelial cells (VA cells) either untreated or treated with increasing concentrations of antimycin A alone or in combination with LPS (0.5 mg/ml) or IL-1β (2 ng/ml) or with LPS or IL-1β alone. B. Northern analysis of RNA from antimcyin-resistant murine fibroblast cells exposed to TNF-α and/or antimycin A. Inhibition of TNF-α-stimulated induction of MnSOD in a murine fibroblast antimycin-resistant cell line (LA9, 31) either untreated or treated with increasing concentrations of antimycin A alone or in combination with TNF-α (10 ng/ml) or TNF-α alone.

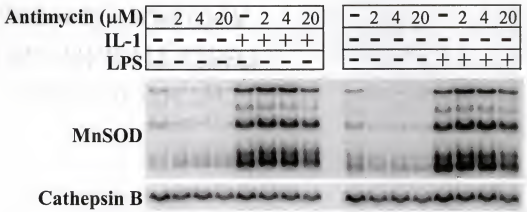
Antimycin (μM) - 2 4 20 - 2 4 20 - 2 4 20 - 2 4 20
IL-1 - - - - + + + + - - - - + + + +
LPS - - - - - - - - - - - - + + + +
MnSOD
Cathepsin B

A

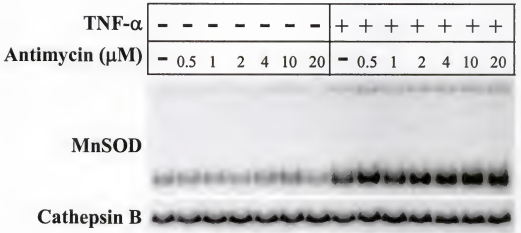
TNF-α - - - - - - - - + + + + + + + +
Antimycin (μM) - 0.5 1 2 4 10 20 - 0.5 1 2 4 10 20
MnSOD
Cathepsin B

B

succinate-cytochrome c oxidoreductase segment of the mitochondrial respiratory chain, which includes cytochrome b, shows resistance to inhibition by antimycin A. Fig. 5-3B illustrates the effect of TNF-α on the expression of MnSOD in the mutant LA9 cells. I should point out that previously it has been demonstrated that the five separate *MnSOD* mRNA transcripts in the rat result from alternative polyadenylation (Hurt et al., 1992); however, there are only two murine *MnSOD* transcripts at 1 Kb and 4 Kb. At concentrations of antimycin A varying from 0.5 to 20 μM, TNF-α continued to induce *MnSOD* mRNA levels demonstrating the specificity of the antimycin action in VA cells.

Inhibition of Mitochondrial ATPase with Oligomycin also Represses TNF-α-Stimulated Expression of *MnSOD*.

Oligomycin, which inhibits F_1F_O ATPase, causes uncoupling of mitochondrial respiratory electron transport and ATPase activity. Previous work by other investigators has demonstrated that cells treated with TNF-α results in an increase in oligomycin-sensitive mitochondrial respiration (Sanchez-Alcazar et al., 1997), with the resultant increase in ROS. However, cells treated with both TNF-α and oligomycin resulted in decreased levels of cellular ATP as well as blockade of the increase in ROS generation (Sanchez-Alcazar et al., 1997). To evaluate whether oligomycin treatment of VA cells would inhibit TNF-α-induction of *MnSOD*, I treated VA cells with increasing concentrations of oligomycin in the presence and absence of TNF-α. The results shown in Fig. 5-4 would indicate that oligomycin inhibits TNF-α-inducible *MnSOD* expression and that this inhibition is likely due to the decreased mitochondrial ATP and/or ROS levels.

Figure 5-4. Northern analysis of RNA from pulmonary artery endothelial cells exposed to TNF-α and oligomycin. Inhibition of TNF-α-stimulated induction of *MnSOD* in rat pulmonary endothelial cells (VA cells) either untreated or treated with increasing concentrations of oligomycin alone or in combination with TNF-α (10 ng/ml) or TNF-α alone.

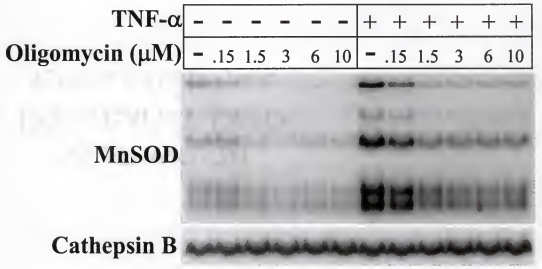
TNF-α - - - - - - + + + + + +
Oligomycin (μM) - .15 1.5 3 6 10 - .15 1.5 3 6 10
MnSOD
Cathepsin B

Figure 5-5. Northern analysis of RNA from pulmonary artery endothelial cells exposed to TNF-α and/or N-acetyl cysteine (NAC). Inhibition of TNF-α-stimulated induction of *MnSOD* in pulmonary artery endothelial cells (VA cells) either untreated or treated with various increasing concentrations of NAC alone or in combination with TNF-α (10 ng/ml) or TNF-α alone.

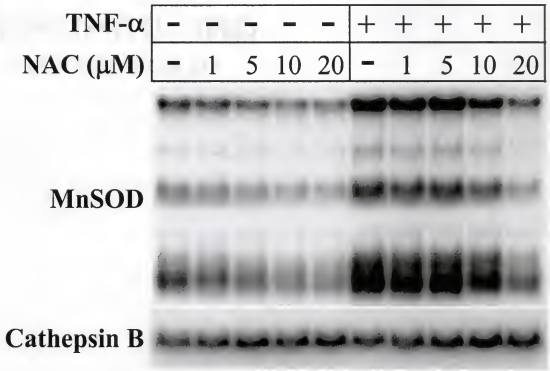
TNF-α - - - - - + + + + +
NAC (μM) - 1 5 10 20 - 1 5 10 20
MnSOD
Cathepsin B

Reactive Oxygen Species Are Important for TNF-α-Stimulated Expression of *MnSOD*.

Since levels of ROS have previously been shown to be decreased in cells treated with antimycin A (Boveris and Chance, 1973; Tan et al., 1998), I made use of the antioxidant, N-acetyl cysteine (NAC), to evaluate whether ROS scavenging can modulate TNF-α-inducible expression of *MnSOD*. NAC caused a dose-dependent decrease in the TNF-α-stimulated expression of *MnSOD* to baseline levels with no detectable effect on cell viability (Fig. 5-5). Of note, the concentrations of NAC capable of decreasing *MnSOD* expression are far below the millimolar levels used in much of the literature, demonstrating the potential importance of ROS in TNF-α-mediated signal transduction and the sensitivity of ROS in retrograde mitochondria-to-nucleus communication.

TNF-α-Stimulated Expression of *MnSOD* in Endothelial Cells Is Dependent on Cytoplasmic Phospholipase A_2 ($cPLA_2$).

Several studies have demonstrated the connection between arachidonic acid and mitochondrial ROS production (Bondy and Marwah, 1995; Li and Cathcart, 1997; Cocco et al., 1999; Woo et al., 2000). To explore whether inhibition of $cPLA_2$ and thus mitochondrial ROS affect *MnSOD* expression, we utilized the potent and selective $cPLA_2$ inhibitor, arachidonyl trifluoromethyl ketone ($AACOCF_3$) (Li and Cathcart, 1997). This inhibitor caused a dose-dependent repression of *MnSOD* expression in TNF-α-stimulated endothelial cells (Fig. 5-6A), whereas $AACOCF_3$ had no effect on IL-1β-stimulated cells (Fig. 5-6B).

Figure 5-6. A. Northern analysis of RNA from pulmonary artery endothelial cells exposed to TNF-α and/or $cPLA_2$ inhibitor ($AACOCF_3$). Inhibition of TNF-α-stimulated induction of *MnSOD* in pulmonary artery endothelial cells (VA cells) either untreated or treated with increasing concentrations of $AACOCF_3$ alone or in combination with TNF-α (10 ng/ml) or TNF-α alone. B. Northern analysis of RNA from pulmonary artery endothelial cells exposed to IL-1β and $cPLA_2$ inhibitor ($AACOCF_3$). Inhibition of IL-1-stimulated induction of MnSOD in pulmonary artery endothelial cells either untreated or treated with increasing concentrations of $AACOCF_3$ alone or in combination with IL-1β(2 ng/ml) or IL-1β alone.

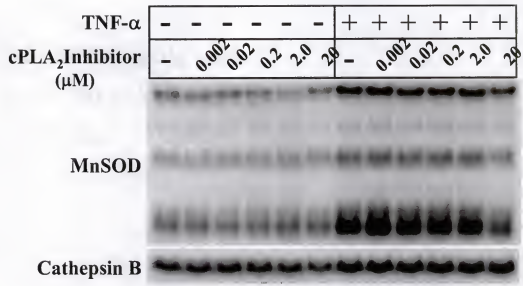
TNF-α
- - - - - - + + + + + +
cPLA2Inhibitor (μM)
- 0.002 0.02 0.2 2.0 20 - 0.002 0.02 0.2 2.0 20
MnSOD
Cathepsin B

A

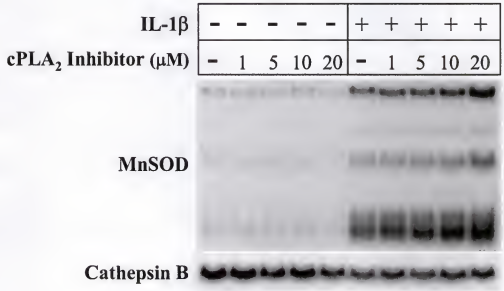
IL-1β
- - - - - + + + + +
cPLA2 Inhibitor (μM)
- 1 5 10 20 - 1 5 10 20
MnSOD
Cathepsin B

B

Figure 5-7. A. Northern analysis of RNA from pulmonary artery endothelial cells exposed to TNF-α and/or I kappa kinase (IκK) inhibitor (Bay 11-7082). Inhibition of TNF-α-stimulated induction of *MnSOD* in pulmonary artery endothelial cells (VA cells) either untreated or treated with increasing concentrations of IκK inhibitor alone or in combination with TNF-α (10 ng/ml) or TNF-α alone. B. Northern analysis of RNA from pulmonary artery endothelial cells exposed to IL-1β and/or I kappa kinase (IκK) inhibitor (Bay 11-7082). Inhibition of IL-1β-stimulated induction of MnSOD in pulmonary artery endothelial cells (VA cells) either untreated or treated with increasing concentrations of IκK inhibitor alone or in combination with IL-1β (2 ng/ml) or IL-1β alone.

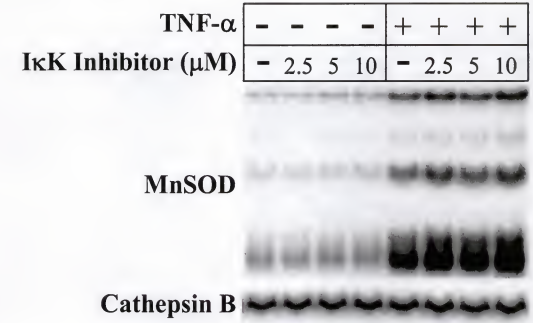
TNF-α
- - - - + + + +
IκK Inhibitor (μM)
- 2.5 5 10 - 2.5 5 10
MnSOD
Cathepsin B

A

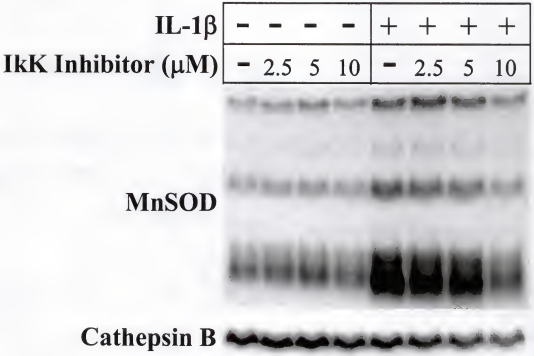
IL-1β
- - - - + + + +
IkK Inhibitor (μM)
- 2.5 5 10 - 2.5 5 10
MnSOD
Cathepsin B

B

Figure 5-8. Northern analysis of RNA from pulmonary artery endothelial cells exposed to TNF-α and/or MAP kinase inhibitor (PD98059). Levels of TNF-α-stimulated induction of *MnSOD* in pulmonary artery endothelial cells (VA cells) either untreated or treated with increasing concentrations of the MAP kinase inhibitor (PD98059) alone or in combination with TNF-α or TNF-α alone. Also, when the MAP kinase inhibitor, SB203580, was used in similar experiments, no alteration in TNF-α-inducible pattern of *MnSOD* was observed, almost identical to the above experiment with PD98059.

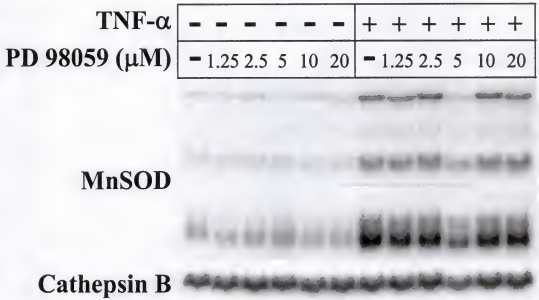
TNF-α
- - - - - - + + + + + +
PD 98059 (μM)
- 1.25 2.5 5 10 20 - 1.25 2.5 5 10 20
MnSOD
Cathepsin B

TNF-α-Inducible Expression of *MnSOD* Is Not Dependent on Nuclear Factor κB (NFκB).

Other investigators have shown that ROS activation by diverse conditions is important for gene activation by NFκB (Cocco et al., 1999). To investigate whether NFκB is important in TNF-α-signaling of *MnSOD*, I utilized the I kappa kinase (IκK) inhibitor, BAY 11-7082 (Pierce et al., 1997). At increasing concentrations of the IκK inhibitor, *MnSOD* expression in IL-1β-stimulated endothelial cells could be reduced to baseline (Fig. 5-7B), with no effect on TNF-α-stimulated cells (Fig. 5-7A). These data suggest that NFκB is activated in the IL-1β signaling pathway, but not in the TNF-α signaling pathway of *MnSOD*. Other kinase signaling pathways were also investigated by using specific inhibitors. The mitogen-activated protein (MAP) kinases are a group of protein serine/threonine kinases that are activated in response to a variety of extracellular stimuli and mediate signal transduction from the cell surface to the nucleus. Two of the MAP kinase pathways that have been implicated in TNF-α and IL-1 signal transduction are JUN/SAPK and p38. The JNK/SAPK (c-Jun kinase/stress activated protein kinase) cascade is activated following exposure to UV radiation, heat shock, or inflammatory cytokines. The p38 kinase (reactivating kinase) is the newest member of the MAP kinase family. It is activated in response to inflammatory cytokines, endotoxins, and osmotic stress. Selective inhibitors of the MKK1/2 (PD 98059) (Kultz et al, 1998) and p38 (SB 203580) (Kramer et al., 1996) were utilized at various concentrations to treat endothelial cells with or without TNF-α. No differences were seen between inducible expression of *MnSOD* with either of the inhibitors (representative example, Fig. 5-8) suggesting that

TNF-α signal transduction for *MnSOD* likely does not occur through these MAP kinase pathways.

Discussion

Manganese superoxide dismutase plays an important role in the cellular defense against superoxide produced by the mitochondrial electron transport chain during normal cellular metabolism (Wong and Goeddel, 1988; Wong et al., 1989; Warner et al., 1991; Wispe et al., 1992). Reduction or deficiency of *MnSOD* has been shown to promote cytotoxicity under conditions of oxidant stress (Li et al., 1995; Melov et al., 1998). A number of laboratories, including our own, have begun to understand the workings of the promoter and the intronic enhancer in causing the dramatic inducible expression of *MnSOD* (Jones et al., 1997; Kuo et al., 1999; Rogers et al., 2000). However, the molecular intracellular signaling pathways and the nature of the induction of *MnSOD* by various inflammatory mediators are still being unraveled.

Retrograde communication from the mitochondria to the nucleus likely consists of metabolic signals and transduction pathways that function across the inner mitochondrial membrane. Since ROS are very short-lived molecules closely regulated by a coordinated enzyme system, they could be potential signal transducers of putative mitochondria-to-nucleus signaling pathways. Production of ROS in the mitochondria is related to changes in electron flux through the respiratory chain, brought about by various physiological conditions, such as heat shock (Lambowitz et al., 1983); variations in oxygen tension (Kramer et al., 1983); and exposure to nitric oxide (Henry and Guissani, 1999). ROS have been found to act as second messengers in cellular functions such as cell growth and differentiation (Hansberg et al., 1993; Remacle et al., 1995). Mitochondrial respiration

has been linked to the expression of the mammalian gene, *GLUT1* (Ebert et al., 1995). Expression of the *GLUT1* gene, one of the isoforms of the glucose transporter, is enhanced by hypoxia and by exposing cells to inhibitors of mitochondrial respiration (Ebert et al., 1995). I, therefore, postulated that inhibition of mitochondrial respiration might also regulate *MnSOD* expression possibly through a mechanism involving intracellular levels of ROS.

Our data show that mitochondrial respiratory chain inhibitors, antimycin A (Fig. 5-1B, 5-2A) and myxothiazole (Fig. 5-2B) as well as the F_1F_O-ATPase inhibitor, oligomycin (Fig.5-4), can repress TNF-α-inducible expression of nuclear-encoded MnSOD. I have also addressed the specificity of the antimycin effects with studies in antimycin A-resistant LA9 mutant cells stimulated with TNF-α (Fig. 5-3B), further implicating ROS, ROS by-products and/or lipid peroxides as likely candidates for signal transduction from the mitochondria to the nucleus. In addition, other investigators have shown that sub-micromolar concentrations of arachidonic acid cause a substantial increase in ROS production in mitochondria (Cocco et al., 1999; Woo et al., 2000). The data in Fig. 5-6 would suggest that decreased levels of arachidonic acid, occurring as a result of selective blockade of $cPLA_2$ enzyme, is sufficient to inhibit the TNF-α-inducible expression of *MnSOD*. Thus oxidative events generated in the mitochondrion, not simply inhibition of energy-coupled processes, are crucial in TNF-α-induced MnSOD gene expression.

ROS or other mitochondrial intermediates may control both the cytotoxic and gene-regulatory effects of TNF-α, thus providing a basis for a mitochondria-to-nucleus signaling pathway, which requires bidirectional communication between the nucleus and

the mitochondria. While the cytotoxic activity of TNF-α seems to be rather restricted to tumor cells, nearly every cell type responds to TNF-α by the activation of a wide range of different genes (Lee et al., 1990). Transcriptional regulation of genes involves interaction of *cis*-acting elements of DNA with their cognate DNA-binding proteins. TNF-α induces activation of nuclear factors that act as 'third' messenger molecules specifically binding to *cis*-acting sequences. Perhaps the best understood example of the second messenger function of ROS is the activation of the mammalian transcription factor, NF-κB (Baeuerle and Baltimore, 1988). When activated, NF-κB induces the expression of various genes involved in inflammatory responses, immune cell regulation and differentiation (Baeuerle and Henkel, 1994). A diverse set of conditions can cause NF-κB activation with the common factor being the generation of ROS within the affected cells (Baeuerle and Baltimore, 1988; Baeuerle and Henkel, 1994). ROS are involved in the TNF-α signaling of *MnSOD* expression (Fig. 5-1,5-2,5-5), however my experiments with the Iκ kinase inhibitor (Fig. 5-7) would indicate that although NF-κB may be involved in IL-1β signaling, it is not involved in TNF-α-inducible expression of *MnSOD*. In addition, my data would also suggest that the MAP kinase pathways involving JNK/SAPK and p38 probably do not regulate expression of *MnSOD* (Fig. 5-8).

Thus, my data would suggest that multiple signaling pathways result in stimulated expression of *MnSOD*. Clearly, inhibition of mitochondrial electron transport alters inducible expression of *MnSOD* by TNF-α, but not IL-1 or LPS. Thus, it would appear that the TNF-α signaling pathway requires retrograde communication from the mitochondria to the nucleus, probably involving ROS. However, due to the high reactivity of ROS and their production within the mitochondrial membrane, it is much

more likely that the cytoplasmic signaling molecule of the TNF-α signaling pathway may be a protein acted upon by a lipid peroxide or other ROS or even the lipid peroxide itself. Our data with the $cPLA_2$ inhibitor would seem to bolster this argument in the TNF-α pathway. Other investigators have shown that TNF-α-induced ROS production requires $cPLA_2$ and 5-lipoxygenase activity, but not cyclooxygenase activity in the Rac signal transduction cascade (Woo et al., 2000). This would suggest that ROS generation is dependent on synthesis of arachidonic acid and its subsequent metabolism to leukotrienes. In fact, exogeneously applied leukotriende B4 could increase mitochondrial ROS (Woo et al., 2000). A model of my proposed *MnSOD* signaling pathways is shown in Fig. 5-9, detailing the differences between the TNF-α and IL-1β pathways. It may be that a yet unidentified signal pathway protein is activated by ROS or a lipid peroxide moiety, causing binding within the enhancer of *MnSOD* to produce the dramatic inductions seen with TNF-α (Fig. 5-9).

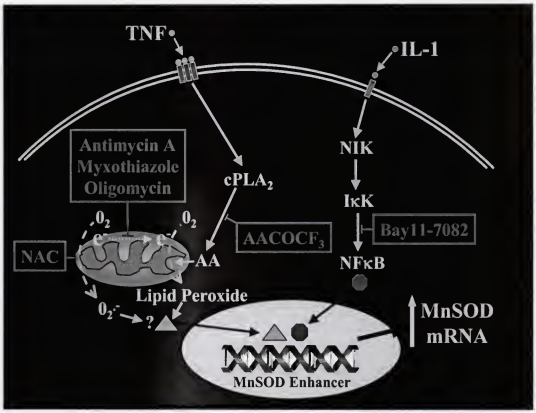

Figure 5-9. Model of TNF-α and IL-1 signal transduction pathways involved in inducible *MnSOD* expression. Mitochondrial inhibitors (antimycin A, myxothiazole) and F_1F_o-ATPase inhibitor (oligomycin) are shown to negatively affect mitochondrial production of ROS, which are involved in the TNF-α signaling pathway, but not the IL-1 pathway. The $cPLA_2$ inhibitor ($AACOCF_3$) diminishes production of arachidonic acid (AA), which increases mitochondrial production of ROS to produce potentially lipid peroxide species. Inhibitory k kinase (IκK) inhibitor (Bay 11-7082) inhibits phosphorylation of the Iκ subunit thus preventing separation of the Iκ subunit from nuclear factor kappa B (NF-κB) and blocking it from translocating into the nucleus.

CHAPTER 6
CONCLUSIONS AND FUTURE DIRECTIONS

Conclusions

Understanding transcriptional regulation began with the pioneering work of Jacob and Monod (Jacob and Monod, 1961) and progresses to this day at a dizzying rate. The interaction of protein transcription factors with DNA plays a critical role in this regulation. These protein-DNA interactions vary in response to both internal and external cellular environmental conditions and stimuli. It is the multitude of possible combinations of protein-DNA interactions, which give the cell such a variety of control mechanism. Perhaps the most thoroughly understood example of protein-DNA interaction involved in transcriptional regulation is the *lac* repressor-operator complex. Isolation of the *lac* repressor (Muller-Hill, 1996) permitted the kinetic studies, which were essential to understanding how protein-binding contributes to the regulatory mechanism. Further refinement of the regulatory mechanism was achieved by an examination *in vivo* of the *lac* repressor-DNA interactions (Nick and Gilbert, 1985). These and hundreds of other pieces of data culminated in understanding the regulatory mechanism of the *lac* operon (Muller-Hill, 1996). Almost 40 years elapsed before a full understanding of the *lac* operon could be attained. A full comprehension of the mechanisms regulating transcription in eukaryotes is unlikely to take less time.

Multiple examples of eukaryotic genes with complex enhancers exist in the literature, β-interferon (Kim and Maniatis, 1997, Merika et al., 1998), T-cell receptor α

(Giese et al., 1995; Mayall et al., 1997), interleukin-4 (Henkel and Brown, 1994; Ranganath et al., 1998), and urokinase (De Cesare et al., 1995; De Cesare et al., 1997), to name a few. From these and other studies two facts have become increasingly clear. First, within the cell the multiple factors that participate in the transcription process also play an active role in the regulation of gene expression. Second, from the data available on eukaryotic transcription, it is also clear that the mechanisms by which transcription is regulated are tremendously complex.

Eukaryotic transcriptional control entails the precise, sequential interaction of a variety of large enzymatic complexes that are recruited by sequence-specific promoter/enhancer-binding proteins. Control of transcriptional regulation is exerted at multiple levels of the process, which includes chromatin recognition and remodeling, covalent modification of histones, recruitment of co-activators and basal transcription components, and the assembly of an elongation-competent transcription complex that is capable of efficient processing through nucleosomal arrays.

Perhaps the earliest step in gene activation involves the mobilization of energy-dependent chromatin remodeling complexes. A number of different complexes capable of assembling and disrupting nucleosome arrays have been identified from yeast, *Drosophila*, and mammalian cells. Generally, these complexes are classified according to the identity of the catalytic ATPase and other shared subunits. Examples of such remodeling complexes in *Drosophila* would be the ACF (ATP-utilizing chromatin assembly and remodeling factor), NURF (nucleosome remodeling factor), and CHRAC (chromatin accessibility complex) complexes, which use the ATPase subunits of the ISWI (nucleosome ATPase) family, as do the two mammalian remodeling complexes,

remodeling and spacing factor (RSF) and human ATP-utilizing chromatin assembly and remodeling factor/Williams syndrome chromatin remodeling factor (hACF/WCRF) (Workman and Kingston, 1998). Other studies would suggest that in addition to the ATPase activity, histone deacetyltransferase complexes (p300 and TIF2) also are required (Kobayashi et al., 2000; Treuter et al., 1999). The interaction appears to be sequential with the ISWI remodeling complex functioning before the acetyltransferases to facilitate tight binding of the nuclear receptor heterodimer to chromatin. In the yeast gene, *PHO8*, transcriptional activation requires chromatin remodeling and acetyltransferase complexes to occur subsequent to binding of factors to the Upstream Activating Sequence (UAS)/enhancer (Gregory et al., 1999).

Histones, whether hypo- or hyperacetylated, contact DNA similarly, however, the acetylated particle is more asymmetric and the histone tails adopt a higher degree of α-helical structure (Workman and Kingston, 1998). In the absence of histone H1, the structural changes result in a less densely packed fiber. Histones H3 and H2B in core particles can also be modified through transglutamination (Ballestar et al., 1996), which provides a sensitive probe for nucleosome structure and possibly an additional regulatory modification *in vivo*. The decrease in chromatin compaction with histone acetylation is very relevant to the effects of acetyltransferases on transcriptional activity.

A number of transcriptional co-activators have been identified: vitamin D receptor interacting protein (DRIP), activator-recruited cofactor (ARC), negative regulator of activated transcription (NAT), thyroid hormone receptor-associated protein (TRAP). The TRAP complex was identified biochemically (Fondell et al., 1996) as a coactivator of the thyroid hormone receptor and has been found to be required for many other

promoter/enhancer-binding factors (Malik et al., 2000). These complexes bind with high affinity to several different types of transcription activation domains and may be a direct connection between promoter/enhancer-binding factors and RNA polymerase II. Coactivators may also act in an architectural manner to promote assembly of enhancer complexes or to regulate binding of specific promoter/enhancer factors to chromatin. One such coactivator, High Mobility Group I protein (HMG I), is distinguished by its ability to bind specifically in the narrow minor groove of AT-rich DNA (Churchill and Travers, 1991). HMG 1 does not function as a transcriptional activator on its own but rather influences the activities of other regulatory factors (Thanos et al., 1993). HMG 1 can interact directly with transcriptional activators of several families, including Rel (Thanos and Maniatis, 1992), bZip (Du et al., 1993), Ets (John et al., 1995), and POU (Leger et al., 1995). HMG I alters the conformation of the DNA (Falvo et al., 1995) and facilitates the assembly of a higher-order nucleoprotein complex in the IFN-β enhancer (Yie et al., 1997).

Most promoter elements contain one of two distinct core promoter structures that comprise a centrally located intiator (Inr) acting in concert with either an upstream TATA box or a downstream promoter element (DPE) to mediate basal transcription (Burke and Kadonaga, 1996; Burke and Kadonaga, 1997). Both the DPE and the TATA box are binding sites for TFIID, and the DPE is as common as the TATA box in *Drosophila* (Kutach and Kadonaga, 2000). Notable differences are observed in the ability of specific core promoters to respond to different enhancers (Ohtsuki et al., 1998). Thus, core promoter components can vary considerably among different tissues and in different

species, and the nature of the core promoter (e.g., containing a TATA box or DPE) will determine the responsiveness to different promoters/enhancers.

Another interesting consideration is that the components of the TFIID complex may also regulate transcription though modification of chromatin or other proteins. The TAFII-250 subunit of TFIID is not only both an acetyltransferase and a protein kinase, but can also catalyze the ATP-dependent ubiquitination of histone H1 *in vitro* (O'Brien and Tijan, 2000). Therefore, TAFII-250 appears to contain both ubiquitin-activating and ubiquitin-conjugating activities. A point mutation in Drosophila TAFII-250 abolished its ubiquitination acitivity *in vitro* and was found to reduce expression of several genes *in vivo* (Pham and Sauer, 2000). The preceding studies underscore the fact that regulatory complexes may contain multiple enzymatic activities and thus suggest a role for TAFII-250 and TFIID in the regulation of gene expression.

Signals in the form of interactions from the enhancer to the core promoter also affect the transition from initiation to elongation, and enhancer/promoter-specific factors may stimulate either or both of these processes. One example would be the HIV-1 Tat protein which associates with P-TEFb-CDK9 and strongly enhances carboxy-terminal-domain (CTD) phosphorylation at the Ser-5 position of RNA polymerase II (Okamoto et al., 1996; Parada and Roeder, 1996). Once initiation is established, however, nucleosomal structures present a barrier to elongation through genes. The chromatin-specific elongation factor, FACT (facilitates chromatin transcription) contains two subunits, Spt16 and SSRP1. The Spt16 subunit interacts directly with the histone deacetylase (HAT) protein, NuA3, whereas SSRP1 binds to the SWI/SNF-related protein, CHD1. An important function of FACT is its ability to facilitate removal of H2A-H2B

from chromatin, and FACT is unable to enhance transcription elongation from chromatin, when H2A-H2B dissociation is prevented by histone cross-linking (Orphanides et al., 1999).

Within eukaryotic chromosomes, open, accessible chromatin typically signifies active genes, which are interspersed with regions of more densely compacted chromatin (heterochromatin), which often harbors inactive genes. Within large regions of the genome, boundary/insulator elements separate independent regions of genetic activity. In *Drosophila*, a unique regulatory element has been defined, the promoter targeting sequence (PTS), which acting in a dominant fashion allows an enhancer to overcome the ability of an insulator to block enhancer-promoter interaction (Zhou and Levine, 1999). Also in *Drosophila*, an intriguing model for long-range enhancer-promoter interactions is proposed involving chromatin condensation whereby promoter-enhancer communication is structurally facilitated (Rollins et al., 1999). This seems to be mediated by a novel class of proteins, Nipped B, a homologue of chromosomal adherins, which have broad functions of sister chromatid cohesion, chromosome condensation, and DNA repair. This last mechanism of promoter-enhancer regulation is reminiscent of the concept of transvection first suggested by E. B. Lewis (Lewis, 1954).

In this research I have demonstrated that a small region of sequence within intron 2 of *MnSOD* is responsible for part of the induction seen when cells are stimulated by inflammatory mediators. Other mechanisms (chromatin remodeling, coactivators, posttranslational modifications), which may contribute to the transcriptional regulation, will be found through further study and experimentation. In addition, I have shown that the signaling pathways from the cell surface to the *MnSOD* gene are different and

dependent on the inflammatory stimulus. The result, increased *MnSOD* expression, may be similar for each of the inflammatory stimuli, but the pathways to the end are very different. This should come as no surprise. Each stimulus, as well as the level of stimulation, likely causes changes (both induction and suppression) in a variety of genes. It is the combination of expression products, which gives rise to the final cellular response.

Future Directions

The observation that the *MnSOD* gene has a complex enhancer element, which is responsive to multiple inflammatory stimuli is consistent with the observations of enhancers in other inducible genes (Kim and Maniatis, 1997; Giese et al., 1995; Henkel and Brown, 1994; De Cesare et al., 1995). As opposed to some of these other inducible enhancers, the transcription factors that bind to the *MnSOD* enhancer have yet to be identified. It will be necessary to start with these proteins as they are the first layer of the protein-enhancer complex which must form to cause the inducible expression seen by northern analysis.

To fully characterize the regulatory proteins that bind to the *MnSOD* enhancer element, it will be necessary to utilize a variety of techniques. As previously shown, the enhancer element can be shown to cause an inducible shift pattern on electromobility gel shift assay (EMSA). Further observations can be made by using the mutated regions for these same shifts under the same conditions as the wild-type enhancer to ascertain if the shifts are altered by the mutations. Data from such experiments might lend further support for a large inducible protein-DNA complex. Some evidence of functional alterations has been shown by transient transfections and northern analysis (Chapter 5).

If a transcription factor can be identified or speculated on by consensus-sequence, then further information could be obtained by super-shift EMSA with the transcription factor antibody, if available.

Since we have not identified any transcription factors, it will be necessary to choose a technique, which could provide these factors with a high-degree of reliability. One such commercially available technique would be the yeast one-hybrid system, using the enhancer sequence binding site(s) as bait to obtain the primary clone(s) of the trans-acting factors. Other techniques, which could be used to obtain proteins binding to the enhancer regions, would include: (1) the creation of a biotinylated enhancer region using biotinylated oligonucleotides as primers for PCR and using these DNA fragments in combination with streptavidin-coated magnetic beads to isolate nuclear proteins which would bind to the enhancer element. These nuclear fractions could be labeled with ^{35}S-methionine to allow identification on 2-D polyacrylamide gel electrophoresis. (2) the identification of proteins which interact with the transcription factors bound to the enhancer region could be isolated using the technique of *in vivo* formaldehyde cross-linking. Intact cells are treated with dilute solutions of formaldehyde, which produces protein-protein, protein-RNA, and protein-DNA cross-links within minutes. This would be followed by the lysis of cells and the isolation of virtually intact chromatin. The chromatin would be mechanically sheared to produce optimal chromatin DNA of around 600 bp. An important point of this technique is that at least one protein binding to the area of interest must be known for the next step. The sheared-soluble chromatin is immunoprecipitated with the antibody of the known binding protein to obtain a pure immuno-complex of all the proteins binding to the region of interest. The formaldehyde

cross-links are reversed and the DNA purified. The purified DNA can be used in one of two ways: (1) quantitative PCR analysis of genomic fragments using specific pairs of primers or (2) the immunoprecipitated DNA can be used as probe to scan specific genomic regions by Southern analysis.

In addition, further work is needed to characterize, in more detail, the transmembrane receptor-mediated intracellular signaling pathways, which all seem to culminate with increased expression of *MnSOD*. Knowing the diversity of signaling pathways inside the cell and the numerous proteins involved in the different pathways, it will be a challenging task to dissect out the individual elements to gain a keener understanding of the key regulatory elements. Possible avenues of experimentation would include obtaining plasmids containing the wild-type as well as mutated forms of the various intracellular signaling proteins that have thus far been identified (NF-κB, members of the TRAF family of proteins, members of the leukotriene enzyme cascade, to name a few), all with the intent of performing *in vivo* over-expression and dominant-negative studies as another means to elucidate which parts of the pathways are important for the individual transmembrane-receptor-mediated signals. Another possible series of experiments might involve obtaining either cells or the animals themselves of the "knock-outs" of the individual proteins of the signaling pathways. As more transgenic "knock-out" mice are created, a series of animals with specific deletions of signal pathway proteins may allow very precise *in vivo* experimentation of signal transduction pathways.

REFERENCES

Aggarwal, B. B., Kohr, W. J., Hass, P. E., Moffat, B., Spencer, S. A., Henzel, W. J., Bringman, T. S., Nedwin, G. E., Goeddel, D. V., and Harkins, R. N. (1985). Human Tumor Necrosis Factor. Production, Purification, and Characterization. J. Biol. Chem. 260:2345-2354.

Akashi, M., Hachiya, M., Paquette, R. L., Osawa, Y., Shimizu, S., and Suzuki, G. (1995). Irradiation Increases Manganese Superoxide Dismutase mRNA Levels in Human Fibroblasts. J. Biol. Chem. 270:15864-15869.

Andrews, N. C. and Faller, D. V. (1991). A Rapid Micropreparation Technique for Extraction of DNA-Binding Proteins from Limiting Numbers of Mammalian Cells. Nucleic Acids Res. 19:2499.

Arai, T., Kelly, S. A., Brengman, M. L., Takano, M., Smith, E. H., Goldschmidt-Clermon, P. J., and Bulkley, G. B. (1998). Ambient but Not Incremental Oxidant Generation Effects Intercellular Adhesion Molecule 1 Induction by Tumor Necrosis Factor alpha in Endothelium. Biochem. J. 331:853-861.

Assayama, K., and Burr, I. M. (1985). Rat Superoxide Dismutases. J. Biol. Chem. 260:2212-2217.

Auron, P. E., Webb, A. C., Rosenwasser, L. J., Mucci, S. F., Rich, A., Wolff, S. M., and Dinarello, C. A. (1984). Nucleotide Sequence of Human Monocyte Interleukin-1 Precursor cDNA. Proc. Natl. Acad. Sci. USA 81:7907-7911.

Auron, P. E., Rosenwasser, L. J., Matsushima, K., Copeland, T., Dinarello, C. A., Oppenheim, J. J., and Webb, A. C. (1985). Human and Murine Interleukin 1 Possess Sequence and Structural Similarities. J. Mol. Cell. Immunol. 2, 169-177.

Baeuerle, P. A., and Baltimore, D. (1988). I kappa B: A Specific Inhibitor of the NF-kappa B Transcription Factor. Science 242:540-546.

Baeuerle, P. A., and Henkel, T. (1994). Function and Activation of NF-kappa B in the Immune System. Ann. Rev. Immunol. 12:141-179.

Baker, K., Marcus, C. B., Huffman, K., Kruk, H., Malfroy, B., and Doctrow, S. R. (1998). Synthetic Combined Superoxide Dismutase/Catalase Mimetics Are Protective as A Displayed Treatment in a Rat Stroke Model: A Key Role for Reactive Oxygen Species in Ischemic Brain Injury. J. Pharmacol. Exp. Ther. 284:215-221.

Balentine, J. D. (1982). Pathology of Oxygen Toxicity. Academic Press, New York.

Ballestar, E., Abad, C., Franco, L. (1996). Core Histones Are Glutaminyl Substrates for Tissue Transglutaminase. J. Biol. Chem. 271:18817-18824.

Banerji, J., Rusconi, S., Schaffner, W. (1981). Expression of a β-Globin Gene is Enhanced by Remote SV40 DNA Sequences. Cell 27:299-308.

Banerji, J., Olson, L., and Schaffner, W. (1983). A Lymphocyte-Specific Cellular Enhancer Is Located Downstream of the Joining Region in Immunoglobulin Heavy Chain Genes. Cell 33, 729-740.

Bankers-Fulbright, J. L., Kalli, K. R., and McKean, D. J. (1996). Interleukin-1 Signal Transduction. Life Sci. 59:61-83.

Bannister, J. V., Bannister, W. H., and Rotilio, G. (1987). Aspects of the Structure, Function, and Applications of Superoxide Dismutase. CRC Crit. Rev. Biochem. 22:111-180.

Benoist, C., and Chambon, P. (1980). Deletions Covering the Putative Promoter Region of Early mRNAs of Simian Virus 40 Do Not Abolish T-Antigen Expression. Proc. Natl. Acad. Sci. USA 77:3865-69.

Benoist, C., and Chambon, P. (1981). *In Vivo* Sequence Requirements of the SV40 Early Promoter Region. Nature 290:304-10.

Beutler, B., Greenwald, D., Hulmes, J. D., Chang, M., Pan, Y. C., Mathison, J., Ulevitch, R., and Cerami, A. (1985). Identity of Tumor Necrosis Factor and the Macrophage Secreted Factor Cachectin. Nature 316, 552-554.

Beutler, B. and Cerami, A. (1989). The Biology of Cachectin/TNF – A Primary Mediator of the Host Response. Annu. Rev. Immunol. 7:625-655.

Beyer, R. E. (1990) The Participation of Coenzyme Q in Free Radical Generation and as An Antiooxidant. Free Rad. Biol. Med. 8:545-65.

Bigdeli, N., Niemann, A., Sandler, S., and Eizirik, D. L. (1994). Dissociation between Interleukin-1 beta-Induced Expression of mRNA for Superoxide Dismutase and Nitric Oxide Synthase in Insulin-Producing Cells. Biochem. Biophys. Res. Commun. 203:1542-1547.

Bondy, S. C., and Marwah, S. (1995). Stimulation of Synaptosomal Free Radical Production by Fatty Acids: Relation to Esterification and to Degree of Unsaturation. FEBS Lett. 375:53-55.

Borg, L. A., Cagliero, E., Sandler, S., Welsh, N., and Eizirik, D. L. (1992). Interleukin-1 beta Increases the Activity of Superoxide Dismutase in Rat Pancreatic Islets. Endocrinol. 130:2851-2857.

Boveris, A., and Chance, B. (1973). The Mitochondrial Generation of Hydrogen Peroxide. General Properties and Effect of Hyperbaric Oxygen. Biochem. J. 134:707-716.

Brody, D. T. and Durum, S. K. (1989). Membrane IL-1: IL-1 alpha Precursor Binds to the Plasma Membrane Via a Lectin-Like Interaction. J. Immunol. 143:1183.

Burke, T. W., Kadonaga, J.T. (1996). Drosophila TFIID Binds to a Conserved Downstream Basal Promoter Element that is Present in Many TATA-Box-Deficient Promoters. Genes Dev. 10:711-724.

Burke, T. W., Kadonaga, J.T. (1997). The Downstream Core Promoter Element, DPE, Is Conserved from Drosophila to Humans and Is Recognized by TAFII60 of Drosophila. Genes Dev. 11:3020-3031.

Callis, J., Fromm, M., and Walbot, V. (1987). Introns Increase Gene Expression in Cultured Maize Cells. Genes Dev. 1:1183-1200.

Carey, M., Lin, Y. S., Green, M. R., and Ptashne, M. (1990). A Mechanism for Synergistic Activation of a Mammalian Gene by GAL4 Derivatives. Nature 345:361-364.

Cerretti, D. P., Kozlosky, C. J., Mosley, B., Nelson, N., Van Ness, K., Greenstreet, T. A., March, C. J., Kronheim, S. R., Druck, T., Cannazarro, L. A. (1992). Molecular Cloning of the Interleukin-1 Beta Converting Enzyme. Science 256:97-100.

Chance, B., Sies, H., and Boveris, A. (1979). Hydroperoxide Metabolism in Mammalian Organisms. Physiol. Rev. 59:527-605.

Chandel, N. S., and Schumacker, P. T. (1999). Cells Depleted of Mitochondrial DNA (rho 0) Yield Insight into Physiological Mechanisms. FEBS Lett. 454:173-176.

Chesrown, S. E. (1994). Regulation of Manganese Superoxide Dismutase. Ph. D. Dissertation, University of Florida.

Chomczynski, P. and Sacchi, N. (1987). Single-step Method of RNA Isolation by Acid. Guanidinium Thio Cyanate-Phenol-Chloroform Extraction. Anal. Biochem. 162:156-159.

Church, G. M. and Gilbert, W. (1984). Genomic Sequencing. Proc. Natl. Acad. Sci. USA 81:1991-1995.

Churchill, M. E. A., and Travers, A. A. (1991). Protein Motifs that Recognize Structural Features of DNA. Trends Biochem. Sci. 16:92-97.

Clark, B. D., Collins, K. L., Gandy, M. S., Webb, A. C., and Auron, P. E. (1986). Genomic Sequence for Human Prointerleukin-1 beta: Possible evolution from a Reverse Transcribed Prointerleukin-1 alpha Gene. Nucl. Acids Res. 14:7897-7914.

Cocco, T., Di Paola, M., Papa, S., and Lorusso, M. (1999). Arachidonic Acid Interaction with the Mitochondrial Electron Transport Chain Promotes Reactive Oxygen Species Generation. Free Rad. Biol. Med. 27:51-59.

Cseh, K., and Beutler, B. (1989). Alternative Cleavage of the Cachectin/Tumor Necrosis Factor Propeptide Results in A Larger, Inactive Form of Secreted Protein. J. Biol. Chem. 264, 16256-16260.

De Cesare, D., Vallone, D., Caracciolo, A., Sassone-Corse, P., Nerlov, C., Verde, P. (1995). Heterodimerization of c-Jun with ATF-2 and c-Fos Is Required for Positive and Negative Regulation of the Human Urokinase Enhancer. Oncogene 11:365-376.

De Cesare, D., Palazzolo, M., Berthelsen, J., and Blasi, F. (1997). Characterization of UEF-4, A DNA-Binding Protein Required for Transcriptional Synergism between Two AP-1 Sites in the Human Urokinase Enhancer. J. Biol. Chem. 272:23921-23929.

Del Maestro, R. and McDonald, W. (1989). Subcellular Localization of Superoxide Dismutases, Glutathione Peroxidase, and Catalase in Developing Rat Cerebral Cortex. Mech. Aging Dev. 48:15-31.

Del-Vecchio, P. J., and Shaffer, J. B. (1991). Regulation of Antioxidant Enzyme Expression in LPS-treated Bovine Retinal Pigment Epithelial and Corneal Endothelial Cells. Curr. Eye Res. 10:919-925.

De Keulenaer, G. W., Ushio-Fukai, M., Yin, Q., Chung, A. B., Lyons, P. R., Ishizaka, N., Rengarajan, K., Taylor, W. R., Alexander, R. W., Griendling, K. K. (2000). Convergence of Redox Sensitive and Mitogen-Activated Protein Kinase Signaling Pathways in Tumor Necrosis Factor-Alpha-Mediated Monocyte Chemoattractant Protein-1 Induction in Vascular Smooth Muscle Cells. Arterioscler. Thromb. Vasc. Biol. 20:385-391.

De Villiers, J., and Schaffner, W. (1981). A Small Segment of Polyoma Virus DNA Enhances the Expression of a Cloned Beta-Globin Gene over a Distance of 1400 Base Pairs. Nucl. Acids Res. 9, 6251-6264.

Dinarello, C. A. (1992). The Biology of Interleukin-1. Chem. Immunol. 51:1-32.

Dougall, W. C. (1990). The Rat Manganese Superoxide Dismutase: Cloning and Gene Regulation. Ph.D. Dissertation, University of Florida.

Dougall, W. C. and Nick, H. S. (1991). Manganese Superoxide Dismutase:A Hepatic Acute Phase Protein Regulated by Interleukin-6 and Glucocorticoids. Endocrinology 129:2376-2384.

Du, W., Thanos, D., and Maniatis, T. (1993). Mechanisms of Transcriptional Synergism between Distinct Virus-Inducible Enhancer Elements. Cell 74:887-898.

Duriez, P. J., Wong, F., Dorovini-Zis, K., Shahidi, R., and Karsan, A. (2000). A1 Functions at the Mitochondria to Delay Endothelial Apoptosis in Response to Tumor Necrosis Factor. J. Biol. Chem. 275,18099-18107.

Eastgate, J., Moreb, J., Nick, H. S., Suzuki, K., Taniguchi, N., and Zucali, J. R. (1993). A Role for Manganese Superoxide Dismutasein Radioprotection of Hemopoeitic Stem Cells by Interleukin-1. Blood 81:639-646.

Ebert, B. L., Firth, J. D., and Ratcliffe, P. J. (1995). Hypoxia and Mitochondrial Inhibitors Regulate Expression of Glucose Transporter-1 Via Distinct *Cis*-Acting Sequences. J. Biol. Chem. 270:29083-29089.

Eddy, L. J., Goeddel, D. V., and Wong, G. H. (1992). Tumor Necrosis Factor-alpha Pretreatment is Protective in a Rat Model of Myocardial Ischemia-Reperfusion Injury. Biochem. Biophys. Res. Commun. 184:1056-1059.

Falvo, J. V., Thanos, D., and Maniatis, T. (1995). Reversal of Intrinsic DNA Bends in the IFNb Gene Enhancer by Transcription Factors and the Architectural Protein HMG I (Y). Cell 83:1101-1111.

Feng, L., Xia, Y., Garcia, G. E., Hwang, D., and Wilson, C. B. (1995). Involvement of Reactive Oxygen Intermediates in Cyclooxygenase-2 Expression Induced by Interleukin-1, Tumor Necrosis Factor Alpha, and Lipopolysaccharide. J. Clin. Invest. 95:1669-1675.

Fibbe, W. E., Schaafsma, M. R., Falkenburg, J. H. F., and Willemze, R. (1989). The Biological Activities of Interleukin-1. Blut. 59:147-156.

Fischer, E., Marano, M. A., Barber, A. E., Hudson, A., Lee, K., Rock, C.S., Hawes, A.S., Thompson, R. C., Hayes, T. J., Anderson, T. D. (1991). Comparison Between Effects of Interleukin-1 Alpha Administration and Sublethal Endotoxemia in Primates. Am. J. Physiol. 261:R442-452.

Flint, D. H., Tuminello, J. F., Emptage, M. H. (1993). The Inactivation of Fe-S Cluster Containing Hydro-lyases by $O_2^{\bullet-}$. J. Biol. Chem. 268:22369-22376.

Fondell, J.D., Ge, H., Roeder, R.G. (1996). Ligand Induction of Transcriptionally Active Thyroid Hormone Receptor Coactivator Complex. Proc. Natl. Acad. Sci. U S A 93:8329-8333.

Freeman, B. A. and Crapo, J. D. (1982). Free Radicals and Tissue Injury. Lab. Invest. 47:412-426.

Freeman, B. A., Mason, R. J., William, M. C., and Crapo, J. D. (1986). Antioxidant Enzyme Activity in Alveolar Type II Cells after Exposure of Rats to Hyperoxia. Exp. Lung Res. 10:203-222.

Fridovich, I. (1974). Superoxide Dismutases. Adv. Enzymol. 41:36-97.

Fridovich, I. (1975). Superoxide Dismutases. Ann. Rev. Biochem. 44:147-159.

Fridovich, I. (1978). The Biology of Oxygen Radicals. Science 201:875-880.

Fridovich, I. (1986). Superoxide Dismutases. Adv. Enzymol. 58:61-97.

Fridovich, I. (1986). Biological Effects of the Superoxide Radical. Arch. Biochem. Biophys. 247:1-11.

Fridovich, I. (1989). Superoxide Dismutases: An Adaptation to a Paramagnetic Gas. J. Biol. Chem. 264:7761-7764.

Fried, M. and Crothers, D. M. (1981). Equilibria and Kinetics of lac Repressor-Operator Interactions by Polyacrylamide Gel Electrophoresis. Nucl. Acids Res. 9:6505-6525.

Fromm, M., and Berg, P. (1983). Simian Virus 40 Early and Late Region Promoter Functions Are Enhanced by the 72 Base Pair Repeat Inserted at Distant Locations and Inverted Orientations. Mol. Cell. Biol. 3:991-99.

Fujii, J., and Taniguchi, N. (1991) Phorbol Ester Induces Manganese-Superoxide Dismutase in Tumor Necrosis Factor-Resistant Cells. J. Biol. Chem. **266,** 23142-23146.

Gallon, J. R. (1981). The Oxygen-sensitivity of Nitrogenase: A Problem for Biochemists and Microoganisms. Trends Biochem. Sci. 19.

Garrity, P. A. and Wold, B. J. (1992). Effects of Different DNA Polymerases in Ligation-Mediated PCR Enhanced Genomic Sequencing and *In Vivo* Footprinting. Proc. Natl. Acad. Sci. USA 89:1021-1025.

Ghosh, S., Latimer, R. D., Gary, B. M., Harwood, R. J., and Oduro, A. (1993). Endotoxin-induced Organ Injury. Crit. Care Med. 21:s19-24.

Gibbs, L. S., Del-Vecchio, P. J., and Shaffer, J. B. (1992). Mn and Cu/Zn SOD Expression in Cells from LPS-Sensitive and LPS-Resistant Mice. Free Rad. Biol. Med. 12:107-111.

Giese, K., Kingsley, C., Kirshner, J. R., Grosschedl, R. (1995). Assembly and Function of a TCR alpha Enhancer Complex is Dependent on LEF-1-Induced DNA Bending and Multiple Protein-Protein Interactions. Genes Dev. 9:995-1008.

Gilbert, D. L. (ed.) (1981). Oxygen and Living Processes: An Inter-Disciplinary Approach. Springer, New York.

Gillies, S. D., Morrison, S. L., Oi, V. T., Tonegawa, S. (1983). A Tissue-Specific Transcription Enhancer Element is Located in the Major Intron of a Rearranged Immunoglobulin Heavy Chain Gene. Cell 33:717-28.

Goeddel, D. V., Aggarwal, B. B., Gray, P. W., Leung, D. W., Nedwin, G. E., Palladino, M. A., Patton, J. S., Pennica, D., Shepard, H. M., and Sugarman, B. J. (1986). Tumor Necrosis Factors: Gene Structure and Biological Activities. Cold Spring Harb. Symp. Quant. Biol. 51 Pt 1:597-609.

Goodwin, R. G., Anderson, D., Jerzy, R., Davis, T., Brannan, C. I., Copeland, N. G., Jenkins, N. A., and Smith, C. A. (1991). Molecular Cloning and Expression of the Type 1 and Type 2 Murine Receptors for Tumor Necrosis Factor. Mol. Cell. Biol. 11:3020-3026.

Goossens, V., Grooten, J., and Fiers, W. (1996). The Oxidative Metabolism of Glutamine. A Modulator of Reactive Oxygen Intermediate-Mediated Cytotoxicity of Tumor Necrosis Factor in L929 Fibrosarcoma Cells. J. Biol. Chem. 271:192-196.

Gottlieb, E., Vaner Heiden, M. G., and Thompson, C. B. (2000). Bcl-x(L) Prevents the Initial Decrease in Mitochondrial Membrane Potential and Subsequent Reactive Oxygen Species Production during Tumor Necrosis Factor alpha-Induced Apoptosis. Mol. Cell. Biol. 20:5680-5689.

Gorman, C. M., Merlino, G. T., Willingham, M. C., Pastan, I., and Howard, B. H. (1982). The Rous Sarcoma Virus Long Terminal Repeat Is a Strong Promoter when Introduced into a Variety of Eukaryotic Cells by DNA-Mediated Transfection. Proc. Natl. Acad. Sci. USA 79, 6777-6781.

Gregory P. D., Schmid, A., Zavari, M., Munsterkotter, M., and Horz, W. (1999) Chromatin Remodelling at the *PHO8* Promoter Requires SWI-SNF and SAGA at a Step Subsequent to Activator Binding. EMBO J.18:6407-6414.

Grosschedl, R., and Birnstiel, M. L. (1980a). Identification of Regulatory Sequences in the Prelude Sequence of an H2A Histone Gene by the Study of Specific Deletion Mutants *In Vivo*. Proc. Natl. Acad. Sci. USA 77:1432-36.

Grosschedl, R., and Birnstie., M. L. (1980b). Spacer DNA Sequences Upstream of the TATAATA Sequence are Essential for Promotion of H2A Histone Gene Transcription *In Vivo*. Proc. Natl. Acad. Sci. USA 77:7102-6.

Grosschedl, R. (1995). Higher-Order Nucleoprotein Complexes in Transcription:Analogies with Site-Specific Recombination. Curr. Opin. Cell Biol. 7:362-370.

Gruss, P., Dhar, R., Khoury, G. (1981). Simian Virus 40 Tandem Repeated Sequences as an Element of the Early Pomoter. Proc. Natl. Acad. Sci. USA 78:943-47.

Gullberg, U., Lantz, M., Lindvall, L., Olsson, I., and Himmler, A. (1992). Involvement of an Asn/Val Cleavage Site in the Production of a Soluble Form of a Human Tumor Necrosis Factor (TNF) Receptor. Site-Directed Mutagenesis of a Putative Cleavage Site in the p55 TNF Receptor Chain. Eur. J. Cell. Biol. 58:307-412.

Gwinner, W., Tisher, C. C., and Nick, H. S. (1995). Regulation of Manganese Superoxide Dismutase in Glomerular Epithelial Cells: Mechanisms of Interleukin-1 Induction. Kidney Int. 48:354-362.

Halliwell, B. (1984). Chloroplast Metabolism. Oxford University Press, Oxford.

Halliwell, B. and Gutteridge, J. M. (1990). Role of Free Radicals and Catalytic Metal Ions in Human Disease: An Overview. Methods Enzymol. 186:1-85.

Halliwell, B. and Gutteridge, J. M. C. (1999). Free Radicals in Biology and Medicine. Oxford Science Publications, Oxford.

Hansberg, W., de Groot, H., and Sies, H. (1993). Reactive Oxygen Species Associated with Cell Differentiation in Neurospora crassa. Free Rad. Biol. Med. 14:287-293.

Harris, C. A., Derbin, K. S., Hunte McDonough, B., Krauss, M. R., Chen, K. T., Smith, D. M., and Epstein, L. B. (1991). Manganese Superoxide Dismutase is Induced by IFN-gamma in Multiple Cell Types. Synergistic Induction by IFN-gamma and Tumor Necrosis Factor or IL-1. J. Immunol. 147, 149-154.

Hassan, H. M., and Sun, H. C. (1992). Regulatory Roles of Fnr, Fur, and Arc in Expression of Manganese-Containing Superoxide Dismutase in Escherichia coli. Proc. Natl. Acad. Sci. USA 89, 3217-3221.

Haugaard, N. (1968). Cellular Mechanisms of Oxygen Toxicity. Physiol. Rev. 48:229.

Hausladen, A., and Fridovich, I. (1994). Superoxide and Peroxynitrite Inactivate Aconitases, but Nitric Oxide Does Not. J. Biol. Chem. 269, 29405-29408.

Heller, R. A., Song, K, Fan, N., and Chang, D. J. (1992). The p70 Tumor Necrosis Factor Receptor Mediates Cytotoxicity. Cell 70:47-56.

Henkel, G. and Brown, M. A. (1994). PU.1 and GATA:Components of a Mast Cell-Specific Interleukin 4 Intronic Enhancer. Proc. Natl. Acad. Sci. USA 91:7737-7741.

Henry, Y., and Guissani, A. (1999). Interactions of Nitric Oxide with Hemoproteins: Roles of Nitric Oxide in Mitochondria. Cell. Mol. Life Sci. 55:1003-1014.

Hjalmarsson, K., Marklund, S., Engstrom, A., and Edlund, T. (1987). Isolation and Sequence of Complementary DNA Encoding Human Extracellular Superoxide Dismutase. Proc. Natl. Acad. Sci. USA 84:6340-6344.

Ho, S. N., Hunt, H. D., Horton, R. M., Pullen, J. K., and Pease, L. R. (1989). Site-directed Mutagenesis by Overlap Extension Using the Polymerase Chain Reaction. Gene 77:51-59.

Ho, Y. S. and Crapo, J. D. (1987). Nucleotide Sequence of cDNAs Coding for Rat Manganese-Containing Superoxide Dismutase. Nucl. Acids Res. 15:10070.

Ho, Y. S. and Crapo, J. D. (1988). Isolation and Characterization of Complementary DNAs Encoding Human Manganese-Containing Superoxide Dismutase. FEBS Lett. 229:256-260.

Ho, Y. S., Howard, A. J., and Crapo, J. D. (1991). Molecular Structure of a Functional Rat Gene for Manganese-Containing Superoxide Dismutase. Am. J. Respir. Cell Mol. Biol. 4:278-286.

Hohmann, H. P., Remy, R., Poschl, B., and Loon, A. P. G. M. (1990). Tumor Necrosis Factors-α and -β Bind to the Same Two Types of Tumor Necrosis Factor Receptors and Maximally Activate the Transcription Factor NF-kB at Low Receptor Occupancy and within Minutes after Receptor Binding. J. Biol. Chem. 265:15183-15188.

Hori, S. (1982). Study on Hyperbaric Oxygen-Induced Convulsion with Particular Reference to Gamma-Aminobutyric Acid in Synaptosomes. J. Biochem. (Tokyo) 91:443-448.

Hornstra, I. K., and Yang, T. P. (1993). *In Vivo* Footprinting and Genomic Sequencing by Ligation-Mediated PCR. Anal. Biochem. 213:179-193.

Howell, N., Huang, P., Kelliher, K., and Ryan, M. L. (1983). Mitochondrial Genetics of Mammalian Cells: A Mouse Antimycin-Resistant Mutant with a Probable Alteration of Cytochrome b. Somatic Cell Genetics 9:143-163.

Hsu, J. L. (1993). The Characterization of Rat Cu/ZnSOD and MnSOD Genes. Ph. D. Dissertation, University of Florida.

Hurt, J., Hsu, J-L., Dougall, W. C., Visner, G. A., Burr, I. M., and Nick, H. S. (1992). Multiple mRNA Species Generated by Alternate Polyadenylation from the Rat Manganese Superoxide Dismutase Gene. Nucl. Acids Res. 20:2985-2990.

Ichas, F., and Mazat, J. P. (1998). From Calcium Signaling to Cell Death: Two Conformations for the Mitochondrial Permeability Transition Pore. Switching from Low- to High-Conductance State. Biochim. Biophys. Acta 1366:33-50.

Ikejima, T., Okusawa, S., van der Meer, J. W., and Dinarello, C. A. (1988). Induction by Toxic-Shock-Syndrome Toxin-1 of a Circulating Tumor Necrosis Factor-like Substance in Rabbits and of Immunoreactive Tumor Necrosis Factor and Interleukin-1 from Human Mononuclear Cells. J. Inf. Dis. 158:1017-1025.

Iwata, S., Lee, J. W., Okada, K., Lee, J. K., Iwata, M., Rasmussen, B., Link, T. A., Ramaswamy, S., and Jap, B. K. (1998). Complete Structure of the 11-Subunit Bovine Mitochondrial Cytochrome bc1 Complex. Science 281:64-71.

Jacob, F., and Monod, J. (1961). Genetic Regulatory Mechanisms in the Synthesis of Proteins. J. Mol. Biol. 3:318-356.

Jacoby, D. B., and Choi, A. M. (1994). Influenza Virus Induces Expression of Antioxidant Genes in Human Epithelial Cells. Free Rad. Biol Med. 16:821-824.

John, S., Reeves, R., Lin, J., Child, R., Leiden, J., Thompson, C. B., and Leonard, W. J. (1995). Regulation of Cell-Type-Specific Interleukin-2 Receptor α-Chain Gene Expression: Potential Role of Physical Interactions between Elf-1, HMG I(Y), and NF-κB Family Proteins. Mol. Cell. Biol. 15:1786-1796.

Jones, P. L., Kucera, G., Gordon, H., and Boss, J. M. (1995). Cloning and Characterization of the Murine Manganous Superoxide Dismutase-Encoding Gene. Gene 153:155-161.

Jones, P. L., Ping, D., and Boss, J. M. (1997). Tumor Necrosis Factor Alpha and Interleukin-1β Regulate the Murine Manganese Superoxide Dismutase Gene through a Complex Intronic Enhancer Involving C/EBPβ and NF-κB. Mol. Cell. Biol. 17:6970-6981.

Judde, J. and Max, E. E. (1992). Characterization of the Human Immunoglobulin Kappa Gene 3' Enhancer: Functional Importance of Three Motifs that Demonstrate B-cell-Specific *In Vivo* Footprints. Mol. Cell. Biol. 12:5206-5216.

Kifle, Y., Monnier, J., Chesrown, S. E., Raizada, M. K., and Nick, H. S. (1996). Regulation of the Manganese Superoxide Dismutase and Inducible Nitric Oxide Synthase Gene in Rat Neuronal and Glial Cells. J. Neurochem. 66:2128-2135.

Kim, T. K. and Maniatis, T. (1997). The Mechanism of Transcriptional Synergy of an *In Vitro* Assembled Interferon-β Enhanceosome. Mol. Cell 1:119-129.

Kinnula, V. L., Aito, H., Klefstrom, J., Alitalo, K., and Raivio, K. O. (1998). Similarities between TNF and Exogenous Oxidants on the Cytotoxic Response of c-Myc-Expressing Fibroblasts *In Vitro*. Cancer Lett. 125:191-198.

Kobayashi, Y., Kitamoto, T., Masuhiro, Y., Watanabe, M., Kase, T., Metzger, D., Yanagisawa, J., Kato, S. (2000). p300 Mediates Functional Synergism between AF-1 and AF-2 of Estrogen Receptor alpha and beta by Interacting Directly with the N-terminal A/B Domains. J. Biol. Chem. 275:15645-15651.

Koleske, A. J., and Young, R. A. (1995). The RNA Polymerase II Holoenzyme and Its Implications for Gene Regulation. Trends Biochem. Sci. 20, 113-116.

Krall, J., Bagley, A. C., Mullenbach, G. T., Hallewell, R. A., and Lynch, R. E. (1988). Superoxide Mediates the Toxicity of Paraquat for cultured Mammalian Cells. J. Biol. Chem. 263:1910-1914.

Kramer, R. S., and Pearlstein, R. D. (1983). Reversible Uncoupling of Oxidative Phosphorylation at Low Oxygen Tension. Proc. Natl. Acad. Sci. 80:5807-5811.

Kramer, R. M., Roberts, E. F., Um, S. L., Borsch-Haubold, A. G., Watson, S. P., Fisher, M. J., and Jakubowski, J. A. (1996). p38 Mitogen-Activated Protein Kinase Phosphorylates Cytosolic Phospholipase A_2 ($cPLA_2$) in Thrombin-Stimulated Platelets. Evidence that Proline-Directed Phosphorylation Is Not Required for Mobilization of Arachidonic Acid by $cPLA_2$. J. Biol. Chem. 271:27723-27729.

Kriegler, M. (1990). Gene Transfer and Expression: A Laboratory Manual. Stockton Press, New York.

Kuo, S. (1998). The Regulation of Rat Manganese Superoxide Dismutase Gene: Detection and Characterization of *Trans*-Acting Factors. Ph. D. Dissertation, University of Florida.

Kuo, S., Chesrown, S. E., Mellot, J., Rogers, R. J., Hsu, J-L., and Nick, H. S. (1999). *In Vivo* Architecture of the Manganese Superoxide Dismutase Promoter. J. Biol. Chem. 274:3345-3354.

Kultz, D., Madhany, S., and Burg, M. B. (1998). Hyperosmolality Causes Growth Arrest of Murine Kidney Cells. Induction of GADD45 and GADD153 by Osmosensing via Stress-Activated Protein Kinase 2. J. Biol. Chem. 273:13645-13651.

Kushner, I., Ganapathi, M., and Schultz, D. (1989). The Acute Phase Response is Mediated by Heterogeneous Mechanisms. Annals N. Y. Acad. Sci. 557:19-30.

Kutach, A. K., and Kadonaga, J.T. (2000). The Downstream Promoter Element DPE Appears To Be as Widely Used as the TATA Box in Drosophila Core Promoters. Mol. Cel.l Biol. 20:4754-4764.

Lambowitz, A. M., Koboyashi, G. S., Painter, A., and Medoff, G. (1983). Possible Relationship of Morphogenesis in Pathogenic Fungus, Histoplasma capsulatum, to Heat Shock Response. Nature 303:806-808.

Lantz, M., Gullberg, U., Nilsson, E., and Olsson, I. (1990). Characterization *In Vitro* of a Human Tumor Necrosis Factor-Binding Protein. A Soluble Form of a Tumor Necrosis Factor Receptor. J. Clin. Invest. 86:1396-1402.

Lee, T. H., Lee, G. W., Ziff, E. B., and Vilcek, J. (1990). Isolation and Characterization of Eight Tumor Necrosis Factor-Induced Gene Sequences from Human Fibroblasts. Mol. Cell. Biol. 10:1982-1988.

Lei, M. and Morrison, D. C. (1988). Specific Endotoxic Lipopolysaccharide-Binding Proteins on Murine Splenocytes. J. Immunol. 141:1006-1011.

Lerger, H., Sock, E., Renner, K., Grummt, F., and Wegner, M. (1995). Functional Interaction between the POU Domain Protein Tst/Oct-6 and the High-Mobility-Group Protein HMG I(Y). J. Biol. Chem. 15:3738-3747.

Levinson, B., Khoury, G., Woude, G. V., and Gruss, P. (1982). Activation of SV40 Genome by 72-Base Pair Tandem Repeats of Moloney Sarcoma Virus. Nature 295, 568-572.

Lewis, E. B. (1954). The Theory and Application of a New Method of Detecting Chromosomal Rearrangements in *Drosophila melanogaster*. Am. Nat. 88:225-239.

Li, Q., and Cathcart, M. K. (1997). Selective Inhibition of Cytosolic Phospholipase A_2 in Activated Human Monocytes. Regulation of Superoxide Anion Production and Low Density Lipoprotein Oxidation. J. Biol. Chem. 272:2404-2411.

Li, Y., Huang, T-T., Carlson, E. J., Melov, S., Ursell, P. C., Olson, J. L., Noble, L. J., Yoshimura, M. P., Berger, C., Chan, P. H., Wallace, D. H., and Epstein, C. J. (1995). Dilated Cardiomyopathy and Neonatal Lethality in Mutant Mice Lacking Manganese Superoxide Dismutase. Nat. Genet. 11:376-381.

Lin, Y.S., Carey, M., Ptashne, M., and Green, M. R. (1990). How Different Eukaryotic Transcriptional Activators Can Cooperate Promiscuously. Nature 345:359-361.

Lomedico, P. T., Gubler, U., Hellmann, C. P., Dukovich, M., Giri, J. G., Pan, Y. C., Collier, K., Semionov, R., Chua, A. O., and Mizel, S. B. (1984). Cloning and Expression of Murine Interleukin-1 cDNA in *Escherichia coli*. Nature 312:458-462.

Lontz, W., Sirsjo, A., Liu, W., Lindberg, M., Rollman, O., and Torma, H. (1995). Increase mRNA Expression of Manganese Superoxide Dismutase in Psoriasis Skin Lesions and in Cultured Human Keratinocytes Exposed to IL-1 beta and TNF-alpha. Free Rad. Biol. Med. 18:349-355.

Manganaro, F., Chopra, V. S., Mydlarski, M. B., Bernatchez, G., and Schipper, H. M. (1995). Redox Perturbations in Cysteamine-Stressed Astroglia: Implications for Inclusion Formation and Gliosis in the Aging Brain. Free Radicals Biol. Med. 19:823-835.

Maniatis, T., Goodburn, S., and Fischer, J. A. (1987). Regulation of Inducible and Tissue-Specific Gene Expression. Science 236:1237-45.

Maniatis, T., Whittmore, L. A., Du, W., Fan, C. M., Keller, A. D., Palombella, V. J., Thanos, D. (1992). Positive and Negative Control of Human Interferon-b Gene Expression. In Transcriptional Regulation, S. L. McKnight and K. R. Yamamoto, eds. (Cold Spring Harbor Laboratory Press: Cold Spring Harbor, New York).

Marklund, S. L. (1984). Extracellular Superoxide Dismutase and Other Superoxide Dismutase Isoenzymes in Tissues from Nine Other Mammalian Species. Biochem. J. 222:649-655.

Massaro, D., Rahman, I., Clerch, L. B., and Iqbal, J. (1992). Tolerance of Rats to Hyperoxia: Lung Antioxidant Enzyme Gene Expression. FASEB J. 6:A1816.

Mayall, T. P., Sheridan, P. L., Montiminy, M. R., and Jones, K. A. (1997). Distinct Roles for P-CREB and LEF-1 in TCR alpha Enhancer Assembly and Activation on Chromatin Templates *In Vitro*. Genes Dev. 11:887-899.

Maxam, A. M. and Gilbert, W. (1980). Sequencing End-Labeled DNA with Base-Specific Chemical Cleavages. Methods Enzymol. 65:499-560.

McCord, J. M. and Roy, R. S. (1982). The Pathophysiology of Superoxide: Roles in Inflammation and Ischemia. Can. J. Physiol. Pharmacol. 60:1346-1352.

McKnight, S. and Yamamoto, K. R. (1992). Transcriptional Regulation. Cold Spring Harbor Laboratory Press: Cold Spring Harbor, New York.

Melendez, J. A., and Baglioni, C. (1993). Differential Induction and Decay of Manganese Superoxide Dismutase mRNAs. Moll. Cell. Biol. 10:1680-1688.

Melov, S., Schneider, J. A., Day, B. J., Hinerfeld, D., Coskun, P., Mirra, S. S., Crapo, J. D., and Wallace, D. C. (1998). A Novel Neurological Phenotype in Mice Lacking Mitochondrial Manganese Superoxide Dismutase. Nat. Genet. 18:159-163.

Mercola, M, Wang, X-F., Olsen, J., and Calame, K. (1983). Transcriptional Enhancer Elements in the Mouse Immunoglobulin Heavy Chain Locus. Science 221:663-65.

Merika, M., Williams, A. J., Chen, G., Collins, T., and Thanos, D. (1998). Recruitment of CBP/p300 by the IFN beta Enhanceosome Is Required for Synergistic Activation of Transcription. Mol. Cell 1:277-287.

Mignotte, B., and Vayssiere, J. L. (1998). Mitochondria and Apoptosis. Eur. J. Biochem. 252:1-15.

Molloy, R. G., Mannick, J. A., and Rodrick, M. L. (1993). Cytokines, Sepsis and Immunomodulation. Br. J. Surg. 80:289-297.

Moreau, P., Hen, R., Wasylyk, B., Everrett, R., Gaub, M. et al (1981). The SV40 72-bp Repeat Has a Striking Effect on Gene Expression Both in SV40 and Other Chimeric Recombinants. Nucleic Acids Res. 9:6047-69.

Morton, R. L., Ikle, D., and White, C. W. (1998). Loss of Lung Mitochondrial Aconitase Activity Due to Hyperoxia in Bronchopulmonary Dysplasia in Primates. Am. J. Physiol. 274:L127.

Mueller, P. R. and Wold, B. J. (1989). *In Vivo* Footprinting of a Muscle Specific Enhancer by Ligation-Mediated PCR. Science 246:780-786.

Muller-Hill, B. (1996). The *lac* Operon. A Short History of a Genetic Paradigm. Walter de Gruyter, Berlin, Germany.

Nedwin, G. E., Naylor, S. L., Sakaguchi, A. Y., Smith, D., Jarrett-Nedwin, J., Pennica, D., Goeddel, D. V., and Gray, P. W. (1985). Human Lymphotoxin and Tumor Necrosis Factor Genes: Structure, Homology and Chromosomal Localization. Nucleic Acids Res. 13:6361-6373.

Neta, R., Douches, S., and Oppenheim, J. J. (1986). Interleukin-1 is a Radioprotector. J. Immunol. 136:2483-2485.

Neuberger, M. S. (1983). Expression and Regulation of Immunoglobulin Heavy Chain Gene Transfected into Lymphoid Cells. EMBO J. 2:1373-78.

Nick, H. and Gilbert, W. (1985). Detection of *In Vivo* Protein-DNA Interactions within the lac Operon of *Escherichia coli*. Nature 313:795-798.

Niitsu, Y., Watanabe, N., Sone, H., Neda, H., Yamauchi, N., and Urushizaki, I. (1985). Mechanism of the Cytotoxic Effect of Tumor Necrosis Factor. Jpn. J. Cancer Res. 76:1193-1197.

Nohl, H., Gille, L., Schoneit, K., and Liu, Y. (1996). Conditions Allowing Redox-Cycling Ubisemiquinone in Mitochondria to Establish a Direct Redox Couple with Molecular Oxygen. Free Rad. Biol. Med. 20:207-213.

O'Brien, T., and Tjian, R. (2000). Different Functional Domains of TAFII250 Modulate Expression of Distinct Subsets of Mammalian Genes. Proc. Natl. Acad. Sci. USA 97:2456-2461.

Oberley, L. W., Kasemet St. Clair, P., Autor, A. P., and Oberley, T. D. (1987). Increase in Manganese Superoxide Dismutase Activity in the Mouse Heart After X-irradiation. Arch. Biochem. Biophys. 254:69-80.

Ohtsuki, S., Levine, M., and Cai, H. N. (1998). Different Core Promoters Possess Distinct Regulatory Activities in the Drosophila Embryo. Genes Dev. 12:547-556.

Okamoto, H., Sheline, C. T., Corden, J. L., Jones, K. A., Peterlin, B. M. (1996). Trans-Activation by Human Immunodeficiency Virus Tat Protein Requires the C-terminal Domain of RNA Polymerase II. Proc. Natl. Acad. Sci. USA. 93:11575-11579.

Okusawa, S., Gelfand, J. A., Ikejima, T., Connolly, R. J., and Dinarello, C. A. (1988). Interleukin 1 Induces a Shock-Like State in Rabbits. Synergism with Tumor Necrosis Factor and the Effect of Cyclooxygenase Inhibition. J. Clin. Invest. 81:1162-1172.

Orphaides, G., Lagrange, T., and Reinberg, D. (1996). The General Transcription Factors of RNA Polymerase II. Genes Dev. 10, 2657-2683.

Orphanides, G., Wu, W.H., Lane, W.S., Hampsey, M., Reinberg, D. (1999). The Chromatin-Specific Transcription Elongation Factor FACT Comprises Human SPT16 and SSRP1 Proteins. Nature 400:284-288.

Parada, C. A., and Roeder, R. G. (1996). Enhanced Processivity of RNA Polymerase II Triggered by Tat-Induced Phosphorylation of its Carboxy-Terminal Domain. Nature 384:375-378.

Pennica, D., Newin, G. E., Hayflick, J. S., Seeburg, P. H., Derynck, R., Palladino, M. A., Kohr, W. J., Aggarwal, B. B., and Goeddel, D. V. (1984). Human Tumour Necrosis Factor: Precursor Structure, Expression and Homology to Lymphotoxin. Nature 312:724-729.

Pham, A.D., and Sauer, F. (2000). Ubiquitin-Activating/Conjugating Activity of TAF(II)250, A Mediator of Activation of Gene Expression in Drosophila. Science 289:2357-2360.

Picard, D., and Schaffner, W. (1984). A Lymphocte-Specific Enhancer in the Mouse Immunoglobulin κ Gene. Nature 307:80-82.

Pierce, J. W., Schoenleber, G. J., Jesmok, G., Best, J., Moore, S. A., Collins, T., and Gerritsen, M. E. (1997). Novel Inhibitors of Cytokine-Induced Ikappa B alpha Phosphorylation and Endothelial Cell Adhesion Molecule Expression Show Anti-Inflammatory Effects *In Vivo*. J. Biol. Chem. 272:21096-21103.

Poyton, R. O. and McEwen, J. E. (1996). Crosstalk between Nuclear and Mitochondrial Genomes. Ann. Rev. Biochem. 65:563-607.

Priestle, J. P., Schar, H. P., and Grutter, M. G. (1988). Crystal Structure of the Cytokine Interleukin-1 beta. EMBO J. 7:339-343.

Priestle, J. P., Schar, H. P., and Grutter, M. G. (1989). Crystallographic Refinement of Interleukin 1 beta at 2.0 A Resolution. Proc. Natl. Acad. Sci. USA 86:9667-9671.

Privalle, C. T., and Fridovich, I. (1993). Iron Specificity of the Fur-Dependent Regulation of the Biosynthesis of the Manganese-Containing Superoxide Dismutase in Escherichia Coli. J. Biol. Chem. 269, 5178-5181.

Ptashne, M. (1986). Gene Regulation by Proteins Acting Nearby and at a Distance. Nature 322, 697-701.

Ptashne, M. and Gann, A. (1997). Transcriptional Activation by Recruitment. Nature 386:560-577.

Pugh, B. F. and Tijian, R. (1991). Transcription from a TATA-less Promoter Requires a Multisubunit TFIID Complex. Genes & Dev. 5:1935-1945.

Queen, C. and Baltimore, D. (1983). Immunoglobulin Gene Transcription Is Activated by Downstream Sequence Elements. Cell 33:741-748.

Queen, C. and Stafford, J. (1984). Fine Mapping of an Immunoglobulin Gene Activator. Mol. Cell. Biol. 4:1042-49.

Ranganath, S., Ouyang, W., Bhattarcharya, D., Sha, W. C., Grupe, A., Peltz, G., and Murphy, K. M. (1998). GATA-3-Dependent Enhancer Activity in IL-4 Gene Regulation. J. Immunol. 161:3822-3826.

Remacle, J., Raes, M., Toussaint, O., Renard, P., and Rao, G. (1995). Low Levels of Reactive Oxygen Species as Modulators of Cell Function. Mutat. Res. 316:103-122.

Rietschel, E. H. and Brade, H. (Aug. 1992). Bacterial Endotoxin. Scientific American 54-61.

Roeder, R. G. (1996). The Role of General Initiation Factors in Transcription by RNA Polymerase II. Trends Biochem. Sci. 21, 327-335.

Rogers, R. J., Chesrown, S. E., Kuo, S., Monnier, J. M., and Nick, H. S. (2000). Cytokine-Inducible Enhancer with Promoter Activity in Both the Rat and Human Manganese-Superoxide Dismutase Genes. Biochem. J. 347:233-242.

Rollins, R.A., Morcillo, P., and Dorsett, D. (1999). Nipped-B, A Drosophila Homologue of Chromosomal Adherins, Participates in Activation by Remote Enhancers in the Cut and Ultrabithorax Genes. Genetics 152:577-93.

Rosenberg, M., and Court, D. (1979). Regulatory Sequences Involved in the Promotion and Termination of RNA Transcription. Ann. Rev. Genet. 13:319-53.

Sambrook, J., Fritsch, E. F., and Maniatis, T. (1989). Molecular Cloning: A Laboratory Manual, second edition, Cold Spring Harbor Laboratory Press, Cold Spring Harbor, NY.

Sanchez-Alcazar, J. A., Hernandez, I., del la Torre, M. P., Garcia, I., Santiago, E., Munoz-Yague, M. T., and Solis-Herruzo, J. A. (1995). Down-Regulation of Tumor Necrosis Factor Receptors by Blockade of Mitochondrial Respiration. J. Biol. Chem. 270:23944-23950.

Sanchez-Alcazar, J. A., Ruiz-Cabello, J., Hernandez-Munoz, I., Pombre, P. S., del la Torre, P., Siles-Rivas, E., Garcia, I., Kaplan, O., Munoz-Yague, M. T., and Solis-Herruzo, J. A. (1997). Tumor Necrosis Factor-alpha Increases ATP Content in Metabolically Inhibited L929 Cells Preceding Cell Death. J. Biol. Chem. 272:30167-30177.

Sauer, F., Hansen, S. K., and Tijian, R. (1995). Multiple TAF IIs Directing Synergistic Activation of Transcription. Science 270, 1783-1788.

Schmidt, K. N., Traenckner, E. B., Meier, B., and Baeuerle, P. A. (1995). Induction of Oxidative Stress by Okadaic Acid Is Required for Activation of Transcription Factor NF-kappa B. J. Biol. Chem. 270:27136-27142.

Schreck, R., Rieber, P., and Baeuerle, P. A. (1991). EMBO J. 10:2247-2258.

Schulze-Osthoff, K., Bakker, A. C., Vanhaesebroeck, B., Beyaert, R., Jacob, W. A., and Fiers, W. (1992). Cytotoxic Activity of Tumor Necrosis Factor is Mediated by Early Damage of Mitochondrial Functions. Evidence for the Involvement of Mitochondrial Radical Generation. J. Biol. Chem. 267:5317-5323.

Schulze-Osthoff, K., Beyaert, R., Vandevoorde, V., Haegeman, G., and Fiers, W. (1993). Depletion of the Mitochondrial Electron Transport Abrogates the Cytotoxic and Gene-Inductive Effects of TNF. EMBO J. 12:3095-3104.

Schumann, R. R., Leong, S. R., Glaggs, G. W., Gray, P. W., Wright, S. D., Mathison, J. C., Tobias, P. S., and Ulevitch, R. J. (1990). Structure and Function of Lipopolysaccharide Binding Protein. Science 249:1429-1431.

Selden, R. F., Howie, K. B., Rowe, M. E., Goodman, H. M., and Moore, D. D. (1986). Human Growth Hormone as a Reporter Gene in Regulation Studies Employing Transient Gene Expression. Mol. Cell. Biol. 6:3173-3179.

Shaffer, J. B., Treanor, C. P., and Del-Vecchio, P. J. (1990). Expression of Bovine and Mouse Endothelial Cell Antioxidant Enzymes Following RNF-alpha Exposure. Free Rad. Biol. Med. 8:497-502.

Shields, J.M. and Yang, V.W. (1998). Identification of the DNA Sequence that Interacts with the Gut-Enriched Kruppel-like Factor. Nucleic Acids Res. 26, 796-802.

Shull, S., Heintz, N. H., Periasamy, M., Manohar, M., Janssen, Y. M., Marsh, J. P., and Mossman, B. T. (1991). Differential Regulation of Antioxidant Enzymes in Response to Oxidants. J. Biol. Chem. 266:24398-24403.

Simkevich, C. P., Thompson, J. P., Poppleton, H., and Raghow, R. (1992). The Transcriptional Tissue Specificity of the Human Pro alpha 1 (I) Collagen Gene Is Determined by a Negative *Cis*-Regulatory Element in the Promoter. Biochem. J. 286:179-185.

Slot, J., Geuze, H., Freeman, B., and Crapo, J. D. (1986). Intracellular localization of the Copper-Zinc and Manganese Superoxide Dismutases in Rat Liver Parenchymal Cells. Lab. Invest. 55:363-371.

Stafford, J., and Queen, C. (1983). Cell-Type Specific Expression of a Transfected Immunoglobulin Gene. Nature 306:77-79.

Stephanz, G. B., Gwinner, W., Cannon, J. K., Tisher, C. C., and Nick, H. S. (1996). Heat-Aggregated IgG and Interleukin-1 beta Stimulate Manganese Superoxide Dismutase in Mesangial Cells. Exp. Nephrol. 4:151-158.

Surpin, M., and Chory, J. (1997). The Co-ordination of Nuclear and Organellar Genome Expression in Eukaryotic Cells. Essays Biochem. 32:113-125.

Suzuki, K., Tatsumi, H., Satoh, S., Senda, T., Nakata, T., Fujii, J, and Taniguchi, N. (1993). Manganese-Superoxide Dismutase in Endothelial Cells: Localization and Mechanism of Induction. Am. J. Physiol. 265:H1173-1178.

Takimoto, Y. and Kuramoto, A. (1993). Presence of a Regulatory Element within the First Intron of the Human Platelet-Derived Growth Factor-A Chain Gene. Jpn. J. Cancer Res. 84:1268-1272.

Tan, S., Sagara, Y., Liu, Y., Maher, P., and Schubert, D. (1998). The Regulation of Reactive Oxygen Species Production During Programmed Cell Death. J. Cell Biol. 141:1423-1432.

Tartaglia, L. A. and Goeddel, D. V. (1992). Two TNF Receptors. Immunol. Today 13:151-153.

Tartaglia, L. A., Rothe, M., Hu, Y.-F., and Goeddel, D. V. (1993). Tumor Necrosis Factor's Cytotoxic Activity is Signaled by the p55 TNF Receptor. Cell 73:213-216.

Thanos, D. and Maniatis, T. (1992). The High Mobility Group Protein HMG I(Y) Is Required for NF-κB Dependent Virus Induction of the Human IFN-β Gene. Cell 71:777-789.

Thanos, D., Du, W., and Maniatis, T. (1993). The High Mobility Group Protein HMG I(Y) Is An Essential Structural Component of a Virus Inducible Enhancer Complex. Cold Spring Harbor Symp. Quant. Biol. 58:73-81.

Thierbach, G., and Reichenbach, H. (1981). Myxothiazol, A New Inhibitor of the Cytochrome b-c1 Segment of the Respiratory Chain. Biochim. Biophys. Acta 638:282-289.

Thornberry, N. A., Bull, H. G., Calaycay, J. R., Champman, K. T., Howard, A. D., Kostura, M. J., Miller, D. K., Molineaux, S. M., Weidner, J. R., and Anunins, J. (1992). A Novel Heterodimeric Cysteine Protease Is Required for Interleukin-1 beta Processing in Monocytes. Nature 356:768-774.

Tijan, R. and Maniatis, T. (1994). Transcriptional Activation: A Complex Puzzle with Few Easy Pieces. Cell 77:5-8.

Tobias, P. S., Mathison, J. C., and Ulevitch, R. J. (1988). A Family of Lipopolysaccharide Binding Proteins Involved in Responses to Gram-negative Sepsis. J. Biol. Chem. 263:13479-13481.

Treuter, E., Johansson, L., Thomsen, J. S., Warnmark, A., Leers, J., Pelto-Huikko, M., Sjoberg, M., Wright, A. P., Spyrou, G., and Gustafsson, J. A. (1999). Competition between Thyroid Hormone Receptor-Associated Protein (TRAP) 220 and Transcriptional Intermediary Factor (TIF) 2 for Binding to Nuclear Receptors. Implications for the Recruitment of TRAP and p160 Coactivator Complexes. J. Biol. Chem. 274:6667-6677.

Tsujimoto, M., Yip, Y. K., and Vilcek, J. (1985). Tumor Necrosis Factor: Specific Binding and Internalization in Sensitive and Resistant Cells. Proc. Natl. Acad. Sci. USA 82:7626-7630.

Tyndall, C., La Mantia, G., Thacker, C. M., Favaloro, J., and Kamen, R. (1981). A Region of the Polyoma Virus Genome between the Replication Origin and Late Protein Coding Sequences Is Required in Cis for Both Early Gene Expression and Viral DNA Replication. Nucl. Acids Res. 9, 6231-6250.

Valentine, J. F., and Nick, H. S. (1992). Acute-Phase Induction of Manganese Superoxide Dismutase in Intestinal Epithelial Cell Lines. Gastroenterol. 103:90-912.

Vinson, C. R., LaMarco, K. L., Johnson, P. F., Landschulz, W. H., and McKnight, S. L. (1988). In Situ Detection of Sequence-Specific DNA Binding Activity Specified by a Recombinant Bacteriophage. Genes & Dev. 2:801-806.

Visner, G. A., Dougall, W. C., Wilson, J. M., Burr, I. A., and Nick, H. S. (1990). Regulation of Manganese Superoxide Dismutase by Lipopolysaccharide, Interleukin-1, and Tumor Necrosis Factor: Role of the Acute Inflammatory Response. J. Biol. Chem. 265:2856-2864.

Visner, G. A., Block, E. R., Burr, I. M., and Nick, H. S. (1991). Regulation of Manganese Superoxide Dismutase in Porcine Pulmonary Artery Endothelial Cells. Am. J. Physiol. 260:L444-449.

Visner, G. A., Chesrown, S. E., Monnier, J., Ryan, U. S., and Nick, H. S. (1992). Regulation of Manganese Superoxide Dismutase: IL-1 and TNF Induction in Pulmonary Artery and Microvascular Endothelial Cells. Biochem. Biophys. Res. Comm. 188:453-462.

von Sonntag, C. (1987). The Chemical Basis of Radiation Biology. Taylor & Francis, London.

Warner, B. B., Bunhans, M. S., Clark, J. C., and Wispe, J. R. (1991). Tumor Necrosis Factor-alpha Increases Mn-SOD Expression: Protection against Oxidant Injury. Am. J. Physiol. 260:L296-301.

Warner, B. B., Stuart, L., Gebb, S., and Wispe, J. R. (1996). Redox Regulation of Manganese Superoxide Dismutase. Am. J. Physiol. 271:L150-158.

Weisinger, R. A., and Fridovich, I. (1973). Superoxide Dismutase: Organelle Specificity. J. Biol. Chem. 248:3582-3592.

Welbourn, C. R. B. and Young, Y. (1992). Endotoxin, Septic Shock and Acute Lung Injury: Neutrophils, Macrophages and Inflammatory Mediators. Br. J. Surg. 79:998-1003.

Whitsett, J. A., Clark, J. C., Wispe, J. R., and Pryhuber, G. S. (1992). Effects of TNF-alpha and Phorbol Ester on Human Surfactant Protein and MnSOD Gene Transcription *In Vitro*. Am. J. Physiol. 262:L688-693.

Wispe, J. R., Warner, B. B., Clark, J. C., Dey, C. R., Neuman, J., Glasser, S. W., Crapo, J. D., Chang, L., and Whitsett, J. A. (1992). Human Mn-Superoxide Dismutase in Pulmonary Epithelial Cells of Transgenic Mice Confers Protection from Oxygen Injury. J. Biol. Chem. 267:23937-23941.

Wong, G. H. W., and Goeddel, D. V. (1988). Induction of Manganous Superoxide Dismutase by Tumor Necrosis Factor: Possible Protective Mechanism. Science 242:941-944.

Wong, G. H. W., Elwell, J., Oberly, L., and Goeddel, D. V. (1989). Manganous Superoxide Dismutase is Essential for Cellular Resistance to Cytotoxicity of Tumor Necrosis Factor. Cell 58:923-931.

Woo, C. H., Eom, Y. W., Yoo, M. H., You, H. J., Han, H. J., Song, W. K., Yoo, Y. J., Chun, J. S., and Kim, J. H. (2000). Tumor Necrosis Factor-α Generates Reactive Oxygen Species via a Cytosolic Phospholipase A_2-Linked Cascade. J. Biol. Chem. (in press).

Workman, J. L. and Kingston, R. E. (1998). Alteration of Nucleosome Structure as a Mechanism of Transcriptional Regulation. Ann. Rev. Biochem. 67:545-579.

Wright, S. D., Ramos, R. A., Tobias, P. S., Ulevitch, R. J., and Mathison, J. C. (1990). CD14, A Receptor for Complexes of Lipopolysaccharide (LPS) and LPS Binding Protein. Science 249:1431-1433.

Yie, J., Liang, S., Merika, M., and Thanos, D. (1997). Intra- and Intermolecular Cooperative Binding of High-Mobility-Group Protein I (Y) to the Beta-Interferon Promoter. Mol. Cell. Biol. 17:3649-3662.

Zhang, W., Shields, J. M., Sogawa, K., Fujii-Kuriyama, Y., and Yang, V. W. (1998). The Gut-Enriched Kruppel-like Factor Suppresses the Activity of the CYP1A1 Promoter in an Sp1-Dependent Fashion. J. Biol.Chem. 273, 17917-17925.

Zhao, X. J., Raitt, D., Burke, P. V., Clewell, A. S., Kwast, K. E., and Poyton, R. O. (1996). Function and Expression of Flavohemoglobin in Saccharomyces cerevisiae. Evidence for a Role in the Oxidative Stress Response. J. Biol. Chem. 271:25131-25138.

Zhou, J., and Levine, M. (1999). A Novel *Cis*-Regulatory Element, the PTS, Mediates an Anti-Insulator Activity in the Drosophola Embryo. Cell 99:567-575.

BIOGRAPHICAL SKETCH

Richard James Rogers was born on September 24, 1957, to Richard Rowe Rogers and Eleanor Frances Rogers, in Lowell, Massachusetts. He attended Central Catholic High School in Lawrence, Massachusetts, graduating in May 1975. He continued his education by attending Boston College in Chestnut Hill, Massachusetts, graduating summa cum laude with a Bachelor of Science degree in chemistry. After college, he was accepted to the University of Massachusetts Medical School from which he received his Doctor of Medicine degree in June 1983. During the following three years he trained in the medical specialty of internal medicine at the Brigham & Women's Hospital in Boston, Massachusetts, and the Berkshire Medical Center in Pittsfield, Massachusetts. From 1986 to 1991, he served as Director of Emergency Services at Harrington Memorial Hospital in Southbridge, Massachusetts, as well as an Instructor in the Department of Emergency Medicine at the University of Massachusetts Medical Center in Worcester, Massachusetts. From 1991 to 1994, he trained in the medical specialty of anesthesiology in the Department of Anesthesiology at the University of Florida College of Medicine in Gainesville, Florida, where he currently holds the title of Instructor and is involved the clinical care of patients and the supervision and teaching of resident physicians and medical students. He entered the doctoral program in biochemistry and molecular biology at the University of Florida in the fall of 1994. Upon completion of the Doctor of Philosophy degree, he will continue as an Assistant Professor in the Department of Anesthesiology at the University of Florida College of Medicine in Gainesville, Florida.

I certify that I have read this study and that in my opinion it conforms to acceptable standards of scholarly presentation and is fully adequate, in scope and quality, as a dissertation for the degree of Doctor of Philosophy.

Harry S. Nick, Chair
Professor of Neuroscience

I certify that I have read this study and that in my opinion it conforms to acceptable standards of scholarly presentation and is fully adequate, in scope and quality, as a dissertation for the degree of Doctor of Philosophy.

Michael S. Kilberg
Professor of Biochemistry and Molecular Biology

I certify that I have read this study and that in my opinion it conforms to acceptable standards of scholarly presentation and is fully adequate, in scope and quality, as a dissertation for the degree of Doctor of Philosophy.

Brian D. Cain
Professor of Biochemistry and Molecular Biology

I certify that I have read this study and that in my opinion it conforms to acceptable standards of scholarly presentation and is fully adequate, in scope and quality, as a dissertation for the degree of Doctor of Philosophy.

Sarah E. Chesrown
Associate Professor of Biochemistry and Molecular Biology

I certify that I have read this study and that in my opinion it conforms to acceptable standards of scholarly presentation and is fully adequate, in scope and quality, as a dissertation for the degree of Doctor of Philosophy.

Robert J. Ferl
Professor of Horticultural Science

This dissertation was submitted to the Graduate Faculty of the College of Medicine and to the Graduate School and was accepted as partial fulfillment of the requirements for the degree of Doctor of Philosophy.

December 2000

Dean, College of Medicine

Dean, Graduate School

UNIVERSITY OF FLORIDA
3 1262 08555 2700